Modelling Growth Patterns of Bird Species Using Non-Linear Mixed Effects Models

by
D Ntirampeba

A thesis in partial fulfilment of the requirements for the degree of
Master of Science in Statistical Sciences

Supervisors: Dr Francesca Little & Dr Birgit Erni

Department of Statistical Sciences
University of Cape Town

May 21, 2008

Acknowledgements

I would like to thank my supervisors, Dr Francesca Little and Dr Birgit Erni for the brilliant ideas, guidance, and dedication to the work throughout the research. I express gratitude to Prof Les Underhill for valuable suggestions in this work. My gratitude to Greg for his assistance with R. I am grateful to Bizimana family, the Department of Statistical Sciences, and Avian Demography Unit for financial support.

Abstract

The analysis of growth data is important as it allows us to assess how fast things grow and determine various factors that have impact on their growth. In the current study, growth measurements on body features (body mass, wing length, head length, bill (culmen) length, foot length, and tarsus length) for Grey-headed Gulls populating Bonaero Park and Modderfontein Pan in Gauteng province, South Africa, and for Swift Terns on Robben Island were taken. Different methods such as polynomial regressions, non-parametric models and non-linear mixed effects models have been used to fit models to growth data. In recent years, non-linear mixed effects models have become an important tool for growth models. We have fitted univariate inverse exponential, Gompertz, logistic, and Richards non-linear mixed effects models to each of the six body features. We have modeled these six features simultaneously by adding a categorical covariate, which distinguishes between different features, to the model. This approach allows for straightforward comparison of growth between the different body features. In growth studies, the knowledge of the age of each individual is an essential information for growth analysis. For Swift Terns, the exact age of most chicks was unknown, but a small portion of the sample was followed from nestling up to the end of the study period. For chicks with unknown age, we estimated age by fitting the growth curve, obtained from birds with known age, to the mass measurements of the chick with unknown age.

It was found that the logistic models were most appropriate to describe the growth of body mass and wing length while the Gompertz models provided best fits for bill, tarsus, head and foot for Grey-headed Gulls. For Swift Terns, the inverse exponential model provided the best univariate fit for four of six features. The logistic model, with a variance function increasing as a power of fitted values, with a different power for each feature and autoregressive correlation structure for within bird errors with errors from different features within the same subject assumed to be independent, gave the best model to describe the growth of all body features taken simultaneously for both Grey-headed Gull and Swift Tern data.

It was shown that growth of Grey-headed Gull and Swift Tern chicks occurs in the following order (foot, body mass, tarsus)-(bill, head)-(wing) and (tarsus, foot)-(body mass, bill, head)-(wing), respectively.

Contents

List of Figures

List of Tables

Chapter 1

Introduction

1.1 Background

In many fields, the analysis of growth data is important as it allows us to determine how large things grow, how fast they grow and how factors such as environment and other variables impact on their growth (Seber and Wild, 1989). Based on growth analysis results, decisions that lead to medical, economic, management, social and political changes may be made. Different methods such as polynomial regressions, non-parametric models and non-linear mixed effects models have been used to fit models to growth data. In recent years, non-linear mixed effects models have become an important tool for growth models. However, from the literature, most of the studies have concentrated on univariate non-linear mixed effects modelling to analyze a single growth response variable, very few studies have looked at multiple responses (Hall and Clutter, 2004).

1.2 Problem statement

Two data sets from two different bird species, obtained from the Avian Demography Unit (Department of Statistical Sciences, University of Cape Town), were used in this study: grey-headed gull and swift tern data. For both species, six growth variables were measured repeatedly on each bird. At each measurement occasion, the age of each Grey-headed Gull chick was provided whereas for terns the age information was summarized as a categorical variable:

nestling for chicks found in the nests or runner otherwise.

A univariate non-linear mixed effects modelling approach is appropriate to fit growth curves for each response separately. But this approach fails to capture the possible correlations between different growth variables and does not allow for formal comparison of the growth trajectories of different responses. The question that arises is "how do we model jointly all the growth variables so that correlations between response variables may be accounted for, thus allowing for formal comparisons between different growth trajectories?" For the tern data, the age variable does not appear in a form that can be readily used for growth analysis as the ages at the beginning of the follow-up period for chicks followed from runner stage were unknown. This leads to the question: "how do we predict the age of a runner chick using the available information?"

1.3 Objectives of the research study

This study intends to use non-linear mixed effects models to describe the growth of grey-headed gulls and swift terns. To attain this, we aim to achieve the following specific objectives:

For the gull data:

- fit growth curve models to each growth variable separately,
- fit the growth curves to all growth variables simultaneously,
- undertake intra-specific comparisons of growth for different growth variables.

For the tern data, the objectives are the same as for gulls. In addition, we have to predict the age at the first catch for each tern chick followed from the running stage.

1.4 Outline of this thesis

Chapter 2 gives a detailed review on growth curves. It highlights the main differences between linear and non-linear growth curve models. Two categories of non-linear mixed effects growth curve models, namely concave and s-shaped growth curves, are reviewed. Some examples for each category are given. For s-shaped growth models, the impact of changing parameters on growth curves is assessed.

Chapter 3 describes the data sets that are analyzed in this study. It also provides a brief review of the non-linear mixed effects method that we use to model the growth data sets.

Chapter 4 presents a detailed application of non-linear mixed effects modelling to fit growth curves to Grey-headed Gull and Swift Tern data. It presents the optimization method used to predict ages of swift terns captured at running stage at the first catch. Also, the results of each method (univariate and multivariate modelling approach) for each data set are presented in this chapter.

Chapter 5 gives conclusions for the study and recommendations for possible areas of improvement.

Chapter 2

Growth curves

2.1 Introduction

Measurements of size of an individual or an object, or a population are often collected on several occasions in order to determine how fast is the growth or how the growth is influenced by various treatments or other covariate characteristics. The resulting data set is usually referred to as longitudinal data or is sometimes known as growth data (Seber and Wild, 1989). By merely looking at a growth data set it is invariably difficult if not impossible to describe the growth patterns embedded in the data and to understand their underlying mechanisms. Scholars suggest two types of methods to describe a data set (Mendenhall et al., 1996): graphical descriptive method and numerical descriptive method. Moreover, it is argued that a data set is easier described by a "picture" than "words"(Mendenhall et al., 1996). Seber and Wild (1989) define an empirical growth curve as a scatterplot of growth data taken on a individual or an object over time. If the random fluctuations are assumed to be non-present, the growth represented by this scatterplot is expected to follow a smooth curve, which is theoretically assumed to belong to a known family of curves $f(x, \phi)$ where ϕ is a vector of parameters to be estimated and x represents time (Seber and Wild, 1989). According to Narushin and Takma (2003), a model of a growth curve is an equation, which describes the increase and/or decrease of the size of a specific feature of an individual against time. Therefore, a growth curve may be viewed as a function that represents growth data. Growth curves are mainly divided into two categories as defined below.

Linear trajectory

A linear trajectory for an individual subject is a plot of a constant and systematic growth over time represented by a polynomial of degree one (Raudenbush and Bryk, 2002)

$$y_{ij} = \beta_{0i} + \beta_{1i} t_{ij} + \varepsilon_{ij},$$

where y_{ij} is the measurement taken on the i^{th} subject at the j^{th} occasion, β_{0j} is the intercept or expected outcome when $t_{ij} = 0$, it is also called initial status of the specified individual, and β_{1i} is the growth rate of the i^{th} individual.

Nonlinear trajectory

Nonlinear trajectories, also known as curvilinear growth trajectories, are curves of systematic growth over time represented either by a polynomial of degree p ($p > 1$) or a nonlinear model such as Gompertz, exponential, or logistic, for example. Nonlinear trajectories may be viewed as a succession of infinitely many piecewise linear growth curves where a curvilinear trajectory is broken up into many separate linear trajectories (Raudenbush and Bryk, 2002). A particular advantage of representing a nonlinear trajectory using piecewise linear growth trajectories is that piecewise linear functions enable the comparison of growth rates for different periods. However, this may not be easy to achieve especially when dealing with complex curves with many periods of interest and when selecting nodes (values at which growth rates change) (Tom and Roel, 2002). Therefore, this representation may lead to a cumbersome and impractical exercise.

2.2 Individual change over time

The graphical description of individual change over time is achieved by means of empirical growth plots, which are the graphs of raw measurements against time for each individual. Empirical growth plots are useful in detecting patterns of individual change over time; and evaluating these patterns for an individual relative to other population members. However, it becomes spatially impossible to display and compare a large number of plots. In this case, it has been proposed to randomly select a few number of individuals to be included in the exploratory analysis (Singer and Willett, 2003), and each individual empirical growth record should be summarized using a smooth trajectory fitted by using either a non-parametric approach or a parametric approach (Jacoby, 2000).

2.2.1 Nonparametric approach: Loess curve

The nonparametric approach to analyzing growth trajectory involves graphical methods of depicting relationships between variables whereby the data dictate the shape of smoothed trajectory without resorting to a specific functional form (Singer and Willett, 2003). The fitted smooth trajectories are superimposed on empirical growth records. Since they do not require any functional form, there are no conditions or assumptions imposed on them (Singer and Willett, 2003; Jacoby, 2000). The main objective of using a nonparametric approach is to assess visually the relationship or possible functional tendency between variables. Therefore, this approach is useful at the exploratory analysis stage. There exist many kinds of smoothing techniques such as kernel smoothing, moving average smoothing, spline smoothing, locally weighted scatter smoothing. In this section, we review briefly the most popular nonparametric smoothing method, the loess also known as a locally weighted scatter smoother "lowess" (Jacoby, 2000). The loess curve is a function of the parameters α and γ. α determines the proportion of the total data points to be considered in each local regression. In other words, this parameter is used to determine the size of the local regression window. γ is used to determine the degree of the local polynomial, which specifies the type of the local regression. It can only take on the values $\gamma = 1$ implying a linear equation, and $\gamma = 2$ for a quadratic equation.

Jacoby (2000) recommended that if the cloud of points conforms to a general monotone pattern (either increasing or decreasing), then γ should be given a value of 1 and if the cloud of points shows some non-monotone pattern with local minima or maxima then γ is set to be 2.
The choice of α is trickier as it assumes any value in the interval $[0, 1]$. The rule of thumb suggests that a typical α should fall in the interval $[0.4, 0.8]$ (Jacoby, 2000). Ideally, one prefers a loess curve that passes through the center of a cloud of empirical records. A right choice of α and γ leads to a loess curve that enables a general view about the pattern of change of a population from which the sample was drawn.

2.2.2 Parametric approach

Parametric methods for analyzing growth data assume a common functional form for all individuals. This approach generates numerical statistics, such as intercept, slope, and asymptotes, that can be useful to describe the underlying characteristics of growth. There exist many classes of parametric functions. These include polynomials, inverse polynomials, piecewise functions, spline functions, exponential curves, restricted growth curves, logistic curves, Gompertz curves, Richards equation, Weibull function, hyperbola functions, parabolic growth curve, Von Bertalanffy equation. Parametric functions have a vast range of applications in real life. The subsequent paragraph highlights some applications of these functions.

Polynomial growth curves are frequently used to estimate growth curves by socioscientists (Burchinal and Appelbaum, 1991). Logistic, exponential and Gompertz growth curves have been used successfully in ecological modeling (Gamito, 1998), for eample, growth of individual plants (Wiener et al., 1998), growth of a clonal eucalyptus plantation (Calegario et al., 2005), growth in Indian Barn-Owls (Nagarajan et al., 2002), wing and primary growth of the Wandering Albatross (Berrow et al., 2002), and modeling the influence of parental experience on the growth of Wandering Albatross (Benoit and Henri, 1990). The Von Bertalanffy' s growth curve is commonly used in biology (Gamito, 1998).

According to Gamito (1998), the logistic growth curve is perceived to be appropriate for a description of laboratory growth of organisms with simple life cycles. Logistic and Gompertz curves are also applied in time series forecasting (Philip, 1994).

Generally, these growth curves differ according to the parameters that describe their functional form. Firstly the challenge is to choose a good functional form that represents all individual trajectories. After the selection of a parametric model, another important point to consider is whether the empirical record really reflects changes or is simply the result of random fluctuations. The determination of the functional form is often based on an average change trajectory for all the individuals. Singer and Willett (2003) suggest two procedures to derive an average trajectory from individual growth trajectories:
The first method is known as *curve of averages*, in which the average outcome at each occasion is computed and then a curve through the obtained averages is plotted. The second method is called the *average of curves*. With this method, one needs to estimate the growth parameters for each individual trajectory, average them and use these averages to predict the curve. It is further recommended that, for an average trajectory to suggest a proper communal representation of individual change trajectories, it must satisfy the property of *dynamic consistency* (i.e. the following conditions should be satisfied: (1) the curve of averages and average of curves must be identical, (2) the average trajectory should have the same functional form as the individual trajectories).

Many authors, including Holmes (1983) and Ricklefs (1967), have developed various graphical procedures to identify a common functional form for different individual growth trajectories. Two major problems surface when graphical methods are used to infer about a common functional form: these methods are subject to subjectivity arising from performing an eye comparison of different curves; and they may not distinguish all the curves such as the logistic from Gompertz and the exponential from the logarithmic parabolic curve. As these methods do not provide a standard way of choosing an appropriate functional form, we will consider a combination of nonparametric methods (loess), previous knowledge, and analytical comparison

based on various statistics such as log-likelihood ratio, AIC and BIC in order to decide which form best fits our data set. To address the question whether individual growth records reflect real changes or whether they are simply results of random fluctuations, requires modeling both intra and inter-individual variation, which will be discussed in the next chapter.

A review of some examples of parametric functional forms is presented in sections 2.3 - 2.5.

2.3 Polynomial growth curve models

According to Burchinal and Appelbaum (1991), when the parametric family is unknown or unknowable, polynomial growth curves are used to approximate the true functional form. They provide good fits or good approximations if an appropriate order has been selected and if there are sufficient number of observations for each individual (Burchinal and Appelbaum, 1991). For n data points (t, y), one needs a polynomial of at most $n-1$ degree that interpolates these points. Mathematically, it is expressed as:

$$y = p(t) = a_0 + a_1 t + a_2 t^2 + \ldots + a_n t^{n-1} \tag{2.1}$$

The degree of a polynomial is determined by its highest power in the independent variable. If $n = 0$, then $p(t) = a_0$, which is just a constant. If $n = 1$, $p(t) = a_0 + a_1 t$. This is a linear trajectory (a straight line), with a_0 being the initial status at time zero and a_1 is the slope of the trajectory. If $n = 2$, then $p(t) = a_0 + a_1 t + a_2 t^2$. This represents a quadratic change trajectory. Where a_0, a_1, and a_2 are intercept, instantaneous rate of change, and curvature parameter respectively. If $n = 3$ then $p(t) = a_0 + a_1 t + a_2 t^2 + a_3 t^3$ is a cubic change trajectory. As the degree of the polynomial becomes higher the more difficult it is to interpret the growth parameters. Equation 2.1 is a polynomial interpolation of n data points. The choice of order of a polynomial is a trade-off between parsimony and accurately describing the complexity of the longitudinal change. It can be based on either testing the significance of parameter estimates, or alternatively, carry out a comparison of different models (i.e. polynomials of different degrees) by using statistics such as AIC and BIC across a series of models.

If all individual polynomial growth curves appear to be of the same order, the mean of estimated individual polynomial growth curves is the same as the estimated population polynomial growth curve since linear models are dynamically consistent. Thus, the mean estimated polynomial growth is used to interpolate the data points.

2.4 Piecewise linear functions

Piecewise linear functions are a flexible class of continuous functions with constant slopes between nodes (values of t at which growth rate changes), but these functions may be changing discontinuously between nodes (Tom and Roel, 2002). With piecewise linear growth models, two major drawbacks are inevitable: Piecewise linear growth models have angular appearances, and the choice of nodes is cumbersome as there are no existing methods to determine them (Tom and Roel, 2002). An individual growth curve can be defined as a linear combination of the basic piecewise linear functions, where a basic piecewise linear function is a polynomial of order one in interval (t_1,t_2) (i.e. it is a straight line within this interval) and is constant outside this interval. A basic piecewise linear function is defined as (Tom and Roel, 2002):

$$f(t) = \begin{cases} a & \text{if } t \leq t_1 \\ mt + c & \text{if } t_1 < t \leq t_2 \\ b & \text{if } t > t_2 \end{cases} \tag{2.2}$$

where a and b are constants, $m = \frac{b-a}{t_2-t_1}$ and $c = a - t_1\frac{b-a}{t_2-t_1}$ are gradient and intercept, respectively.

2.5 Non-linear growth curve models

We begin this section with the clarification of the concept "non-linear model", as opposed to "linear model". A model is said to be linear if it is linear in parameters, otherwise it is non-linear (Burchinal and Appelbaum, 1991). Ratkowsky (1990) explains further how to distinguish between a linear and a non-linear function by making use of the derivatives concept. Let $f(x, \phi)$ be a function of time x and the vector of parameters ϕ. f is said to be non-linear if at least one of its partial

derivatives with respect to elements of β is a function of at least one of the elements of ϕ, otherwise f is linear. From this definition it is clear that the non-linear concept is referring to parameters but not to the shape of the growth trajectory. Non-linear models are mechanistic models in that their parameters have physical meaning of the underlying process or the mechanism generating the data. These models are developed through mathematical constructions that are based on derivatives. They are therefore mechanistic models resulting from differential equations. Within the non-linear models family, some models can be transformed to a linear form. An example of this type is the proportional hazards model given by:

$$h(t) = h_0(t) \exp(\sum_{i=1}^{p} \beta_i x_i), \tag{2.3}$$

which is non-linear in parameters β_i. However, it is linearized by taking the logarithm of both sides:

$$\ln(h(t)) = ln(h_0(t)) + \sum_{i=1}^{p} \beta_i x_i \tag{2.4}$$

Other models cannot be directly transformed into a linear form in all parameters. These functions are known as "inherent non-linear models" (e.g. logistic, Gompertz, Richards equation). For linear models and transformable non-linear models, parameter estimates can be found using linear regression methods whereas for inherent non-linear models there is no closed form solution for parameter estimation. Non-linear parameter estimation requires iterative methods. Another important feature of distinguishing between linear and non-linear growth curves is that the former are dynamically consistent whereas the latter are not. Although parameter estimation for linear models is much easier than for non-linear models, and despite that linear growth models sometimes provide good approximation to non-linear growth models, there are good reasons why non-linear growth models may be preferred over linear models. For instance non-linear models provide a meaningful description of the underlying process through their parameters, non-linear models are better than linear models when extrapolating outside of the observed frame, and non-linear models give a parsimonious interpretation of the growth process compared to linear growth models in general and in particular to polynomial growth models (Pinheiro and Bates, 2000).

For the rest of this study, linear and non-linear will be referring to the concept of linearity or non-linearity in parameters. We now describe the most commonly used growth curves: exponential, Richards, logistic, and Gompertz. These may be classified into two types of structural forms, namely concave and sigmoidal shaped curves.

Concave growth curves are described by Ratkowsky (1990) as consisting of two categories of curves: convex and concave. Convex curves are curves whose second derivative is always greater than zero for all values of the explanatory variable and concave curves refer to curves whose second derivative is always less than zero for all values of the explanatory variable. Thus, a convex curve has only an upwards concavity whereas a concave curve has only a downwards concavity. From this definition, it follows that convex and concave curves have no points of inflection. Since these curves are distinguished by orientation of their concavities, it is preferable to adopt the term "concave" curves for convex and concave curves. This study focuses on exponential and inverse exponential as examples of concave curve.

Sigmoidal shaped curves are curves that have only one point of inflection but without maxima or minima (Ratkowsky, 1990). Therefore, the sigmoidal curve can be regarded as a curve with both upwards and downwards concavity with the change of concavity occurring at the inflection point. Thus, in some sense, a sigmoidal curve is considered as two concave curves of different concavities joined together at the inflection point. Sigmoidal curves can be either descending or ascending. In this study we explore only the most commonly used sigmoidal curves: Richards, logistic and Gompertz curves.

The number of parameters in both concave and sigmoidal growth curves can be as many as the data set permits, however, it is desirable to have fewer parameters in the model unless it is proven that more parameters are needed. Ratkowsky (1990) argues that when a model with more than three parameters is used to fit a concave curve, it is seldom parsimonious. It generally results in over-parameterization, which may cause convergence problems. To circumvent the estimation problems, one needs to resort to a re-parameterization process. This means that the parameters that are responsible for a non-linear behaviour are replaced by new ones that are functions

of the old parameters (Ratkowsky, 1990).

2.5.1 Concave growth curves

Under this section, we will discuss only the exponential growth curve. According to Gamito (1998), the growth rate (β) of any quantity changing exponentially is expressed as follows:

$$\beta = \frac{\ln(y_t) - \ln(\gamma)}{t} \tag{2.5}$$

Where y_t is the quantity at t and γ is the initial quantity at time $t = 0$. Through algebraic manipulation, the changing quantity can be expressed as a function of the initial value and time as follows:

$$y_t = \gamma \exp(\beta t) \tag{2.6}$$

The exponential growth curve is shown in Figure 2.1. The exponential growth model is known for its special property, "doubling times", which entails that the initial quantity doubles at doubling times and continues to double over and over again at these times.

Calculating the doubling time:

The doubling time is the time at which the growing quantity has reached twice of its initial value. This can be found as follows: $2\gamma = \gamma \exp(\beta t)$.
Solving for t, we get: $t = \frac{\ln 2}{\beta}$.
Although exponential growth is moderate initially, it increases rapidly as consequence of the doubling time effect. Gamito (1998), while modeling growth of a fish population, concluded that exponential growth curves provided a meaningful fit but recommended that exponential growth curves should not be used to model growth over extended time periods. Many other authors, among others, Sterman (2000), stressed that "in the real world nothing can grow indefinitely". Therefore, there is a need for other growth models that take into consideration stages where the growth starts leveling off before it eventually reaches its maximum. Most of these models belong to the category of s-shaped growth models also known as sigmoidal models.

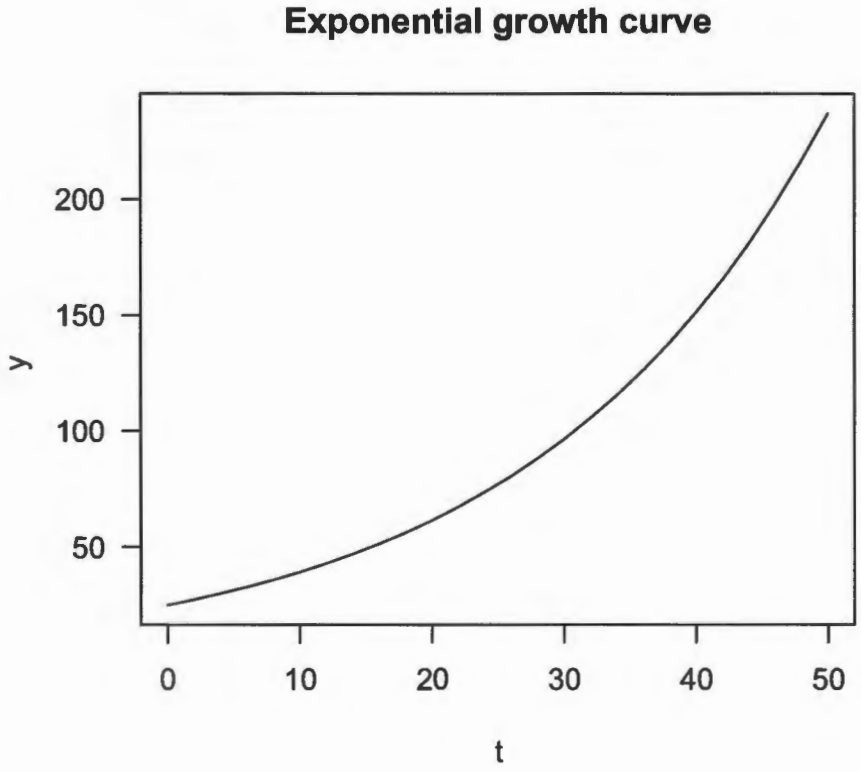

Figure 2.1: An example of a hypothetical exponential growth curve with parameters $\gamma = 25$ and a constant growth rate $\beta = 0.045$.

Before we discuss the s-shaped growth curves, let us just mention a special case of the exponential, which includes a ceiling beyond which the curve cannot rise. This model is called inverse exponential (Gamito, 1998) and is given by:

$$y_t = \alpha - (\alpha - \gamma)\exp(-\beta t) \tag{2.7}$$

Where y_t denotes the value of y at time t, α is the ceiling quantity (maximum), γ is the initial value of y at $t = 0$, and β is the growth rate. Note that y_t can be any quantity (e.g. length, size of a population). This model is believed to be appropriate for situations where the growth rate decreases to zero as the quantity increases up to its upper limit (Gamito, 1998), and is also called the *restricted growth curve.* Figure 2.2 depicts an example of an inverse exponential growth curve.

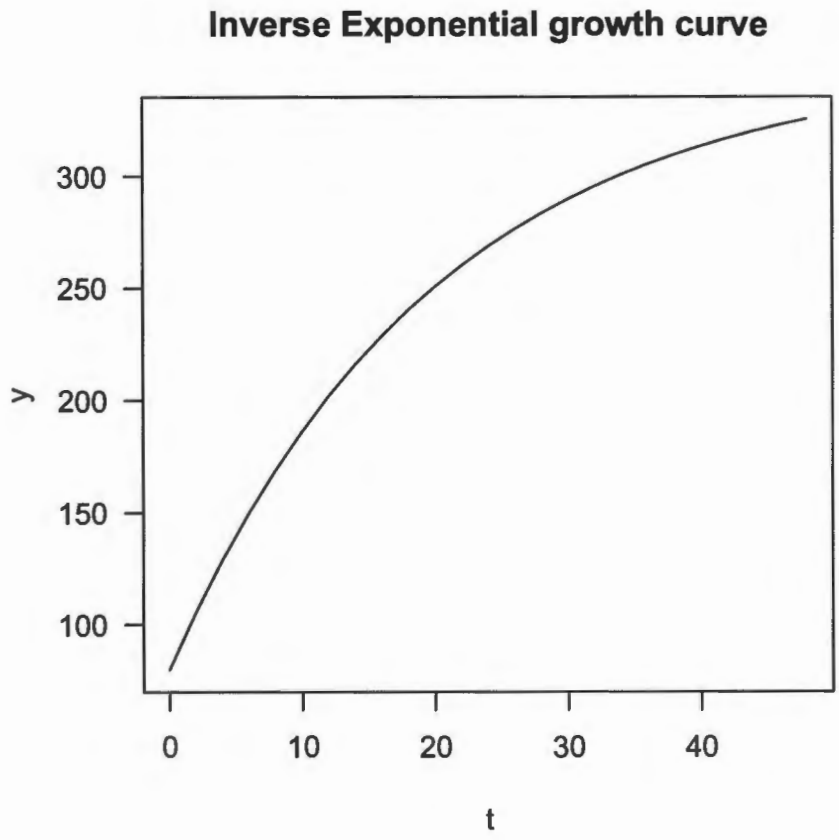

Figure 2.2: A theoretical example of an inverse exponential growth curve with fixed parameters $\alpha = 350$, $\gamma = 20$ and $\beta = 0.025$

2.5.2 S-shaped or Sigmoidal Growth Curves

"Everything that rises must converge" (Sterman, 2000). As no quantity can grow for ever, its growth rate declines until it reaches zero at some point in time due to diverse limiting factors such as competition within the population or other natural factors. In such situations, it is common to observe that the growth phenomena have the following chronological patterns: a gradual increase of the growth rate from the beginning until the point of inflection is reached, and thereafter the growth rate decreases until the maximum quantity is reached (upper asymptote) (Kumar, 1998; Ratkowsky, 1983).

These patterns are graphically represented by an s-shaped growth curve known as sigmoidal growth curve. Some s-shaped growth curves, such as the logistic growth curve, hypothesize that the instantaneous growth changes linearly in the population while others like Gompertz and Richards growth curves assume non-linearity of the instantaneous growth rate. In sections (2.5.2.1-2.5.2.3) we review Richards, logistic and Gompertz models. We also assess the impact of changing parameters on the growth curve for each of these models.

2.5.2.1 Richards growth curves

Mathematically, Richards growth curve is expressed as follows:

$$y = \frac{\alpha}{(1 + \exp(\beta - \mu t))^{\frac{1}{\delta}}} \tag{2.8}$$

where α is an upper asymptote, β and μ are growth parameters, and δ is the shape parameter. Like any other s-shaped growth curve, Richards growth curve has two concavities which change at the point of inflection. It has also two asymptotes, lower and upper asymptote. From Richards growth model, two three-parameter models, logistic and Gompertz, can be derived by letting $\delta = 1$ and δ approaches zero, respectively. It is generally believed that at least two of Richards growth parameters have poor statistical properties (poor estimation properties). For this reason Ratkowsky (1990) does not encourage the use of this model. A Richards growth curve is shown in Figure 2.3. We have simulated Richards growth model with different values of parameters in order to assess the effect of changing parameters on its form. The following was observed: Figure 2.4 (a) indicates that as δ, the shape parameter, changes the shape of the curve changes as well. For very small δ, the growth curve tends to be asymmetric. The change of δ impacts on both the initial and later part of the growth. It is noted that for $\delta = 1$ Richards curve becomes a logistic curve and for δ close to zero Richards model changes to a Gompertz curve. As the growth parameter μ increases the upper asymptote is reached in shorter time. For instance, if $\mu = 0.95$ the growth reaches the peak near t= 18 whereas when $\mu = 0.45$ the peak growth is reached near $t = 35$. This indicates that an increase in μ accelerates the growth rate.

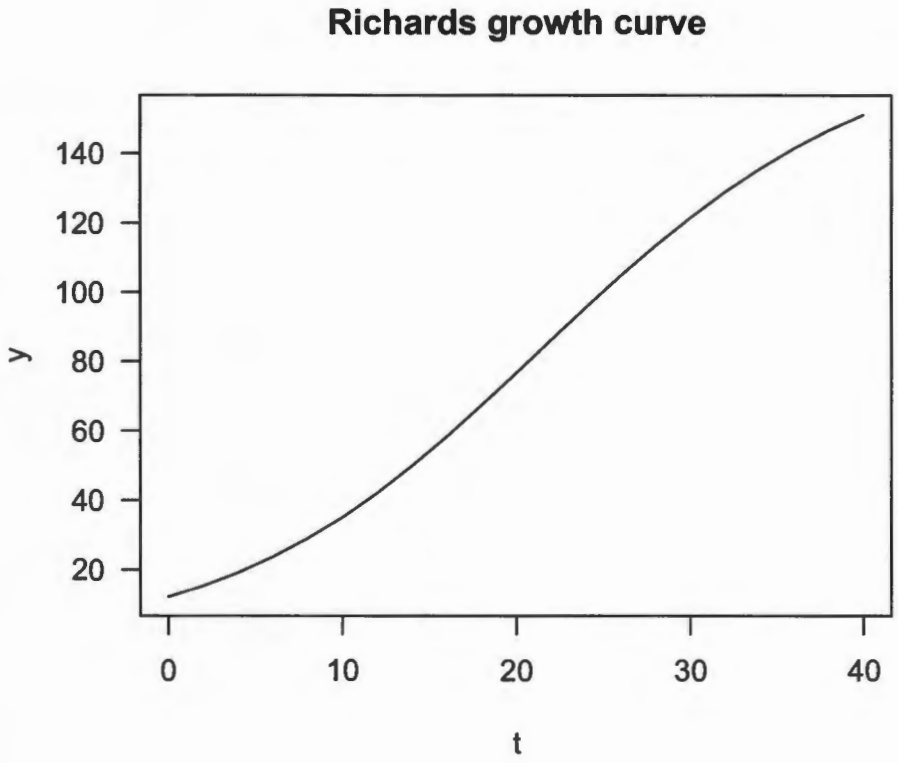

Figure 2.3: An example of a theoretical Richards growth curve, with parameters $\alpha = 175$, $\mu = 0.010$, $\delta = 0.75$, and $\beta = 1.85$.

From Figure 2.4(c), it can be observed that initial growth rate decreases as the value of β (growth parameter) increases. In the interval of $[t = 0, t = 20]$, if $\beta = 12$, y changes from approximately 20 to about 100; but if $\beta = 14$, y changes from 20 to 70. From this observation, it may be concluded that β and μ govern the growth. Figure 2.4 (d) shows that changing α affect the shape and the growth rates. It is noted that larger α leads to steeper curves, which implies higher maximum value of the curve and a larger grow rate.

2.5.2.2 Logistic growth curves

The logistic growth curve, also called the Verhulst growth curve, was named after Francois Pierre Verhulst who, in 1938, derived the logistic equation to describe the

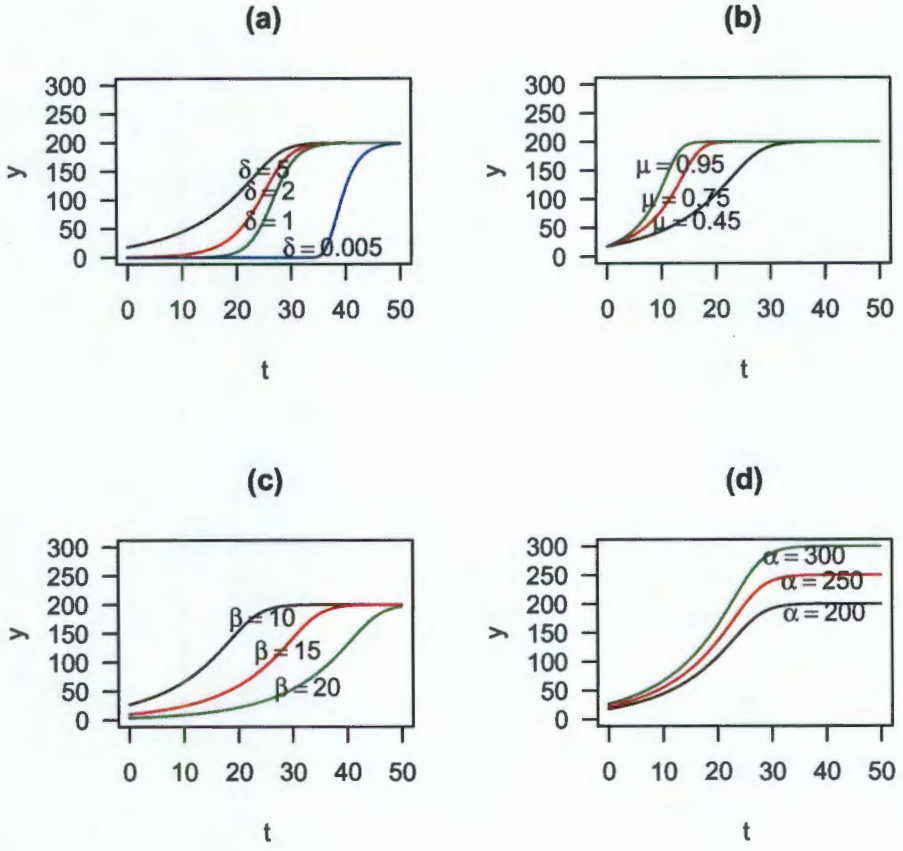

Figure 2.4: Richards growth curves with changing (a) δ (shape-parameter), (b) μ (growth parameter), (c) β (growth parameter), and α (asymptote)

self-limiting growth of a biological population. This equation describes a growth that increases exponentially at the beginning and the middle of the growth and slows down to level off at the asymptotic value after some time (Weisstein, 1999). One of the parameterizations of the logistic growth model, commonly used, is:

$$y_t = \gamma + \frac{\alpha}{1 + \exp(-\frac{t-\mu}{\beta})} \tag{2.9}$$

where γ and α are the lower and upper asymptotes, respectively, β is the time elapsed between the quantity reaching half and approximately $\frac{3}{4}$ of the upper asymptote (it is also known as scale parameter) and μ is the time at which the quantity reaches half of its asymptotic value. Figure 2.5 depicts a logistic growth curve.

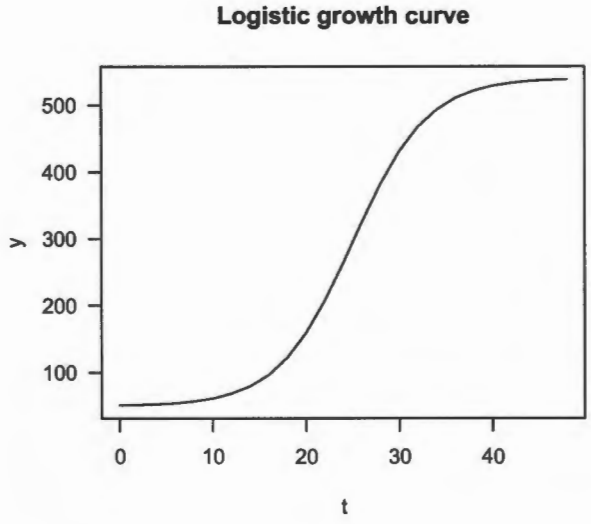

Figure 2.5: An example of a theoretical logistic growth curve, with lower and upper asymptotes $\gamma = 50$ and $\alpha = 490$, and growth parameters $\mu = 25$ and $\beta = 0.25$.

The logistic growth curve assumes that the instantaneous growth rate declines linearly in the population. To relax this restrictive assumption, other s-shape growth models, generally not symmetric, are suggested (Sterman, 2000). These include Richards, Gompertz and Weibull growth models. In the following paragraph, we assess the impact of changing parameters on the logistic growth curve.

When the α (asymptote) and μ (time to half of the asymptotic growth) parameters are kept constant and the parameter β (estimated time to grow from half of asymptote to three quarters of asymptote) takes on different values, the growth curves change. For small values of β the curve becomes steeper compared to curves with large values. When the α and β parameters are kept constant and μ, the time it takes to grow up to $\frac{1}{2}$ of upper asymptote, is allowed to change, the shape of the curves change in the interval of $t = 0$ and the t-value corresponding to $\frac{1}{2}$ of the asymptote. In this interval, changing μ affects the initial steepness of the curve. It may be concluded that the change of μ affects the growth rate. α is the upper asymptote and hence changing α affects the maximum value of the growth and the growth rates.

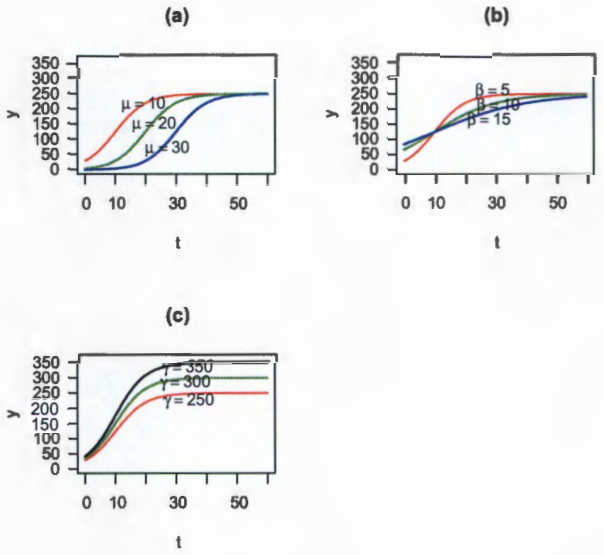

Figure 2.6: Logistic growth curves with changing (a) estimate of time to half of asymptote (μ), (b) estimate of time from half to three quarters of asymptotes (β) and (c) asymptote (α).

2.5.2.3 Gompertz growth curves

The Gompertz growth model named after Bejamin Gompertz who, in 1825, published a paper "on the nature of the function expressive of the law of mortality", is defined as:

$$y_t = \gamma \exp(\beta(1 - \exp(-\mu t))) \tag{2.10}$$

where γ is the theoretical value of y at $t = 0$ (lower asymptote), β is the initial instantaneous growth rate, and μ is the rate at which the growth rate β decreases. This growth curve was long used mostly in actuarial sciences to determine the number of humans surviving up to any age (Winsor, 1932; Olshansky and Bruce, 1997), but now is used in other fields to model growth for biological and economic phenomena. The Gompertz growth curve is often presented as a 3-parameter equation that describes a sigmoidal growth processes. However, it has various parameterizations. The Gompertz growth curve is characterized mainly by the following features: it is non-symmetric which means that it may assume shorter increasing growth rate

period than decreasing growth rate period or vice versa (Philip, 1994); and it has a point of inflection, one or two asymptotes, and a growth rate which is always positive. A Gompertz curve is depicted in Figure 2.7 and Figure 2.8 illustrates the impact of changing parameters on Gompertz growth curve.

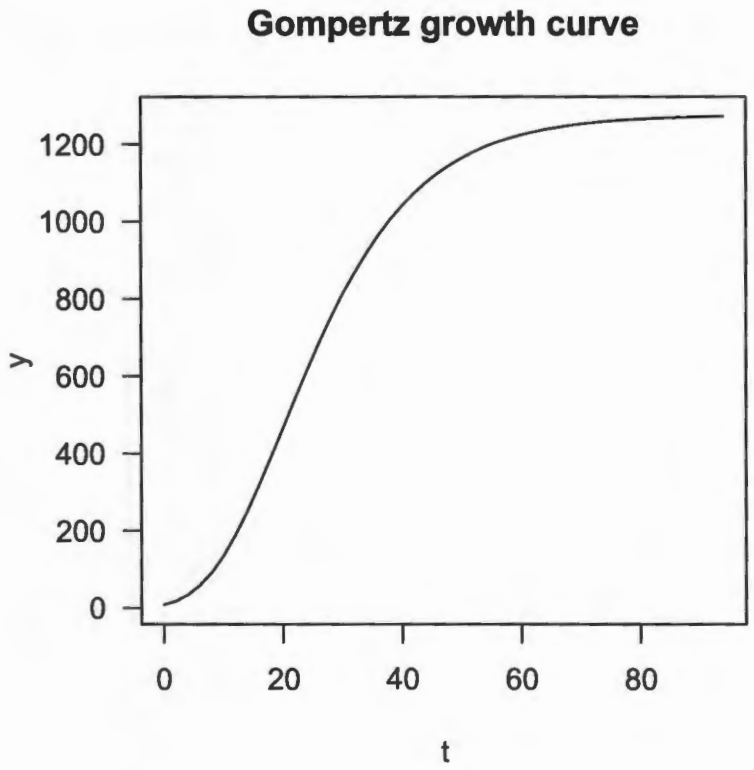

Figure 2.7: An example of a hypothetical Gompertz growth curve with a lower asymptote $\gamma = 50$, and growth rates $\beta = 3.35$ and $\mu = 0.08$.

Figure 2.8 (a) indicates that when the growth rate μ increases while other parameters remain constant the asymptote increases as well. Although bigger values of μ correspond to bigger asymptotes, it takes exactly equal time to reach the asymptotes. This implies that the time to reach the asymptote is the same for all μ.
If the rate β is increased while the other parameters are kept constant the time it takes to reach the asymptote is shortened.

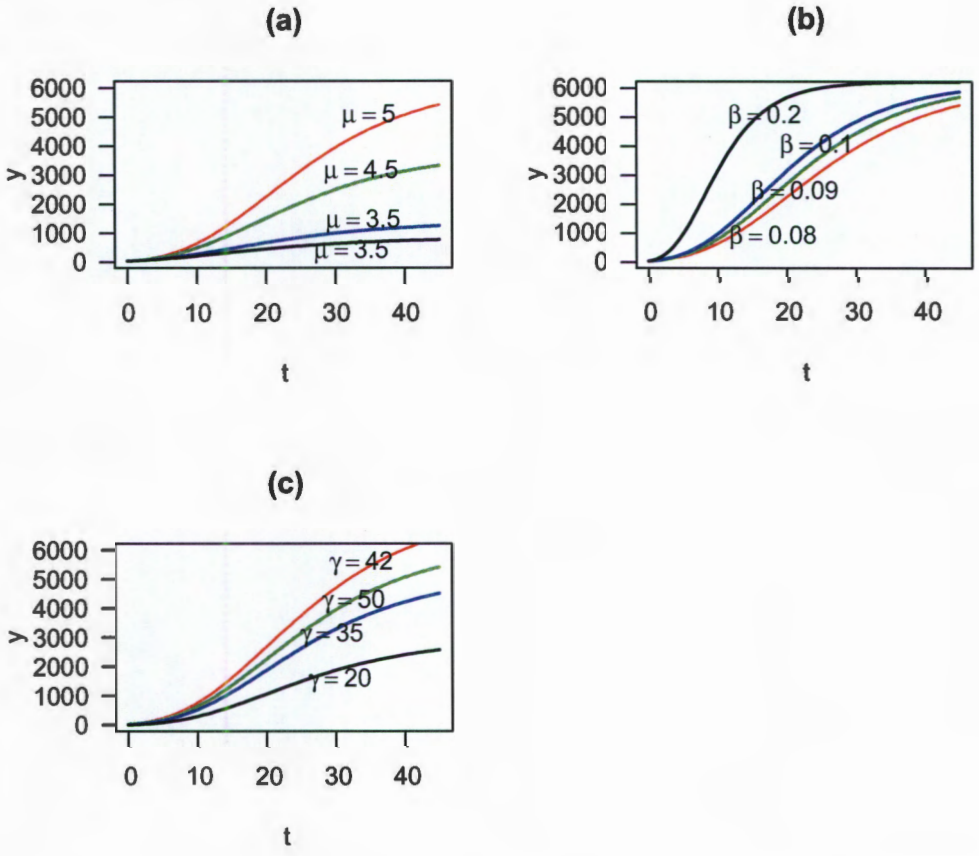

Figure 2.8: Gompertz growth curves with changing (a) initial instantaneous growth rate (β), (b) growth rate (μ) at which β decreases, and initial value at time $t = 0$ (γ).

For example, from Figure 2.8 (b), if $\mu = 0.2$ the growth reaches the asymptote at $t = 30$ while if $\mu = 0.08$ the growth still has to reach the asymptote after $t = 40$. Therefore, the change of the μ parameter affects the growth rate, which is what is expected by defiriti on. By inspecting Figure 2.8 (c), it can be noted that as the value of γ (initial value) increases the upper asymptote becomes higher. Note that the initial values are not clearly distinguished due to the scale.

2.5.2.4 Comparison of logistic and Gompertz growth curves

Due to the simplicity and the physical interpretation of logistic and Gompertz parameter estimates, these two growth curve models are most commonly used among sigmoidal growth processes. The logistic growth model is symmetric about the point of inflection whereas the Gompertz curve is non-symmetric. Both logistic and Gompertz growth curves have one point of inflection but with different locations as the former is symmetric and the latter is non-symmetric. They both have one or two asymptotes. Although, theoretically, both the logistic and Gompertz curve are not dynamically consistent, in practice the sum or average of several logistic or Gompertz curves can be approximated by another logistic or Gompertz (Winsor, 1932). It is argued that not many growth processes satisfy the logistic growth rate symmetry property whereas the feature of non-symmetry may be well satisfied in some growth processes (Vieira and Hoffmann, 1977). A summary of some of the mathematical properties that shows the parallelism between these two growth models is shown in Table 2.1. This table is adopted from (Winsor, 1932; Ricklefs, 1967; Vieira and Hoffmann, 1977).

Table 2.1: Mathematical properties of Gompertz and Logistic curves pointing out some of their commonalities.

Property	Gompertz	Logistic
Equation	$\gamma \exp(\beta(1-\exp(-\mu t)))$	$\gamma + \frac{\alpha}{1+\exp(-\frac{t-\mu}{\beta})}$
No. of parameters	3	4
Asymptotes	$\gamma(lower)$*	$\gamma(lower), \alpha(upper)$
Inflection	$\frac{1}{e}$	$\frac{1}{2}$
Symmetric	Asymmetrical	Symmetrical about inflection
Dynamically consistent	No	No

* there are alternative parameterizations of Gompertz curve with upper asymptotes.

Chapter 3

Data and Methodology

3.1 Data

3.1.1 Swift tern (*Sterna bergii*)

The swift tern (*Sterna bergii*), also known as greater crested tern, is a nomadic seabird species dispersed around the southern African coastlines (Namibia, Angola, South Africa and Mozambique) (Cooper et al., 1990; Hockey et al., 2005). It has an incubation period of about 28 days and chicks remain in the nests for about two to four days after hatching (Le Roux, 2006). Swift terns feed mainly on fish captured by plunge-diving into waters (Hockey et al., 2005). The data set used in this study was supplied by the Avian Demography Unit (Department of Statistical Sciences, University of Cape Town). It consists of measurements of body mass (grams), wing length (mm), foot length (mm), head length (mm) and culmen length (mm) taken on several unequally spaced occasions during the period of May to July 2001. Chicks were not all measured from day of hatching. Thus, the time or occasion of measurement is not equivalent to age. From a sample of 253 chicks only 34 chicks were followed from nestling stage, others were first captured when they were already runners. With this available information, growth curves cannot directly be fitted to body features without estimating the true ages at first capture of all birds handled at runner stage. Thus, one important aspect of this thesis is the age determination of chicks followed from when they were already runners. This problem is addressed in chapter 4.

3.1.2 Grey-headed gull (*Larus cirrocephalus*)

Gulls are a multi-ethnic group with about 50 extant species related to terns, skuas and jaegers, and skimmers (McIntyre, 2006). The group of interest for this study is the grey-headed gull, which comprises two subspecies namely *Larus c. cirrocephalus* found in South America and *Larus c. Poiocephalus* from Africa (McIntyre, 2006). In Africa, grey-headed gulls are mostly found at wetlands both inland and the coast (Brooke, 1997; Brooke et al., 1999). They are believed to have expanded along range in South Africa during the 20^{th} century, the first known breeding locality was at Broedenhurst Pan in the Northern Cape (Brooke et al., 1999). The data set on grey-headed gulls comes from the Avian Demography Unit (Department of Statistical Sciences, University of Cape Town). This data set contains growth information for grey-headed gulls breeding at Bonaero Park and Modderfontein Pan located in Gauteng (South Africa). The measurements collected from each chick were chick mass (grams), wing length (mm), culmen (bill) length measured with dial callipers to the nearest 0.1 mm, head length measured to the nearest mm, tarsus length measured to the nearest 0.1 mm, foot length measured to the nearest mm, and age measured in days. These measurements were taken on several irregular spaced occasions between 13 May and 15 July 2005 every two to five days. The sample includes 190 birds, of which 114 were from Bonaero Park and 76 from Modderfontein Pan.

To avoid estimation problems, for both Grey-headed Gull and Swift Tern data, only chicks that were caught on at least four occasions were included in the data analysis.

3.2 Methodology: Non-linear mixed effects modelling

For repeated measurements, every individual is observed at several occasions. Such data can be viewed as having a two-level hierarchical structure where level-one is the repeated observations over time nested in level two that refers to the individuals (Raudenbush and Bryk, 2002). Non-linear mixed effects models for repeated measurements are viewed as a hierarchical model where each level of the hierarchical data is represented by its own submodel. The first stage of a hierarchical non-linear model known as the intra-individual variability model intends to describe the pattern of change of measurements over occasions within an individual. It involves choosing a functional form to describe the pattern of growth over time. This pattern is often "non-linear". At the second stage, the aim is to try to give an account for inter-individual variation among the parameter estimates and often involves incorporation of covariates that describe individual-specific characteristics. The parameters that describe the functional form of the model are *fixed* effects. The parameters that refer to inter-individual variability are *random* effects, hence the term *mixed effects* modelling.

3.2.1 Non-linear mixed effects modelling for a single response variable

A basic non-linear model for a single response variable is defined as follows (Davidian and Giltinan, 1995) :

Stage 1: Intra-individual variation

Assume y_{ij}, the j^{th} response for individual i taken at occasion x_{ij} $(i = 1, 2, \ldots, N;$ $j = 1, 2, \ldots, n_i)$ follows a non-linear model. Then the relationship between y_{ij} and x_{ij} can be modelled as

$$y_{ij} = f(x_{ij}, \phi_i) + \varepsilon_{ij} \tag{3.1}$$

where ϕ_i is a $p \times 1$ vector of parameters defining the specific structural form of the relationship for individual i and ε_{ij} represents the random variation of response

within individual i. n_i is the number of observations for individual i and N is the number of individuals. f is a non-linear functional form characterizing the relationship between y_{ij} and x_{ij}. For instance if the relationship between y_{ij} and x_{ij} is described by a logistic structural form expressed as $y_{ij} = \frac{\alpha_i}{1+\exp(-\frac{x_{ij}-\mu_i}{\beta_i})} + \varepsilon_{ij}$, the vector of parameters is $\boldsymbol{\phi_i} = \begin{bmatrix} \alpha_i \\ \mu_i \\ \beta_i \end{bmatrix}$, where α_i is the upper asymptote, μ_i is the estimate of time to grow to half of the asymptote , and β_i is the estimate of time to grow from half to three quarters of the asymptote for individual i. The within individual errors, ε_{ij}, may be heterogeneous and correlated. Individuals may have a common intra-individual variance structure that can be modelled using a variance function $G(\boldsymbol{\phi_i}, \boldsymbol{\theta})$ with $\boldsymbol{\theta}$ representing parameters of this variance function. The following are examples of intra-individual variance functions: A constant variance function for all individuals ($var(\varepsilon_{ij}) = \sigma^2$), a variance function in which the variance increases linearly with fitted values ($var(\varepsilon_{ij}) = \sigma^2|\mu_{ij}|^{2\delta}$), and a variance function with different variances that increase as power function of fitted values for each body feature k ($k = 1, 2, \ldots, 6$) ($var(\varepsilon_{ij}) = \sigma^2|\mu_{ij}|^{2\delta_k}$). Similarly, the correlation of within individual errors can be represented by a function $\Gamma(\alpha)$. The correlation function $\Gamma(\alpha)$ may assume various forms such a compound symmetry, a first order autoregressive function (AR1), and a moving average function (MAR). Quite often, the ε_{ij} may be heterogeneous and at the same time correlated. Thus, this leads to the following specification of the variance-covariance structure for intra-individual variation as described by Davidian and Giltinan (1995) :

$$Cov(\boldsymbol{\varepsilon_{ij}}|\boldsymbol{\phi_i}) = \sigma^2 G^{\frac{1}{2}}(\boldsymbol{\phi_i}, \boldsymbol{\theta}) \Gamma(\alpha) G^{\frac{1}{2}}(\boldsymbol{\phi_i}, \boldsymbol{\theta}) = \boldsymbol{R_i}(\boldsymbol{\phi_i}, \xi), \boldsymbol{\xi} = (\sigma, \boldsymbol{\theta}, \alpha) \tag{3.2}$$

where $G^{\frac{1}{2}}(\boldsymbol{\phi_i}, \boldsymbol{\theta})$ is an $n_i \times n_i$ diagonal matrix representing the intra-individual variance and $\Gamma(\alpha)$ is correlation matrix describing the correlation patterns of measurements for the i^{th} individual.

The description of the first stage can then be summarized as follows:

$$\boldsymbol{y_i} = f_i(\boldsymbol{\phi_i}) + \boldsymbol{\varepsilon_i}, (\boldsymbol{\varepsilon_i}|\boldsymbol{\phi_i}) \sim \left(0, \boldsymbol{R_i}(\boldsymbol{\phi_i}, \boldsymbol{\xi})\right) \tag{3.3}$$

where $\boldsymbol{y_i}$ is a $n_i \times 1$ vector of responses for individual i, $\boldsymbol{\varepsilon_i}$ is a $n_i \times 1$ vector of errors for individual i,

and $f_i(\phi_i)$= $\begin{bmatrix} f(x_{i1}, \phi_i) \\ f(x_{i2}, \phi_i) \\ \vdots \\ f(x_{in_i}, \phi_i) \end{bmatrix}$.

Stage 2: Inter-individual variation

Variability among different individuals is manifested by the variation of individual specific regression parameters ϕ_i. This variation may be due to systematic dependence on individual characteristic and /or may be due to random variation in a population of individuals. The between-subject variability is modeled by expressing ϕ_i as a function of covariate values and/ or random variation.

For our example of the logistic model in stage 1 we have three parameters and hence three functions. We also assume that the between-subject variability may be explained by the difference in covariate site for gull data and some random variation for each parameter. Therefore, the three functions are expressed as follows:

$\alpha_i = \alpha_{00} + \alpha_{01} \times \text{site} + \text{b}_{0i}$

$\mu_i = \alpha_{10} + \alpha_{11} \times \text{site} + \text{b}_{1i}$

$\beta_i = \alpha_{20} + \alpha_{21} \times \text{site} + \text{b}_{2i}$.

In general,

$$\phi_i = d(a_i, \alpha, b_i), b_i \sim (0, D) \tag{3.4}$$

where ϕ_i is a vector of regression parameters for individual i, b_i is a vector of random effects associated with i^{th} individual, α is a vector of fixed effects and a_i is a vector of covariates characterizing the i^{th} individual (e.g for this case a_i = site variable). d is a p-dimensional vector valued function and for each element of ϕ_i may correspond to a different functional form and D is a variance-covariance matrix of random effects.

3.2.2 Multivariate non-linear mixed effects modelling

In situations where measurements on more than one response growth variable are collected repeatedly for each subject, modelling jointly all the response variables is an alternative method of fitting growth curves instead of fitting a separate model for each response variable. Multivariate non-linear mixed effects modelling is an extension of the univariate non-linear mixed effects modelling (Davidian and Giltinan, 1995). The model formulation given below, follows the formulation of multivariate non-linear mixed effects models presented by Davidian and Giltinan (1995), and Hall and Clutter (2004).

Let y_{rij} denote response r for individual i taken at occasion x_{rij} with $i = 1, 2, \ldots, n_{ri}$ (n_{ri}= number of individuals measured for response r),
$j = 1, 2, \ldots, n_{rj}$ (n_{rj}=number of observations on individual i for response r), and $r = 1, 2, \ldots, R$ (R=number of responses).
Let us combine repeated observations for each individual i, relating to a specific response r, into a $n_{ri} \times 1$ vector $\boldsymbol{y_{ri}} = (y_{ri1}, y_{ri2}, \ldots, y_{rin_{rj}})'$ and further concatenate all vectors relating to all observations for R response variables for each individual in $n_i \times 1$ vector, $\boldsymbol{y_i} = (\boldsymbol{y_{1i}}, \boldsymbol{y_{2i}}, \ldots, \boldsymbol{y_{Ri}})'$, where $n_i = \sum_i^R n_{rj}$ is the number of measurements for individual i over all responses at all occasions. Similarly we form a vector of occasions x_i. Then the relationship of each response to the occasions can be modeled by a structural function

$$\boldsymbol{y_i} = f_d(\boldsymbol{x_i}, \boldsymbol{\phi_i}) + \boldsymbol{\varepsilon_i}, \boldsymbol{\varepsilon_i}|\boldsymbol{\phi_i} \sim \big(0, \boldsymbol{R_i}(\boldsymbol{\phi_i}, \boldsymbol{\xi})\big) \tag{3.5}$$

where $\boldsymbol{\phi_i}$ is a vector of all the parameters used in the d functional forms for individual i , $\boldsymbol{\varepsilon_i}$ is a vector of within-individual errors, and $\boldsymbol{\xi}$ is a combined vector of within-subject covariance parameters.

Let $\boldsymbol{a_i}$ be a vector of individual specific attributes or covariates and $\boldsymbol{\alpha}$ be a combined vector of fixed effects. Then stage 2 is expressed as

$$\boldsymbol{\phi_i} = d\big(\boldsymbol{a_i}, \boldsymbol{\alpha}, \boldsymbol{b_i}\big), \boldsymbol{b_i} \sim (0, \boldsymbol{D}) \tag{3.6}$$

where d includes separate models d_k for each response , $\boldsymbol{b_i} = (b_{1i}, b_{2i}, \ldots, b_{ri})'$ and $\boldsymbol{D}$ is the joint covariance matrix for all random effects, which accounts for correlations among the individual specific regression parameters for r different response variables.

An alternative approach that is very simple in that it uses existing univariate modelling techniques and that is applicable when responses follow the same structural model, is to simply distinguish measurements from different response variables by adding a categorical response covariate to the model. So for K responses, we define a k-level factor variable that indicates the specific response that generated each measurement. This is incorporated into the model using dummy variables that compare measurements from K-1 responses to measurements from the chosen reference/baseline response. The model formulation becomes:

$$\boldsymbol{y_i} = f(\boldsymbol{x_{ki}}, \boldsymbol{\phi_i}) + \boldsymbol{\varepsilon_i}, \boldsymbol{\varepsilon_i}|\boldsymbol{\phi_i} \sim \left(0, R_i(\boldsymbol{\phi_i}, \boldsymbol{\xi})\right) \tag{3.7}$$

where $\boldsymbol{\phi_i} = (\phi_{i1}, \phi_{i2}, \ldots, \phi_{ip})$, is a p $\times$ 1 vector of parameters to estimate, and
$\phi_{i1} = \phi_1 + \sum_{k=2}^{K} \tau_k \phi_{1k} + b_{1i}$,
$\phi_{i2} = \phi_2 + \sum_{k=2}^{K} \tau_k \phi_{2k} + b_{2i}$,
$\vdots$
$\phi_{ip} = \phi_p + \sum_{k=2}^{K} \tau_k \phi_{pk} + b_{pi}$,
τ_k is an indicator variable equal to one if response variable equals k, zero else (except for $k = 1$ where $\tau_k = 0$), ϕ_{pk} are differences in parameter values compared to parameter values of baseline response (response variable 1), and b_{pi} is a random effect associated with parameter p for individual i. We thus use a univariate model to solve a multivariate problem. We, however, continue to refer to it as a "multivariate" model to distinguish it from the separate fits. In section 4.3.1, we illustrate this approach using the logistic model (equation 4.6).

3.2.3 Parameter estimation

Under this section, we highlight estimation methods used when sufficient data are available for almost every individual and when dealing with sparse data. For situations where sufficient data are available, Davidian and Giltinan (1995) and Singer and Willett (2003) suggest that the generalized least squares (GLS) method, which is a generalization of the ordinary least squares method (OLS), should be used for estimation. This method relaxes the assumptions of independent and constant variation of residuals assumed for OLS, by allowing autocorrelated and heteroscedastic residuals.

For sparse data, reliable individual specific regression parameters, which constitute the building blocks for further inference, cannot be obtained for most individuals. This renders the estimation method based on GLS inapplicable. For such situations, methods based on linearization of the hierarchical nonlinear model are recommended in order to achieve the estimation of ϕ_i, ξ and D. There exist two types of linear approximation methods, namely: first order linear approximation, which bases the inferences on the joint maximum likelihood and generalized least squares methods; and a conditional first-order linear approximation method considered as a refined linearization in that it takes into account the inter-individual variability (Davidian and Giltinan, 1995).

Estimation procedures for a nonlinear function are iterative and require starting values so that the convergence may be achieved. For estimation of ϕ_i, OLS or nls (non-linear least squares) estimators are used as starting values and the identity matrix can be used as a starting value for estimation of D (Davidian and Giltinan, 1995). Despite a right choice of starting values, estimation procedures do not always converge. Convergence problems may be caused by overparameterization or presence of one or more parameters that prevent the model from exhibiting a close-to linear behaviour (Ratkowsky, 1990). Reparameterization, which is a process of substituting the parameters that are responsible for the non-linearity behaviour by new ones that are functions of only the old parameters, is thought as one way to overcome the convergence problems (Ratkowsky, 1990). The issue of parameterization is not easy to tackle in that it is not straight forward to detect which parameters are responsible

for the non-linearity behaviour; and even if these parameters are known it may not be known which transformations are suitable. Exploratory tools such as the use of histograms to detect parameters that cause non-linearity, and some transformations (e.g. exponential, power transformations, logarithm and expected-value parameter) were suggested by Ratkowsky (1990).

We used the nlme procedure in R to fit the non-linear mixed effects models to our data (R Development Core Team, 2006).

Chapter 4

Application of non-linear mixed effects models: Chick growth curves in Grey-headed Gulls and Swift Terns

4.1 Introduction

In this chapter we will fit univariate and multivariate models to the growth body features in the two data sets. This will involve firstly choosing some structural forms for the models, after which we will iteratively use the last four main steps, described by (Pinheiro and Bates, 2000), to build hierarchical non-linear mixed effects models. The best model will be selected based on the AIC statistic.

Choosing the appropriate structural form of the model

Choosing models is partly determined by mechanistic criteria (i.e. the mechanism of the process that has yielded the data). Looking at the empirical data plots is helpful in narrowing the choice of structural form. Several different structural forms can be fitted to data and then can be compared using Akaike's information criterion (AIC). Empirical data plots (Figure 4.1) suggested that s-shaped curves and concave growth curves were applicable to our data.

Four growth models, logistic, Gompertz, Richards, and inverse exponential were fitted to the two data sets (Grey-headed Gull data and Swift Tern data). In fitting these models, we used non-linear mixed effects modelling. A detailed model building process is shown for the logistic growth model fitted to body mass whereas only the final model is shown for other features and growth curves. The choice of the best growth model was done based on likelihood ratio tests and Akaike information criterion (AIC).

Choosing the random effects to be included in the model

This may be achieved by either using the plot of confidence intervals for parameters obtained from separate fits for each individual, or by fitting different prospective models with random effects for some parameters and then carry out the comparison by making use of a likelihood ratio test or Akaike information criterion (AIC). One may decide to start with models with random effects for all parameters and then eliminate any unnecessary random effects or start with few random effects and add on random effects as long as the model improves.

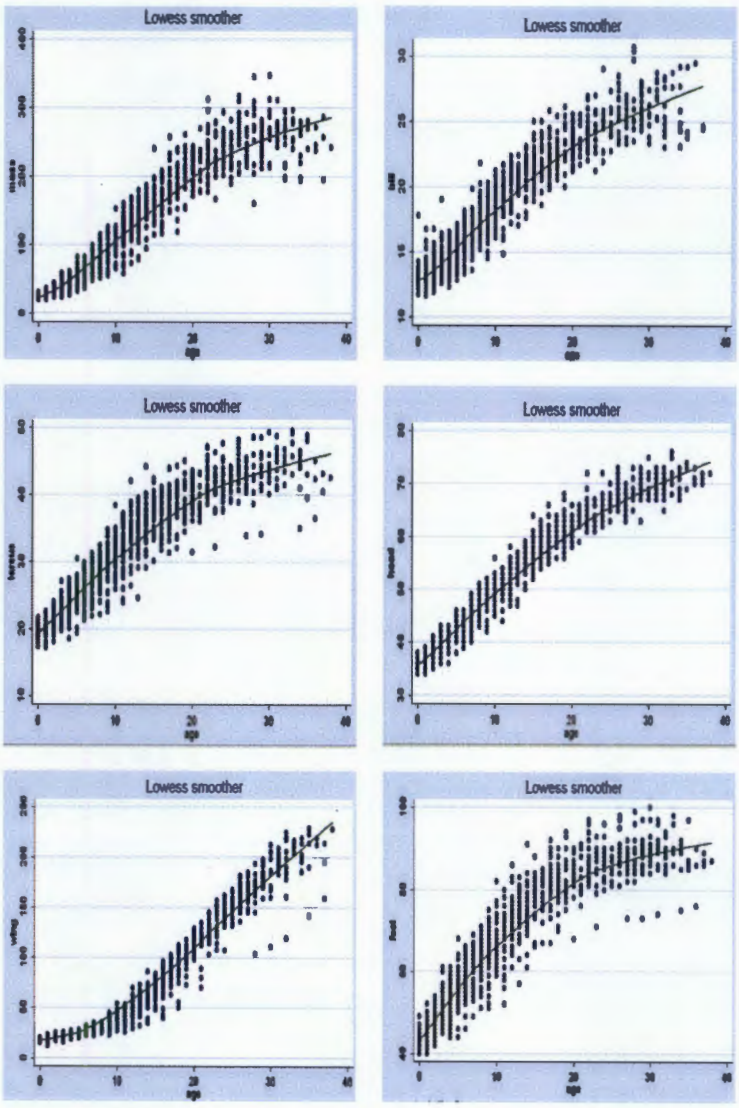

Figure 4.1: Loess curves superimposed on growth data for each of the six body features of Grey-headed Gulls (in mm, except for mass in g), with age in days.

Variance and correlation functions

Whenever there is no prior information about the random effects variance-covariance matrix, different variance and correlation functions can be fitted and compared using the likelihood ratio tests or AIC as for random effects selection. Residual plots can be used as a way to explore possible variance and correlation functions for within-group errors.

Covariate modelling

Some of the variation between individuals can be attributed to the difference in covariate values. An inspection of plots of random effects versus covariates is used to determine which covariates are accountable for random effects variation.

Model diagnostics

The last step for any model building process are the model diagnostics. In order to check whether there are any violations of the assumptions and that the model is adequate, an analysis of residuals is undertaken. This step is usually performed after each major step of the model building process.

4.2 Univariate non-linear mixed effects modelling: Grey-headed Gull data

4.2.1 Single logistic model for body mass

As a start, bird effects were ignored and a single logistic model was fitted to all data. The model for the body mass y_{ij} for bird i at age t_{ij} is:

$$y_{ij} = \frac{\alpha}{1+\exp(-\frac{t_{ij}-\mu}{\beta})} + \varepsilon_{ij}, \varepsilon_{ij} \sim N(0, \sigma^2) \tag{4.1}$$

where α is the asymptotic mass, μ is the time it takes a bird to grow to half of the asymptote and β is the scale parameter (the time it takes to grow from half to three quarters of the asymptote). The ε_{ij} are random errors.

Table 4.1 provides the parameter estimates for this model. The asymptotic mass (α) was estimated to 268.33 g. Half of this mass is attained after 12.69 days (μ, inflection point). The scale parameter of 5.47 informs about how long on average it takes a bird to grow from half (134.17 g) to approximately three quarters of the asymptotic mass (201.25 g). We were unable to fit a logistic parameterization that includes a lower asymptote as given in equation 2.9. The residual standard error of 18.61 is the estimate of σ^2 in equation 4.1. Figure 4.2 indicates that the residuals are mostly negative for some birds and mostly positive for others. This is an indication that the bird effect should be accounted for. One way to include bird effects is to fit separate models for each bird and hence allow different parameters for each bird. This is shown in the next section.

Table 4.1: Parameter estimates for the logistic growth model for all Grey-headed Gull chicks ignoring bird and site effects.

Parameter	Estimate	Std. Error	t- value	$Pr(>\|t\|)$
α	268.33	2.07	129.51	< 0.001
μ	12.69	0.13	93.92	< 0.001
β	5.47	0.09	61.85	< 0.001

Residual standard error: 18.61 on 1244 degrees of freedom

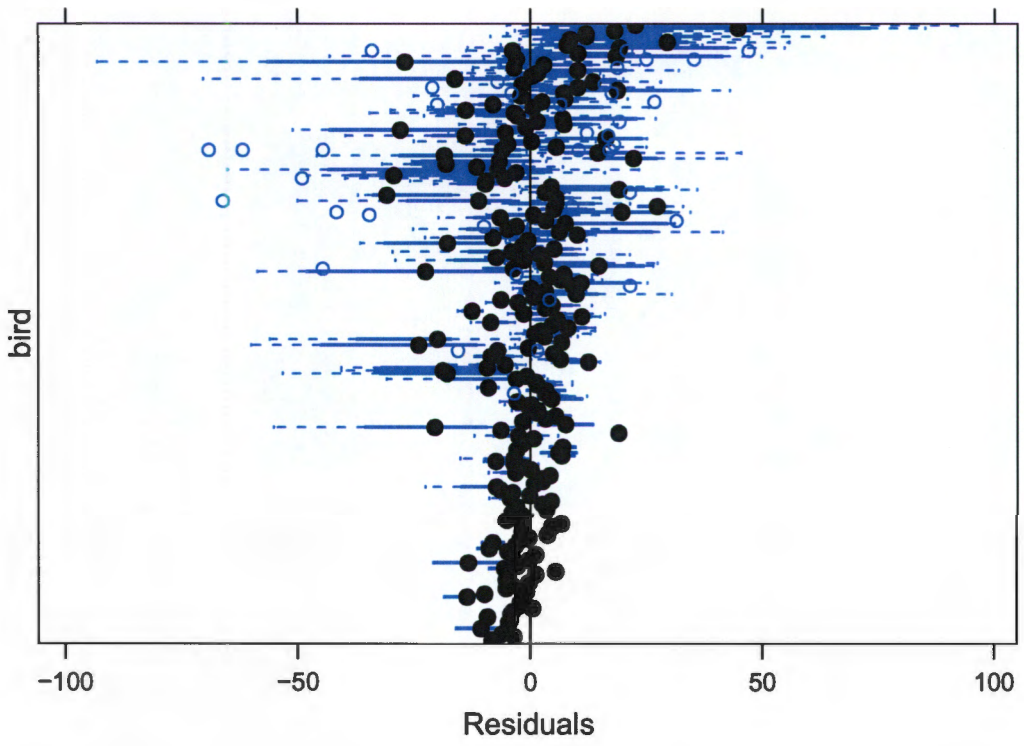

Figure 4.2: Boxplots of residuals by individual Grey-headed Gull chick for the single logistic growth model fitted to all Grey-headed Gull chicks of Bonaero and Modderfontein site.

4.2.2 Bird-specific logistic models for body mass

To allow bird effects to be incorporated in parameter estimates, a separate logistic model for each bird is fitted. The structural model for body mass y_{ij} for i^{th} bird at age t_{ij} is defined as follows:

$$y_{ij} = \frac{\alpha_i}{1 + \exp(-\frac{t_{ij} - \mu_i}{\beta_i})} + \varepsilon_{ij}, \varepsilon_{ij} \sim N(0, \sigma^2) \tag{4.2}$$

where a common variance, σ^2, was assumed for all birds.

Table 4.2 displays the summary of parameter estimates for 12 birds selected, where NA indicates that the logistic model did not fit for that specific bird (bird no 135). There is variability in parameter estimates between birds. The residual standard error has decreased from 18.61 to 9.50. Figure 4.3 shows that the boxplots of residuals are now predominantly centered around zero. The reduction of the residual standard error together with the distribution of boxplots of residuals around the zero suggest that the bird effects have been accounted for by fitting a separate logistic model for each bird. Despite the fact that fitting a separate model for each bird allows to accommodate bird effects, this model has two major drawbacks. Firstly, variation between and within-birds are not accounted for and, secondly, the resulting model is overparameterized. Therefore, neither fitting a single logistic model nor separate models adequately describes the data. A more sensible model that accounts for within and between birds variability with fewer parameters is needed. Non-linear mixed modelling provides a balance between the simple model given by a single non-linear regression and the overparameterized model produced by fitting a separate model for each bird (Pinheiro and Bates, 2000).

However, separate models are useful to decide about the random effects structure and form the basis of non-linear mixed effects modelling in that they may provide starting values for parameter estimation.

Table 4.2: Individual-specific regression parameters obtained from separate logistic growth models for 12 Grey-headed Gull chicks.

Bird	Estimate	S.E	t-statistic	$Pr(>\|t\|)$
		α		
135	NA	NA	NA	NA
186	284.18	6.10	46.56	< 0.001
96	278.49	5.93	46.99	< 0.001
192	280.01	4.90	57.15	< 0.001
151	298.96	7.74	38.62	< 0.001
127	301.60	7.73	39.00	< 0.001
65	323.62	20.47	15.81	< 0.001
147	318.39	7.97	39.95	< 0.001
108	305.35	7.02	43.52	< 0.001
101	311.11	8.53	36.46	< 0.001
110	330.98	16.96	19.51	< 0.001
146	374.79	12.66	29.61	< 0.001
		μ		
135	NA	NA	NA	NA
186	13.06	0.43	30.53	< 0.001
96	13.64	0.41	33.37	< 0.001
192	10.88	0.33	32.57	< 0.001
151	13.30	0.50	26.64	< 0.001
127	11.96	0.48	24.85	< 0.001
65	14.16	1.18	11.96	< 0.001
147	13.92	0.46	30.18	< 0.001
108	13.52	0.44	30.83	< 0.001
101	13.29	0.50	26.61	< 0.001
110	11.29	0.67	16.94	< 0.001
146	15.18	0.58	26.01	< 0.001
		β		
135	NA	NA	NA	NA
186	5.21	0.38	13.64	< 0.001
96	4.90	0.33	14.82	< 0.001
192	4.12	0.29	14.04	< 0.001
151	5.36	0.41	13.20	< 0.001
127	5.58	0.43	13.05	< 0.001
65	6.23	0.67	9.23	< 0.001
147	5.30	0.38	13.78	< 0.001
108	5.25	0.37	14.28	< 0.001
101	5.52	0.38	14.63	< 0.001
110	4.62	0.43	10.82	< 0.001
146	5.77	0.41	13.92	< 0.001

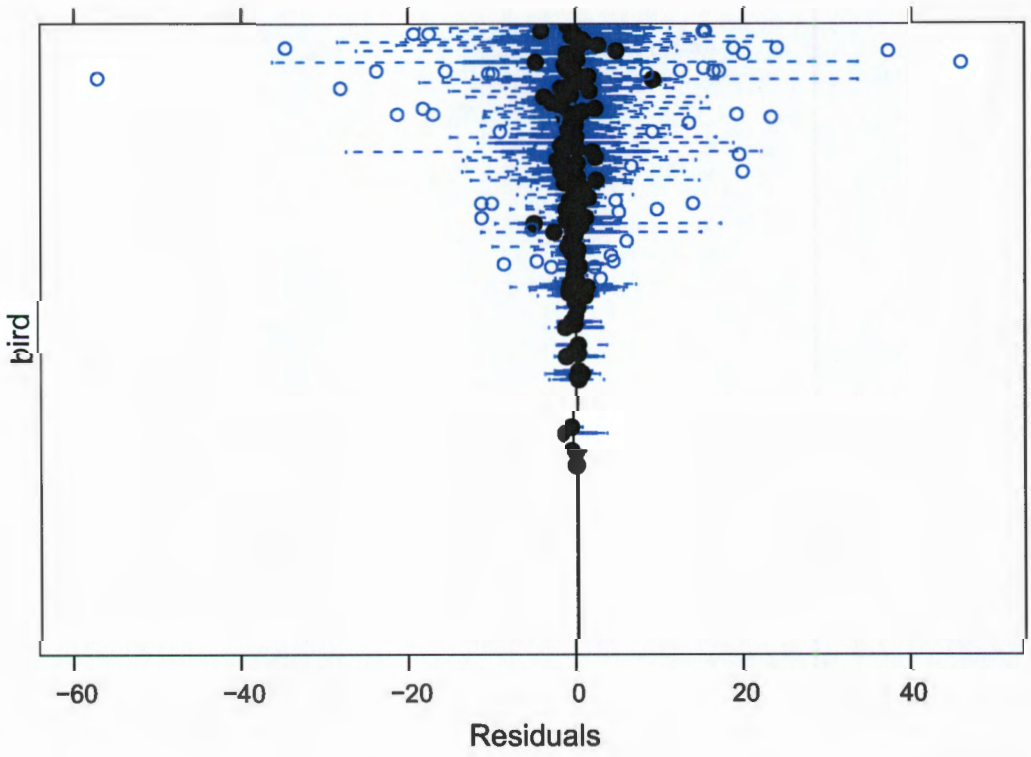

Figure 4.3: Boxplots of residuals by bird for bird specific models on body mass for Grey-headed Gulls.

4.2.3 Mixed effects logistic models

We now add random variation to average population parameters in the population of birds to account for differences between birds in these parameter values. The mixed effects logistic model for body mass y_{ij} for bird i on the j^{th} occasion at age t_{ij} is given by

$$y_{ij} = \frac{\alpha + b_{1i}}{1 + \exp[-\frac{t_{ij}-(\mu+b_{2i})}{\beta+b_{3i}}]} + \varepsilon_{ij}, \varepsilon_{ij} \sim N(0, \sigma^2), \boldsymbol{b_i} \sim N(0, \boldsymbol{D}) \qquad (4.3)$$

where α, μ and β are fixed effects (mean values of parameters in the population of birds), b_{1i}, b_{2i} and b_{3i} are random effects and represent individual deviations from the average population parameters. The random effects $\boldsymbol{b_i}$ are assumed to be independent of each other and distributed with mean zero and variance-covariance

matrix $\boldsymbol{D}$. The within-bird errors (ε_{ij}) are assumed to be independently normally distributed with mean zero and a variance σ^2, and independent to the random effects. The assumption of independence and constant variance for within-bird errors may be relaxed by fitting variance and correlation functions.

4.2.3.1 Random effects selection

One of the key questions to be addressed when fitting non-linear mixed effects models is to choose the parameters to which random effects should be added. The plot of confidence intervals for the bird specific parameters obtained from equation 4.2 depicted in Figure 4.4 indicates a considerable degree of overlap in confidence intervals for individual parameter estimates. It also indicates a few birds with very wide confidence intervals compared to the rest. This suggests that random effects may not be necessary. However, we nonetheless explored a model with random effects on all three parameters. A summary of a model with random effects in all three parameters is shown in Table 4.3. The standard deviations for all random effects are greater than zero, hence this justifies why the random effects may be needed for all parameters. A stepwise elimination method was used to fit models with no random effects for some parameters; comparison of these models with a model with all parameters being associated with random effects is shown in Table 4.4. This table confirms that the model with random effects for all three parameters is well supported by the data.

We have tried to fit both an unstructured variance-covariance (allowing different correlations among random effects) and a diagonal variance-covariance matrix structure (independent random effects). The unstructured variance-covariance structure could not be fitted in most of the cases. Table 4.4 indicates that the model with random effects, assumed independent (diagonal variance-covariance structure matrix), for all parameters is the best as it has the smallest AIC (9802.48).

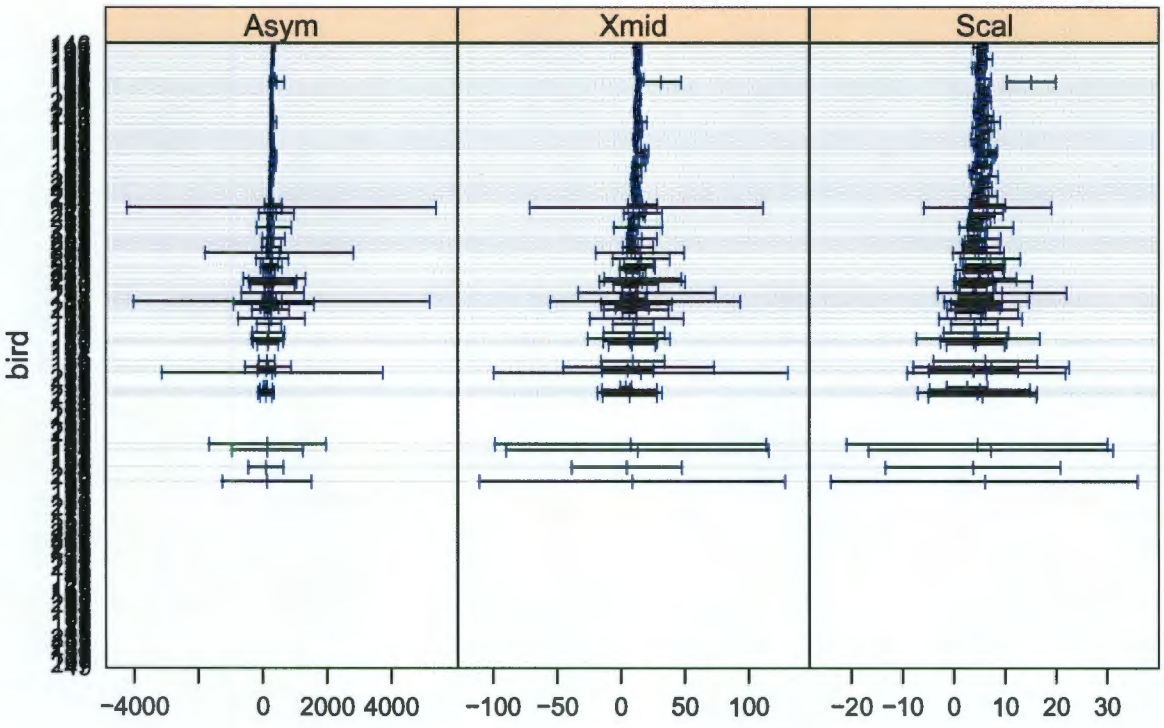

Figure 4.4: Ninety-five per cent confidence intervals on the logistic model parameters for each Grey-headed Gull in Bonaero and Modderfontein site.

4.2.3.2 Variance functions in mixed effects logistic models

So far, the within-bird errors (ε_{ij}) have been assumed to be distributed with mean zero and $\text{var}(\varepsilon_{ij}) = \sigma^2$. However other forms of variability other than constant variation may arise. For instance ε_{ij} may vary with the magnitude of the predicted values or covariates. Figure 4.5 indicates that as the fitted values increase the standardized residuals increase as well.

Table 4.3: Parameter estimates for the non-linear mixed effects model with all fixed effects associated with random effects.

Fixed effects	Value	Std.Error	t-value	p-value	Rand.effects Std.Dev
α	263.17	3.56	73.99	< 0.001	30.39
μ	12.47	0.14	89.60	< 0.001	1.03
β	5.35	0.06	83.21	< 0.001	0.40

residual s.e = 9.48

Table 4.4: Selection of fixed effects to be associated with random effects.

Parameter with random effects in the model	Var-Covariance matrix structure for random effects	AIC	BIC	logLikelihood
α, μ, β	Diagonal	9802.48	9838.38	-4894.24
α, μ	Diagonal	9827.95	9858.72	-4907.98
α, β	Diagonal	9990.60	10021.37	-4989.30
μ, β	Unstructured	10149.50	10185.40	-5067.75
μ, β	Diagonal	10284.96	10315.73	-5136.48
α		9996.28	10021.92	-4993.14
β		10771.76	10797.41	-5380.88
μ		10506.48	10532.12	-5248.24

Thus, the following variance functions were investigated:

1. a variance model in which variance increases linearly with the fitted values: var(ε_{ij})=$\sigma^2|\mu_{ij}|^{2\delta}, \delta = 0.5$.

2. a variance function with a constant plus a power of fitted values: var(ε_{ij})=$\sigma^2(\delta_1 + |\mu_{ij}|^{\delta_2})^2$.

The structural mixed effects logistic model then becomes:

$$y_{ij} = \frac{\alpha + b_{1i}}{1 + \exp[-\frac{t_{ij}-(\mu+b_{2i})}{\beta+b_{3i}}]} + \varepsilon_{ij}, \varepsilon_{ij} \sim N(0, \sigma^2 g^2(\mu_{ij}, \boldsymbol{\delta})), \boldsymbol{b_i} \sim N(0, D) \qquad (4.4)$$

where $g(.)$ is a function of variance covariates such as fitted values, μ_{ij}, and the parameters vector $\boldsymbol{\delta}$.

By assuming heteroscedasticity of within-bird errors, the non-linear mixed effects logistic model has improved (Table 4.5). From the AIC it is noted that variance models assuming heterogeneity are better than the one assuming constant variation of within-bird errors as their associated AICs are less than the AIC of 9802.48 for the model with constant variance.

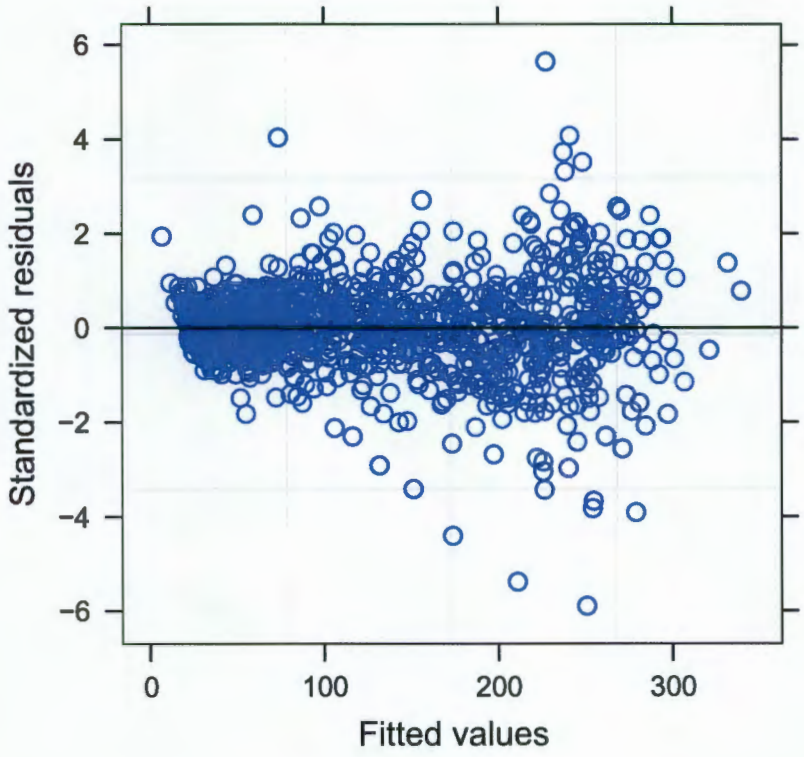

Figure 4.5: Plot of residuals versus fitted values for body mass of Grey-headed Gull chicks.

The variance function with a constant plus a power of fitted values produces the best model (smallest AIC of 9200.37).

4.2.3.3 Correlation functions

Thus far, it has been assumed that the within-bird errors are independent, which means there is no correlation between ε_{ij} and $\varepsilon_{ij'}$ for $j \neq j'$. However, because our data are repeated measures on chick growth, it makes sense to assume that the within-bird errors are serially correlated. Therefore, several correlation structures that include compound symmetry, autoregressive and moving average were considered. From Table 4.6, it seems that within-bird errors are serially correlated and an autoregressive correlation model provides a better description relative to compound symmetry and moving average models (AIC = 8986.06).

Table 4.5: Comparison of models with different variance functions for within-bird errors.

$Var(\varepsilon_{ij})$	AIC	BIC	logLik
σ^2	9802.48	9838.38	-4894.24
$\sigma^2\|\mu_{ij}\|^{2\delta}$	9308.22	9344.12	-4647.11
$\sigma^2(\delta_1 + \mu_{ij}^{\delta_2})^2$	9200.37	9246.52	-4591.18

So far, we may conclude that the best model to describe the body mass is a mixed effects logistic model where all fixed effects are associated with random effects, and the within bird variability is best modelled by a variance function given by $\text{var}(\varepsilon_{ij}) = \sigma^2(\delta_1 + |\mu_{ij}|^{\delta_2})^2$, and within bird errors are modelled by a first order autoregressive correlation function (AR1).

Table 4.6: Comparison of models with different correlation functions for within-bird errors.

$\text{Var}(\varepsilon_{ij})$	$\text{Corr}(\varepsilon_{ij})$	AIC	BIC	logLik
σ^2	uncorrelated	9200.37	9246.52	-4591.18
$\sigma^2(\delta_1 + \mu_{ij}^{\delta_2})^2$	AR1	8986.06	9037.35	-4483.03
$\sigma^2(\delta_1 + \mu_{ij}^{\delta_2})^2$	CompSymm	9175.49	9226.78	-4577.75
$\sigma^2(\delta_1 + \mu_{ij}^{\delta_2})^2$	ARMA	9802.48	9838.38	-4894.24

4.2.3.4 Covariate modelling in mixed effects logistic models

At this point of the model building process, it is interesting to find out whether there is a difference between the Bonaero and Modderfontein sites with respect to growth in mass of birds. One way of checking the site effect is to consider modelling the fixed effects as a function of site taken as a covariate. Plots of random effects versus site were used to determine which random effects variation is explained by the site. The plots displayed by Figure 4.6 indicated that there was no evidence of a difference between asymptotes due to site effects, there might be a small difference in estimates of time to reach half of the asymptote (Xmid), and that there was a clear difference of scale parameters between the sites. Table 4.7 compares models with the site effect added to various combinations of fixed effects parameters and random effects. Dashes indicate that the model with all fixed effects parameters changing between sites and random effects for all parameters did not converge. Based on AIC, the model allowing all parameters to vary between the sites was found to be the best. Therefore, our final model is the mixed effects logistic model that includes site as covariate, and within bird variability and correlation structure for ε_{ij} are modelled by $\sigma^2(\delta_1 + \mu_{ij}^{\delta_2})^2$ and AR(1), respectively. And only α and μ parameters were associated with random effects.

Table 4.7: Comparison of the models including site as a covariate explaining partly the variation of parameters between birds.

$\text{Var}(\varepsilon_{ij})$	$\text{Corr}(\varepsilon_{ij})$	Fixed effects that differ between sites	Fixed effects with random effects	AIC	BIC	logLik
$\sigma^2(\delta_1 + \mu_{ij}^{\delta_2})^2$	AR1	None	α, μ, β	8986.06	9037.35	-4483.03
$\sigma^2(\delta_1 + \mu_{ij}^{\delta_2})^2$	AR1	μ, β	α, μ, β	8964.96	9026.50	-4470.48
$\sigma^2(\delta_1 + \mu_{ij}^{\delta_2})^2$	AR1	α, β	α, μ, β	8959.11	9020.65	-4467.56
$\sigma^2(\delta_1 + \mu_{ij}^{\delta_2})^2$	AR1	α, μ	α, μ, β	8966.20	9027.75	-4471.10
$\sigma^2(\delta_1 + \mu_{ij}^{\delta_2})^2$	AR1	α, μ, β	α, μ, β	–	–	–
$\sigma^2(\delta_1 + \mu_{ij}^{\delta_2})^2$	AR1	α, μ, β	α, μ	8958.80	9020.34	-4467.40
$\sigma^2(\delta_1 + \mu_{ij}^{\delta_2})^2$	AR1	β	α, μ	8974.30	9025.58	-4477.15
$\sigma^2(\delta_1 + \mu_{ij}^{\delta_2})^2$	AR1	β	α, μ, β	8976.30	9032.71	-4477.15

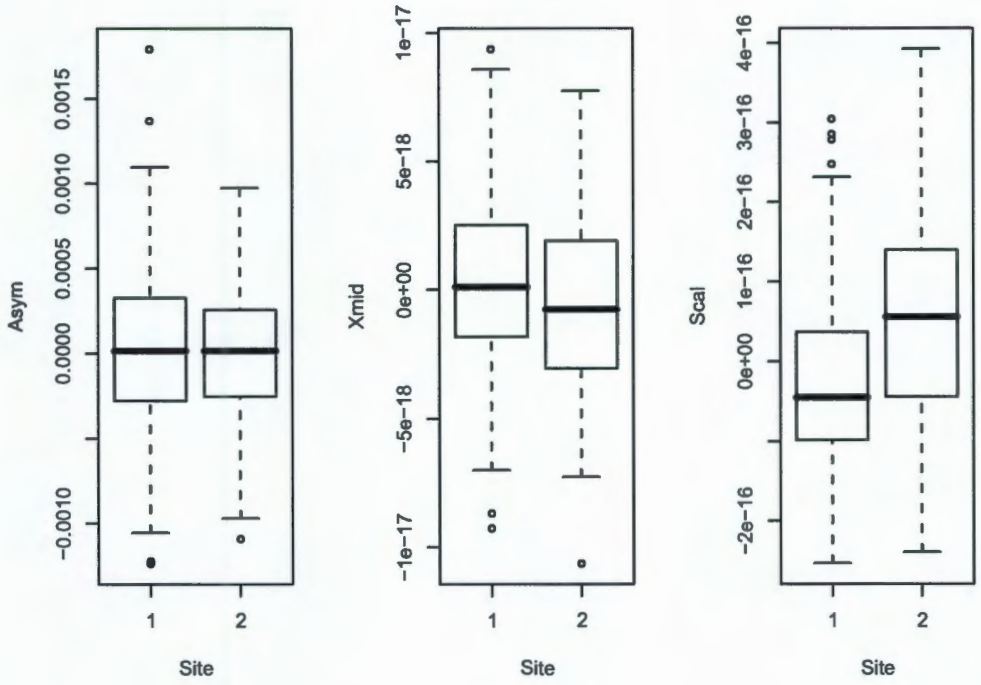

Figure 4.6: Random effects for all three parameters Asym (α), Xmid (μ), and Scal (β) versus site.

4.2.3.5 Model diagnostics

To complete the model building process, it is necessary to examine if the basic assumptions underlying the non-linear mixed effects models are met (within-bird errors independent and identically normally distributed, and they are independent of random effects; the random effects are normally distributed and are independent for different birds). This may be achieved by inspecting the plot of standardized residuals versus fitted values, and normal quantile plots for residuals and random effects. The plot of the standardized residuals versus fitted values, displayed in Figure 4.7, shows that the residuals are scattered evenly around the zero line without any particular systematic patterns. Within-bird errors (Figure 4.8) do not exhibit any serious departures from the assumption of normality.

No evident departure from the assumption of normality for the random effects is shown by the normal plot of the estimated random effects. Figure 4.10 shows that there is no visible difference between the population predictions and the bird-specific predictions. This not surprising given the very small estimates for the random effects as illustrated by the scales for the y-axes in figure 4.6. It is surprising that the AIC statistic (Table 4.4)indicated the need for random effects for all fixed effects. Though not reported, likelihood ratio (LR) test, confirmed the need for those random effect terms. This raises the question as to whether either of these two tests are appropriate for evaluating the need of random effects in the model.

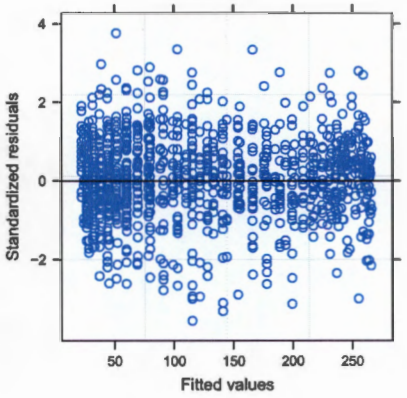

Figure 4.7: Scatter plot for standardized residuals versus fitted values for the final model given in equation 4.5.

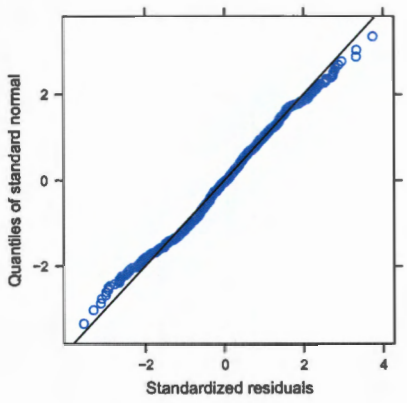

Figure 4.8: Normal plot of standardized residuals for the final model of mass given in equation 4.5.

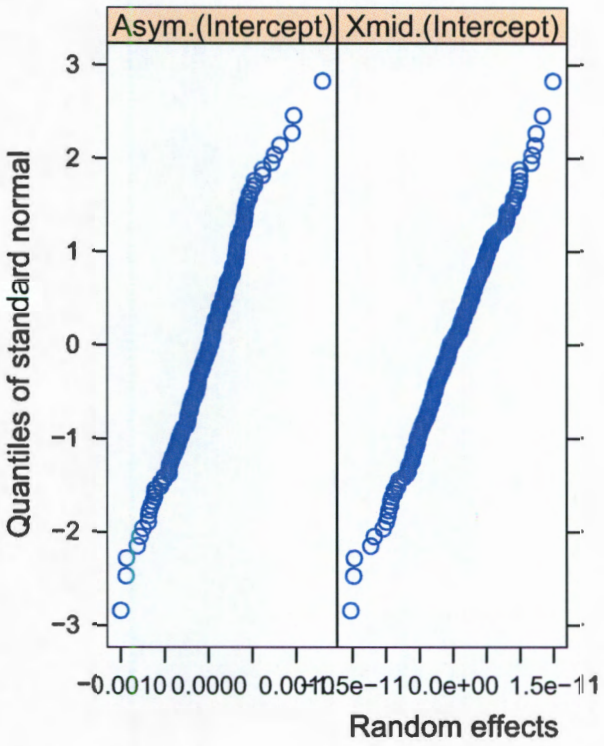

Figure 4.9: Normal plot of estimated random effects for the final model given in equation 4.5 .

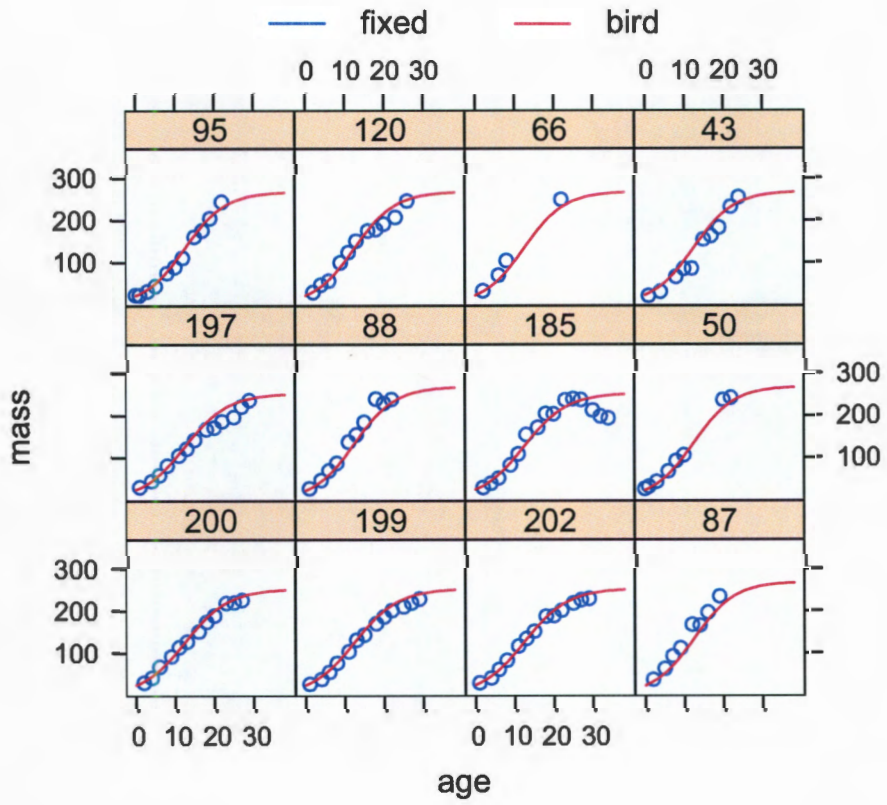

Figure 4.10: Population predictions (fixed, in blue), within-bird predictions (individual bird, in pink) obtained from the final model given in equation 4.5, and observed masses (circles) versus age (days) for Bonaero and Modderfontein sites.

4.2.3.6 Final non-linear mixed effects logistic model for body mass

The change in size of the growth variable mass for Grey-headed Gulls from Bonaero Park and Modderfontein Pan is described by a non-linear logistic model where the within-bird errors correlation is modelled by a first order autoregressive model and their variance is modelled as a variance function with a constant plus a power of fitted values ($\sigma^2(\delta_1 + \mu_{ij}^{\delta_2})^2$); and the between bird variability is accounted for by random effects (b_i) on fixed effects α and μ and distributed with mean zero and diagonal variance-covariance matrix D.

The model is expressed as follows:

$$y_{ij} = \frac{\alpha + \text{site} \times \alpha_{\text{site}} + \text{b}_{1\text{i}}}{1 + \exp[-\frac{t_{ij} - (\mu + \text{site} \times \mu_{\text{site}} + \text{b}_{2\text{i}})}{\beta + \text{site} \times \beta_{\text{site}}}]} + \varepsilon_{ij}, \varepsilon_{ij} \sim N(0, R_i), b_i \sim N(0, D) \qquad (4.5)$$

where $\begin{bmatrix} \alpha \\ \mu \\ \beta \end{bmatrix} = \begin{bmatrix} 268.42 \\ 12.45 \\ 5.21 \end{bmatrix}, \begin{bmatrix} \alpha_{site} \\ \mu_{site} \\ \beta_{site} \end{bmatrix} = \begin{bmatrix} -15.46 \\ -0.05 \\ 0.33 \end{bmatrix}, D = \begin{bmatrix} 0.099 & 0 \\ 0 & 0.000002 \end{bmatrix},$

and $R_i = \sigma^2 G_i^{\frac{1}{2}}(\theta_i, \delta)\Gamma_i(\alpha)G_i^{\frac{1}{2}}(\theta_i, \delta)$ with $\sigma^2 = 0.26^2$, and θ_i is a vector of fixed effects for each individual, $G_i^{\frac{1}{2}} = \text{diag}[\sigma^2(\delta_1 + \mu_{ij}^{\delta_2})^2]$, ($\delta_1 = 5.36 \times 10^{-26}$ and $\delta_2 = 0.87$);

and $\Gamma(\alpha)_i = \begin{bmatrix} 1 & 0.75 & 0.75^2 & \dots & 0.75^{n_i-1} \\ & 1 & 0.75 & \dots & 0.75^{n_i-2} \\ & & \vdots & \dots & \vdots \\ & & & & 1 \end{bmatrix}$.

Site takes the value of zero and one for Bonaero and Modderfontein, respectively.

Estimates of the fixed effect parameters are shown in Table 4.8. As expected, all parameters were significant with exception of the site adjustment to μ. It shows also that the Grey-headed Gull chicks from Modderfontein might have lower asymptotes than those from Bonaero (p-value=0.08) and a significantly slower growth towards the latter part of the growth curve (β_{site}=0.34, p= 0.02). There was no significant difference between initial growth rates of birds from the two sites (p=0.9). Figure 4.11 illustrates the population curves for two sites.

Table 4.8: Fixed effects estimates of the final mixed effects logistic model for body mass of Grey-headed Gulls at Bonaero and Modderfontein sites.

Parameter	Estimate	Std.Error	t-value	p-value
γ	268.42	5.14	52.27	0.00
γ_{site}	-15.46	8.92	-1.73	0.08
μ	12.45	0.22	55.80	0.00
μ_{site}	-0.05	0.43	-0.12	0.90
β	5.21	0.07	70.30	0.00
β_{site}	0.34	0.15	2.30	0.02

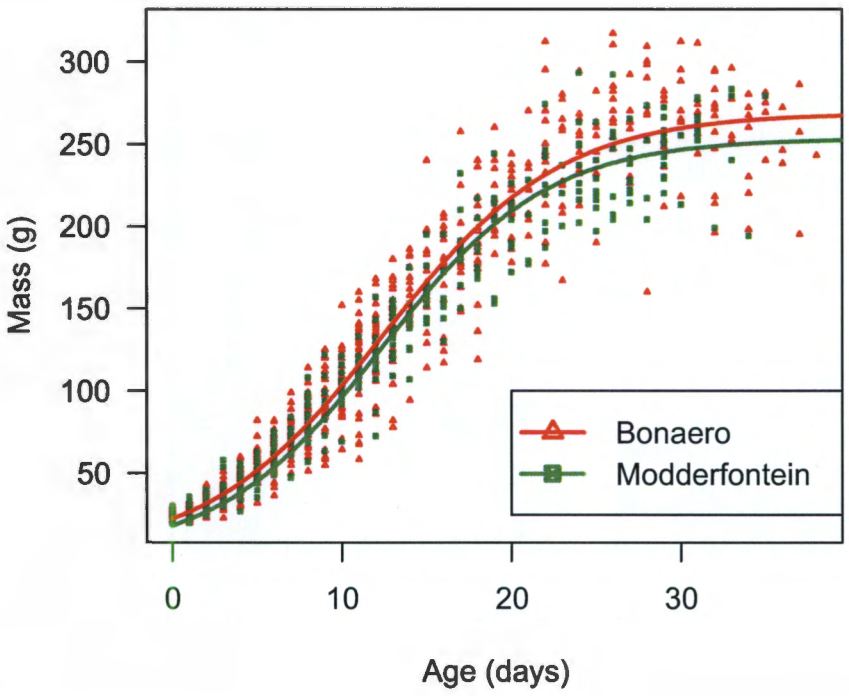

Figure 4.11: Predicted population curves for the two sites superimposed on observed masses of Grey-headed Gulls.

4.2.4 Non-linear mixed effects growth models of the six body features

For each of the six growth variables, the model building procedure illustrated, using body mass in previous section, was followed to fit logistic, Gompertz, inverse exponential, and Richards models. The inverse exponential model could not fit wing length. A variance consisting of a constant plus power function of fitted values and a first order autoregressive correlation function were the best variance and correlation functions for within-bird errors, respectively for the other five body features. The best model for each variable was obtained by using the AIC statistic. The logistic model was found to be the best model for the description of both body mass and

wing growth (Table 4.9). The Gompertz and Richards models provided the best fits for bill length. But, due to the easy interpretation of the Gompertz parameters, this model was preferred over the Richards model. The Gompertz model also provided the best fit for the tarsus growth. The head growth was best described by Richards and logistic models. The Richards model provided the best description of foot length.

One of the questions of interest was to determine whether there is a site effect on each of the growth variables or not. The site effect was tested using a t-test. For instance, an estimate of asymptote is given by: $\gamma + \gamma_{site}$. If the γ_{site} is found to be significantly different from zero then we draw the conclusion that the asymptote varied between site. It was found that there was no site effect on growths of all body features, except for body mass (Table 4.9).

A direct comparison of models with respect to parameter estimates is difficult because different parameterizations result in different mechanistic interpretations of parameters. However, comparisons can be made between models with respect to common parameters: logistic, inverse exponential and Richards models can be compared with respect to upper asymptote estimates, whereas Gompertz and inverse exponential may be compared with respect to lower asymptote and growth rate estimates. Table 4.9 shows that the logistic and Richards models gave similar estimates for upper asymptotes (α), while the estimates for this parameter from the inverse exponential models are much higher. It is also noted that, except for body mass, the Gompertz and Inverse models yielded approximately similar estimates for lower asymptotes (γ). Figure 4.12 gives a graphical comparison of different models for each body feature.

Because both the logistic and Gompertz models gave good descriptions of body features relative to other models, the parameter estimates resulting from these models were used to describe each feature growth in the subsequent paragraphs. The logistic model provides information about the upper asymptote, the estimate of time to reach half of the asymptote, and the estimate of time to grow from half to approximately three quarters of the asymptote. On the other hand, the Gompertz model inform about the lower asymptote, the instantaneous growth rate and the rate at

which the instantaneous growth decreases.

Logistic model (Table 4.9):

From Table 4.9, the asymptotic body mass of a grey-headed gull was estimated to be 268.42 g. Within 13 days of hatching (μ=12.45), the Grey-headed Gull chick mass was estimated to be half of the maximum body mass (134.21 g).
After 3.59 days the bill (culmen) grew up to half of the asymptotic length, which is estimated to 29.2 mm. But a slow growth was followed for the next 11.68 days as the bill length changed from 14.60 mm (half of the asymptote) to 21.90 mm (three quarters of the asymptote).
The tarsus asymptotic length was estimated to 46.22 mm. Half of this length was reached in 3.39 days after hatching and thereafter a slow growth was observed.
The asymptotic wing length was estimated to be 349.40 mm, with half of this length reached within approximately 30 days of hatching and three quarters reached within 40 days.
Approximately 1.36 days (μ=1.36) after hatching a chick had a foot length equal to half of the maximum length (46.50 mm).
The asymptotic head length was estimated to 78.11 mm and half of this length was reached within 2.61 days after hatching. But a slow growth occurred afterwards as it took 13 days for a chick head to grow from half to three quarters of maximum length.

Gompertz model (Table 4.9):

The mass of a Grey-headed Gull chick at hatching was estimated to approximately 21.21 g (lower asymptote). The body mass increased at a rate of 2.83 g/day with a decreasing rate of 0.08 g/day.
At hatching day, the bill was estimated to 12.11 mm long (lower asymptote) and grew at an instantaneous growth rate of 0.93 mm/day with a slowing down rate of 0.06 mm/day.
The tarsus length was approximated to 19.11 mm at day zero and it grew at rate of 1.00 mm/day at a decreasing rate of 0.06 mm per day.
At day zero the wing length of a grey headed gull was estimated to grow from 15.25

mm at rate of 4 mm/day at a decreasing rate of 0.03 mm/day.

At day zero, a Grey-headed Gull chick had an estimated foot length of 42.84 mm and grew at an instantaneous growth rate of 0.82 mm/day at slowing down rate of 0.08 mm/day, with the head growing from 35.15 mm at hatching at a rate of 0.88 mm/day at decreasing rate of 0.05 mm/day. From this analysis, it may be noted that almost half of the growth process for bill, foot, tarsus and head took place during the incubation period whereas for mass and wing the major part of growth occurred after hatching. This is also shown by the Figure 4.13. This figure was obtained by dividing the predictions obtained from the logistic model by the asymptote to get scaled predictions, and these scaled valued were plotted against age. From this figure, it may be noted that the foot, tarsus, bill and head had similar growth patterns and that, indeed, a considerable part of their growth process was completed during the incubation. The wing growth was the longest among all other body features. Interesting that logistic has the lowest AIC for wing length (Table 4.9). But, from Figure 4.12, it looks as if Richards model fits better compared to logistic, Gompertz and exponential models since it allows for slowing of wing growth. Biologists will be able to comment on which is more plausible.

Table 4.9: Fixed effects estimates (with standard errors in brackets) obtained from the univariate **logistic, Gompertz, inverse exponential and Richards** growth models for all six body features of Grey-headed Gulls.

Model		Body feature					
		Mass	Bill	Tarsus	Wing	Head	Foot
Logistic	AIC	**8958.8**	2989.67	3709.4	**6969.43**	3898.36	6521.72
	α	**268.42 (5.13)**	29.19 (0.40)	46.22 (0.41)	**349.40 (14.86)**	78.11 (0.52)	93.10 (0.79)
	α_{site}	−15.46 **(8.92)**	–	–	–	–	–
	μ	**12.45 (0.22)**	3.59 (0.33)	3.39 (0.16)	**29.14 (0.3)**	2.61 (0.17)	1.36 (0.14)
	μ_{site}	−0.05 **(0.43)**	–	–	–	–	–
	β	**5.21 (0.07)**	11.68 (0.31)	9.21 (0.15)	**9.64 (0.13)**	12.98 (0.18)	8.65 (0.19)
	β_{site}	**0.33 (0.14)**	–	–	–	–	–
Gompertz	AIC	9055.68	**2977.56**	**3617.06**	7308.61	3973.46	6523.97
	γ	21.21 (0.34)	**12.11 (0.08)**	**19.11 (0.09)**	15.25 (0.29)	35.15 (0.12)	42.84 (0.20)
	γ_{site}	2.03 (0.61)	–	–	–	–	–
	β	2.83 (0.03)	**0.93 (0.02)**	**1.00 (0.01)**	4.38 (0.11)	0.88 (0.01)	0.82 (0.01)
	β_{site}	−0.16 (0.05)	–	–	–	–	–
	μ	0.08 (0.002)	**0.06 (0.002)**	0.06 (0.002)	0.03 (0.001)	0.05 (0.001)	0.08 (0.003)
	μ_{site}	−0.003 (0.004)	–	–	–	–	–
Inverse exponential	AIC	10605.96	3171.78	3747.47	–	3965.34	6540.35
	γ	7.10 (0.98)	11.92 (0.07)	18.88 (0.10)	–	34.83 (0.11)	41.86 (0.23)
	α	538.58 (25.40)	32.84 (0.73)	49.89 (1.03)	–	89.48 (1.60)	97.67 (1.48)
	β	0.02 (0.001)	0.04 (0.002)	0.05 (0.001)	–	0.03 (0.001)	0.06 (0.002)
Richards	AIC	9047.04	2969.32	3677.72	7172.76	**3869.13**	**6486.59**
	α	291.00 (5.90)	27.10 (0.34)	44.36 (0.37)	236.27 (2.11)	**74.21 (0.68)**	**90.86 (1.36)**
	α_{site}	−26.67 (9.96)	–	–	–	–	–
	μ	1.00 (0.28)	2.66 (0.45)	2.33 (0.25)	4.40 (0.18)	**1.74 (0.24)**	**1.17 (0.45)**
	μ_{site}	0.041 (0.51)	–	–	–	–	–
	β	0.14 (0.008)	0.16 (0.02)	0.17 (0.01)	0.17 (0.006)	**0.11 (0.008)**	**0.14 (0.02)**
	β_{site}	0.01 (0.02)	–	–	–	–	–
	δ	0.51 (0.08)	3.53 (0.60)	2.92 (0.29)	1.58 (0.07)	**2.57 (0.31)**	**1.93 (0.49)**
	δ_{site}	0.17 (0.17)	–	–	–	–	–

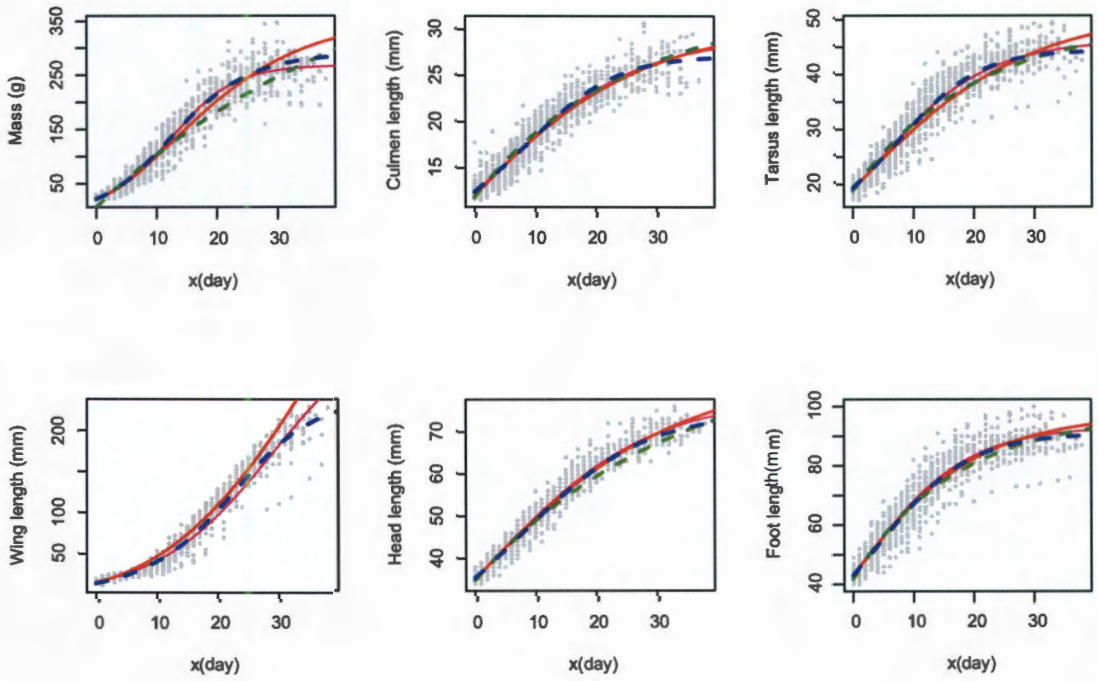

Figure 4.12: Predicted population curves superimposed on observed growth data for the six features of Grey-headed Gulls: observed data (grey dots), logistic (pink line), Gompertz (red line), inverse exponential (green line), and Richards (blue line).

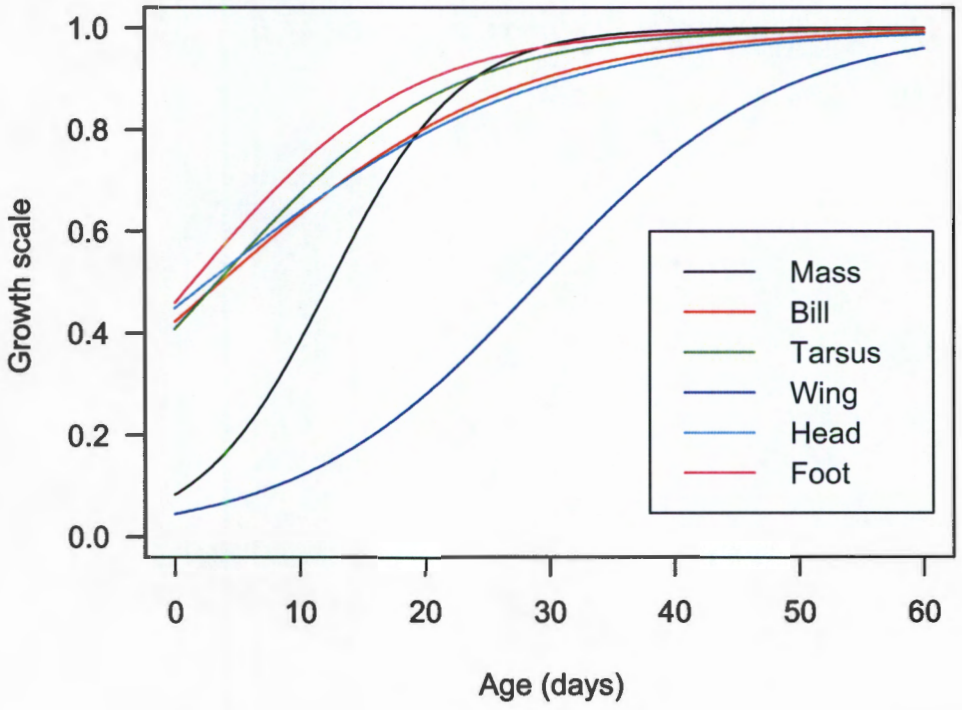

Figure 4.13: Scaled predicted curves obtained from the final univariate logistic models for the body features of Grey-headed Gulls.

4.3 Multivariate non-linear mixed effects modelling: Grey-headed Gull data

Although the term multivariate will be repeatedly used in the subsequent paragraph, this is not really a multivariate model but rather a way of modeling multiple responses. In section 4.2, the growth model of each body feature was obtained separately through univariate analysis techniques. The main weakness of this approach is that it does not capture possible correlations among different body features. We decided to impose a uniform structural function form on all responses and include the feature indicator as a covariate. The following data manipulation is needed: create a single response-vector, $\boldsymbol{y}_i = \begin{bmatrix} y_{i1} & y_{i2} & y_{i3} & y_{i4} & y_{i5} & y_{i6} \end{bmatrix}^T$, in which all six response variables are stacked and create an indicator covariate to distinguish features from one another. In the above vector y_{ik} refers to measurements on feature k for the individual i. In this section a detailed model building process for multivariate non-linear mixed effects modelling using the logistic growth model is presented. Only final models will be presented for the other growth models.

4.3.1 Multivariate logistic models

To fit a multivariate mixed effects logistic model, the indicator variable (feature) was treated as a covariate. This covariate is then used to explain the differences between the logistic growth parameters for the different features. The model is mathematically expressed as:

$$y_{ijk} = \frac{\alpha}{1+\exp[-\frac{t_{ijk}-\mu}{\beta}]} + \varepsilon_{ijk}, \varepsilon_{ijk} \sim N(0, \boldsymbol{R_{ik}}), \boldsymbol{b_i} \sim N(0, \boldsymbol{D}) \qquad (4.6)$$

where:

$\alpha = \alpha_1 + \sum_{k=2}^{6} \tau_k \alpha_k + b_{1i}$,

$\mu = \mu_1 + \sum_{k=2}^{6} \tau_k \mu_k + b_{2i}$,

$\beta = \beta_1 + \sum_{k=2}^{6} \tau_k \beta_k + b_{3i}$,

τ_k is an indicator variable equal to one if feature equals k, zero else (except for k=1 where $\tau_k = 0$). α_k, μ_k and β_k are differences in parameter values compared to parameter values of feature 1. These are added information yielded by the multivariate model. α_1, μ_1 and β_1 are parameter values (fixed effects for feature 1 (mass))

Random effects $\boldsymbol{b}_i$ are assumed to be independent and distributed with mean zero and a diagonal variance-covariance matrix $\boldsymbol{D}$. The within-bird errors are assumed to be independently normally distributed with mean zero and a constant variance σ^2, and independent of the random effects. $k = 1, 2, 3, 4, 5, 6$ and relates to body features by the following relation: $\begin{bmatrix} 1 \\ 2 \\ 3 \\ 4 \\ 5 \\ 6 \end{bmatrix} = \begin{bmatrix} \text{mass} \\ \text{bill} \\ \text{tarsus} \\ \text{head} \\ \text{wing} \\ \text{foot} \end{bmatrix}$.

4.3.1.1 Variance functions (multivariate case)

The within-bird errors given in equation 4.6 are assumed to be distributed with mean zero and a constant variance for all growth variables. However, it may be reasonable to assume that the within-bird errors variance depends on the fitted values and /or covariates as was the case for the univariate models. A variance function in which the variance increases linearly with fitted values ($\text{var}(\varepsilon_{ij}) = \sigma^2|\mu_{ij}|^{2\delta}$, where $\delta = 0.5$), a variance function with different variances for each body feature ($\text{var}(\varepsilon_{ij}) = \sigma^2\delta_k^2$), and a variance function where variance increase as a power of fitted values, with a different power for each feature,($\text{var}(\varepsilon_{ij}) = \sigma^2|\mu_{ij}|^{2\delta_k}$) were fitted and the best variance function was selected based on AIC. $k = 1, 2, 3, 4, 5, 6$ and denotes the body features. The last variance function, with a different power for each feature, was the best since this model has the smallest AIC (59528.61), (Table.4.10).

Table 4.10: Comparison of different variance functions for within-bird errors for the multivariate logistic model.

$Var(\varepsilon_{ij})$	AIC	BIC	logLik
σ^2	72464.72	72512.70	-36225.36
$\sigma^2\|\mu_{ij}\|^{2\delta}$	68990.02	69038.01	-34488.01
$\sigma^2\delta_k^2$	61488.35	61570.61	-30732.17
$\sigma^2\|\mu_{ij}\|^{2\delta_k}$	59528.61	59617.72	-29751.31

4.3.1.2 Correlation functions (multivariate case)

Up to this stage of the model building process, the within-bird errors have been assumed to be uncorrelated. Conceptually a first order autoregressive model seems to an appropriate correlation function for the within-birds errors for each feature. Thus, we used a corAR1 correlation structure (corAR1(form=~1|bird/feature))(AIC=39137.2) and corCompSymm correlation structure (corCompSymm(form=~1|bird/feature)) for the features within subject errors, with errors from different features within the same subject assumed to be independent. The model with compound symmetry correlation structure could not converge.

4.3.1.3 Adding additional covariates

To assess whether the variation in parameters is partially due to the difference in sites, the attribute site was brought in to the model as a covariate. The inclusion of site in the model did not improve the model (AIC=31560.87 against AIC=31556.31 for model without site). This leads us to the conclusion that the parameters do not vary between Bonaero Park and Modderfontein Pan.

4.3.1.4 Final multivariate mixed effects logistic model

The best multivariate non-linear mixed effects logistic model that describes the six growth variables is expressed as follows:

$$y_{ijk} = \frac{\alpha}{1+\exp[-\frac{t_{ijk}-\mu}{\beta}]} + \varepsilon_{ijk}, \varepsilon_{ijk} \sim N(0, \boldsymbol{R_{ik}}), \boldsymbol{b_i} \sim N(0, \boldsymbol{D}) \tag{4.7}$$

Where:

$\alpha = \alpha_1 + \sum_{k=2}^{6} \tau_k \alpha_k + b_{1i}$,

$\mu = \mu_1 + \sum_{k=2}^{6} \tau_k \mu_k + b_{2i}$,

$\beta = \beta_1 + \sum_{k=2}^{6} \tau_k \beta_k + b_{3i}$,

$\boldsymbol{R_{ik}} = \sigma^2 G_{ik}^{\frac{1}{2}}(\boldsymbol{\theta}, \boldsymbol{\delta}) \Gamma_{ik}(\alpha) G_{ik}^{\frac{1}{2}}(\boldsymbol{\theta}, \boldsymbol{\delta})$ with $\sigma = 0.43$,

$G_{ik}^{\frac{1}{2}} = \text{diag}[\sigma^2 |\mu_{ijk}|^{2\delta_k}]$,

$$\delta_k \in \begin{bmatrix} \delta_1 \\ \delta_2 \\ \delta_3 \\ \delta_4 \\ \delta_5 \\ \delta_6 \end{bmatrix} = \begin{bmatrix} 0.75 \\ 0.36 \\ 0.35 \\ 0.32 \\ 0.67 \\ 0.44 \end{bmatrix};$$

$$\boldsymbol{\Gamma}_{ik}(\alpha) = \begin{bmatrix} 1 & 0.74 & 0.74^2 & \dots & 0.74^{n_i-1} \\ & 1 & 0.74 & \dots & 0.74^{n_i-2} \\ & & \vdots & \dots & \vdots \\ & & & & 1 \end{bmatrix},$$

$\boldsymbol{D}$= diag$[1.81^2, 0.70^2, 0.30^2]$ and $\boldsymbol{\theta}$ is a vector of fixed and random effect parameters.

The estimates of reference values (parameters for body mass) and differences in parameter values between other body features and body mass are given in Table 4.11 and the fixed effects estimates and their standard errors are shown in Table 4.12.

Table 4.11: Estimates of reference values (α_1, μ_1 and β_1) and differences to these parameter values for other body features obtained from the multivariate logistic model for Grey-headed Gulls.

Estimates of reference values, differences in parameter values other features	Value	Std.Error	t-value	p-value
α_1 (reference value)	261.48	3.61	72.43	< 0.001
α_2	-231.31	3.63	-63.69	< 0.001
α_3	-214.64	3.62	-59.29	< 0.001
α_4	-182.35	3.64	-50.04	< 0.001
α_5	43.67	9.36	4.36	< 0.001
α_6	-168.59	3.64	-46.34	< 0.001
μ_1 (reference value)	12.39	0.18	68.02	< 0.001
μ_2	-7.94	0.43	-17.49	< 0.001
μ_3	-8.79	0.24	-36.98	< 0.001
μ_4	-9.38	0.27	-35.08	< 0.001
μ_5	14.01	0.53	26.54	< 0.001
μ_6	-11.02	0.20	-53.68	< 0.001
β_1 (reference value)	5.31	0.07	77.21	< 0.001
β_2	7.19	0.37	19.21	< 0.001
β_3	4.22	0.17	24.88	< 0.001
β_4	8.10	0.21	37.54	< 0.001
β_5	3.69	0.13	29.97	< 0.001
β_6	3.26	0.15	22.07	< 0.001

4.3.1.5 Model diagnostics

Having obtained the final model, it is important to assess the goodness of fit of this model by checking if the basic assumptions underlying non-linear mixed effects models are not violated. From the normal quantile plot (Figure.4.14), it appears that there are some departures from the assumption of normality for within-bird errors though Figure 4.15 shows a symmetric distribution for residuals mostly within the ± 2 range with small number of large positive and negative residuals. The plot of standardized residuals versus fitted values for all features (4.16) does not indicate any possible non-constant variance for within bird-errors rather it shows that we have predominantly fitted values less than 100 compared to a smaller number of fitted values greater than 100. Figure 4.17 is a repeat of the plot of standardized residuals versus fitted values but differentiates between different features.

We note that large negative residuals of within bird-errors are mostly associated with wing measurements. The scale of measurement for wing and mass is different from the scale of other features. The normal plots of random effects (Figure 4.18) do not indicate any departures from the normality assumption for random effects.

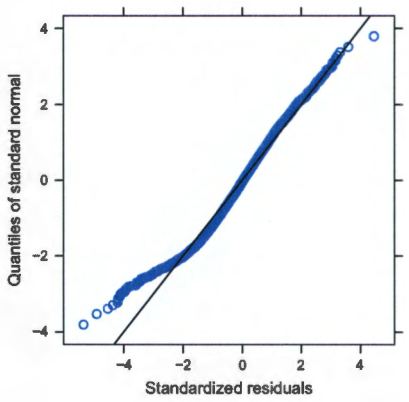

Figure 4.14: Normal quantile plot of standardized residuals from the final multivariate logistic model (eq. 4.7) for Grey-headed Gulls.

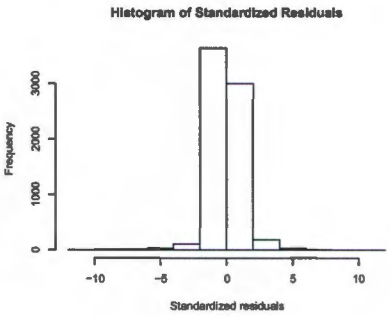

Figure 4.15: Histogram of standardized residuals obtained from the final multivariate logistic model (eq. 4.7) for Grey-headed Gulls.

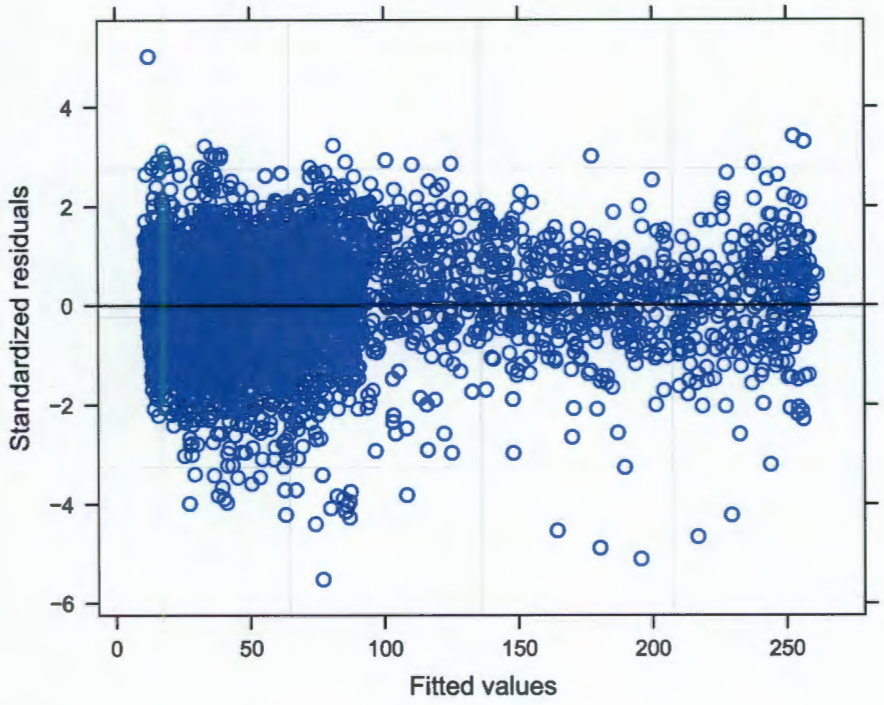

Figure 4.16: Standardized residuals obtained from the final multivariate logistic model (eq. 4.7) versus fitted values for all body features of Grey-headed Gulls.

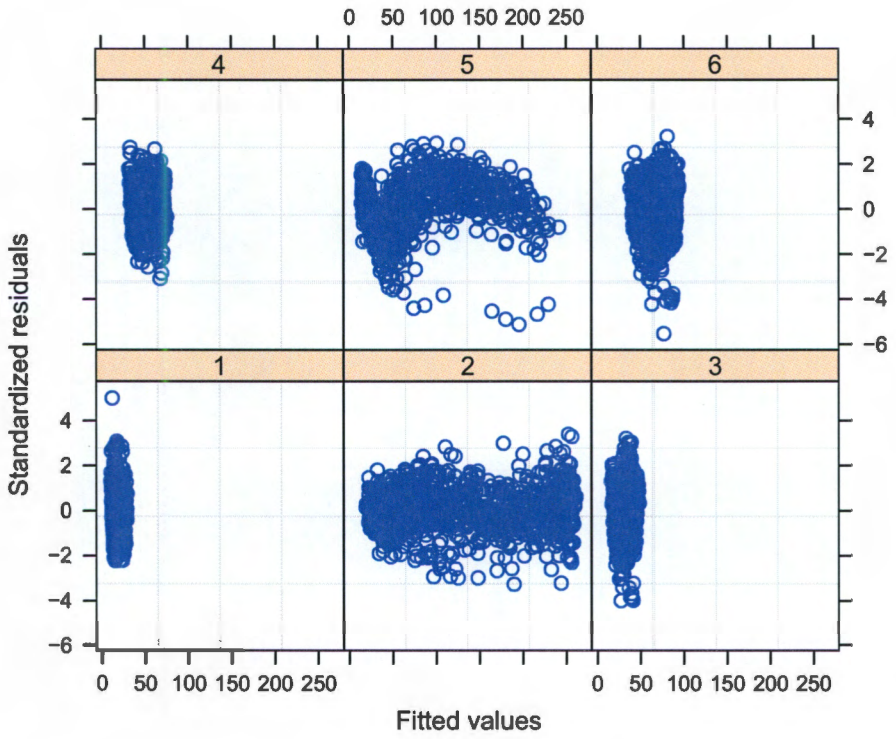

Figure 4.17: Standardized residuals obtained from the final multivariate logistic model (eq. 4.7) versus fitted values for each body feature of Grey-headed Gulls, 1=bill, 2=mass, 3=tarsus, 4=head, 5=wing, and 6=foot.

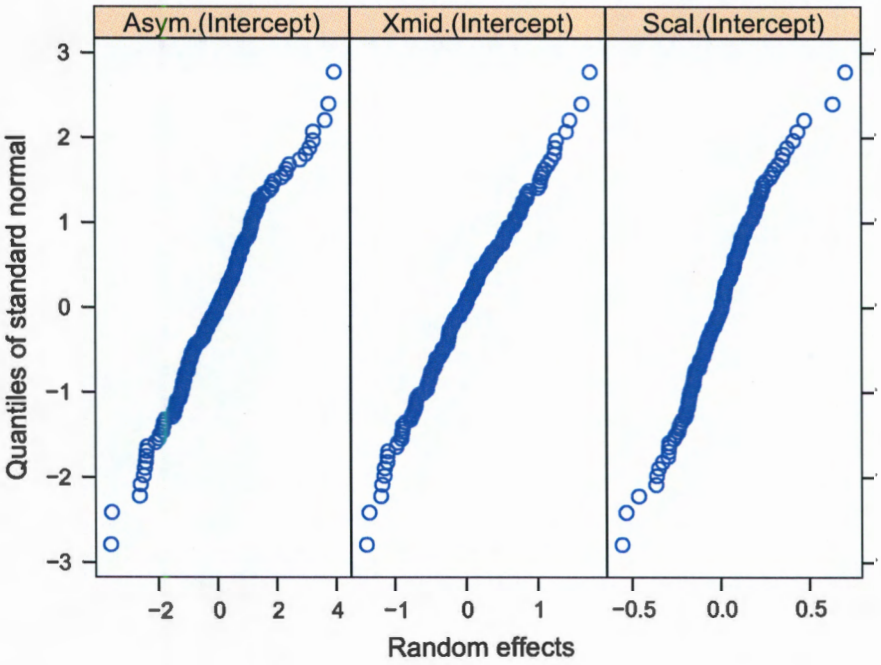

Figure 4.18: Normal plot of the estimated random effects corresponding to the final multivariate logistic model (eq. 4.7) for grey-headed gulls.

4.3.2 Multivariate non-linear mixed effects with other growth models: Gompertz and Richardss models

The strategy of the model building procedure illustrated in previous sections was followed in order to fit the multivariate Gompertz, Richards and inverse exponential models. Due to convergence difficulties, the multivariate inverse exponential model could not be fitted.

Multivariate Richards and Gompertz models

The best multivariate Gompertz model obtained was a three-parameter growth model where two of its fixed effects (lower asymptote and the estimate of instantaneous growth rate) were associated with random effects, with a diagonal variance-covariance structure for $\boldsymbol{D}$. The distribution of within-bird errors were best estimated by a normal distribution with mean zero and a variance power function for each growth variable. A first order autoregressive correlation function provided the best fit of within-bird errors. The fixed effects estimates are shown in Table 4.12.

For the multivariate Richards model, only the asymptote (α parameter) was associated with random effects. The within-bird errors were assumed to be equally correlated irrespective of their positions (ie. compound symmetry correlation structure, with a correlation coefficient $\alpha = 0.43$). It was also assumed that the distribution of within-bird errors followed a normal distribution with mean zero and variance modeled by a variance function changing as a power function of fitted values for each body feature ($\text{var}(\varepsilon_{ij}) = \sigma^2|\mu_{ij}|^{2\delta_k}$). The parameter estimates are provided in Table 4.12.

Table 4.12: Fixed effects estimates (standard errors) obtained from the multivariate **logistic, Gompertz and Richards** models for the six body features of Grey-headed Gulls.

Model		Body feature					
		Mass	Bill	Tarsus	Wing	Head	Foot
Logistic	AIC (30416.39)						
	α	261.48 (3.61)	30.17 (0.49)	46.85 (0.38)	305.18 (8.66)	79.14 (0.60)	92.90 (0.55)
	μ	12.39 (0.18)	4.45 (0.42)	3.60 (0.17)	26.40 (0.50)	3.00 (0.21)	1.37 (0.12)
	β	5.31 (0.07)	12.49 (0.37)	9.54 (0.16)	9.00 (0.11)	13.40 (0.21)	8.57 (0.13)
Gompertz	AIC (31379.95)						
	γ	16.71 (0.93)	12.36 (0.10)	18.90 (0.11)	9.52 (0.37)	35.21 (0.12)	42.55 (0.21)
	β	2.84 (0.05)	0.88 (0.02)	0.89 (0.01)	3.76 (0.03)	0.84 (0.01)	0.76 (0.01)
	μ	0.10 (0.002)	0.06 (0.002)	0.08 (0.002)	0.05 (0.001)	0.05 (0.001)	0.09 (0.002)
Richards	AIC (33101.14)						
	α	270.88 (4.27)	28.57 (0.45)	45.09 (0.35)	201.17 (3.75)	74.66 (0.55)	91.49 (0.55)
	μ	1.91 (0.21)	1.61 (0.39)	2.50 (0.26)	10.91 (1.15)	1.54 (0.20)	1.53 (0.25)
	β	0.17 (0.01)	0.12 (0.01)	0.17 (0.01)	0.40 (0.04)	0.11 (0.06)	0.15 (0.01)
	δ	0.83 (0.08)	2.13 (0.43)	3.05 (0.32)	4.30 (0.48)	2.31 (0.24)	2.31 (0.29)

4.3.3 Multiple comparisons of growth parameters

The asymptotic values for body features are of course expected to be different from each other and hence the multiple comparison for these parameters is of no interest. The multivariate logistic model enables us to compare directly the growth rates of different body features as the growth rates (μ and β) are expressed in the same unit (time). Tables 4.13 and 4.14 provide differences between estimated times to reach half of the asymptotes (μ), and the differences between estimates to grow from half to three quarters of the asymptote (β) for all features relative to one another. The time it takes to reach half of the asymptote for a feature appearing in a row is compared to the time it will take to reach half of the asymptote for a feature located in a corresponding column. A negative number indicates that it takes less time to get to half of the asymptote for a feature in a given row compared to the feature in the corresponding column. For instance, -7.94, in the second row first column of Table 4.13 indicates that to reach half of the asymptotic bill length it took approximately 8 days less than it took the mass of a gull to get to half of the asymptotic mass. The number in row 5 and column 1 (14.00) (Table 4.13) points out that the wing took 14 days longer, to reach half of the asymptote, than the body mass took to reach half of the maximum mass. Table 4.14 can be interpreted in a similar way. From these two tables, we noted that wing took longer than any other body feature to reach half of the asymptotic measurement followed by mass; not much of difference between bill, tarsus, head, and foot was observed. The bill and head took longer than other features to grow from half to three quarters of the asymptotic measurement and tarsus, wing and foot took approximately the same time.

Table 4.13: Estimates of differences (in days) (with standard errors) between parameters μ for the body features of Grey-headed Gulls.

Body feature	Mass	Bill	Tarsus	Head	Wing	Foot
Mass	–					
Bill	-7.94(0.45)	–				
Tarsus	-8.79(0.24)	-0.85(0.43)	–			
Head	-9.39(0.27)	-1.45(0.45)	-0.60(0.25)	–		
Wing	14.00(0.53)	21.95(0.65)	22.80(0.52)	23.39(0.53)	–	
Foot	-11.02(0.21)	-3.08(0.43)	-2.23(0.19)	-1.63(0.23)	-25.03(0.51)	–

Table 4.14: Estimates of differences (in days) (with standard errors) between parameters β for the body features of Grey-headed Gulls.

Body feature	Mass	Bill	Tarsus	Head	Wing	Foot
Mass	–					
Bill	7.19(0.37)	–				
Tarsus	4.22(0.17)	-2.96(0.39)	–			
Head	8.09(0.21)	0.90(0.41)	3.86(0.17)	–		
Wing	3.69(0.13)	-3.49(0.38)	-0.53(0.19)	-4.40(0.23)	–	
Foot	3.25(0.15)	-3.93(0.39)	-0.97(0.20)	-4.83(0.24)	-0.43(0.17)	–

4.4 Comparison of univariate and multivariate growth models

The logistic model was considered to provide a better description of the joint growth body features since it had the smallest AIC (30416.39, Table 4.12) among other multivariate models.

The parameters obtained from the multivariate model for body mass, bill length, tarsus length, head length, and foot length are similar to those obtained from the univariate non-linear mixed effects models (Table 4.15). However, for wing length, there were some differences. For instance, the asymptotic wing length obtained from the multivariate logistic model was 305.18 mm whereas 349.40 mm was the estimate obtained from the univariate logistic model. The estimated time for the wing to grow to half of the asymptotic length was 26.40 days from the multivariate logistic against 29.14 days obtained from the univariate logistic model. Also, the wing growth rate estimates obtained form the multivariate and the univariate Gompertz models were different. The multivariate Gompertz model indicated that the wing grew at rate of 3.76 mm per day with a decreasing rate of 0.05 mm per day whereas the univariate Gompertz gave a growth rate of 4.38 mm per day at decreasing rate of 0.03 mm per day (Table 4.15). For the logistic models, there is a good correspondence between the univariate and multivariate curves (Figure 4.19). From this graph it can be seen that there is good correspondence for ages where lots of data is available and that curves differ only where there is very little data.

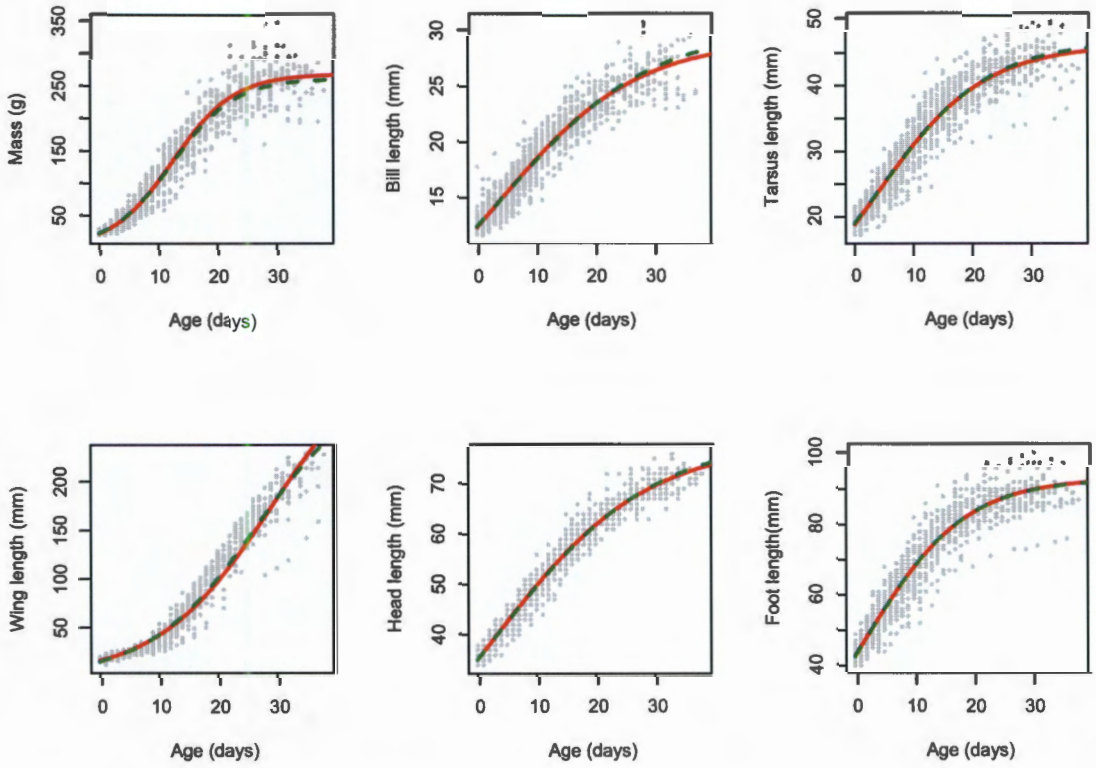

Figure 4.19: Predicted curves from the univariate (solid red line) and multivariate (dotted green line) non-linear mixed effects logistic models superimposed on observed values (grey dots) of the six body features of Grey-headed Gulls.

The major difference between these approaches were that with the multivariate modelling approach it was possible to carry out multiple comparisons between the growth rates for different body features (Tables 4.13, 4.14).

Table 4.15: Comparison of fixed effects estimates obtained from the univariate and multivariate **logistic, Gompertz and Richards** models for the six body features of Grey-headed Gulls.

Model		Body feature					
		Mass	Bill	Tarsus	Wing	Head	Foot
Mult.logistic							
Uni.logistic							
	α	261.48 (3.61)	30.17 (0.49)	46.85 (0.38)	305.18 (8.66)	79.14 (0.60)	92.90 (0.55)
		268.42 (5.13)	29.19 (0.40)	46.22 (0.41)	349.40 (14.86)	78.11 (0.52)	93.10 (0.79)
	μ	12.39 (0.18)	4.45 (0.42)	3.60 (0.17)	26.40 (0.50)	3.00 (0.21)	1.37 (0.12)
		12.45 (0.22)	3.59 (0.33)	3.39 (0.16)	29.14 (0.3)	2.61 (0.14)	1.36 (0.14)
	β	5.31 (0.07)	12.49 (0.37)	9.54 (0.16)	9.00 (0.11)	13.40 (0.21)	8.57 (0.13)
		5.21 (0.07)	11.68 (0.31)	9.21 (0.15)	9.64 (0.13)	12.98 (0.18)	8.65 (0.19)
Mult.Gompertz							
Uni.Gompertz							
	γ	16.71 (0.93)	12.36 (0.10)	18.90 (0.11)	9.52 (0.37)	35.21 (0.12)	42.55 (0.21)
		21.21 (0.34)	12.11 (0.08)	19.11 (0.09)	15.25 (0.12)	35.15 (0.12)	42.84 (0.20)
	β	2.84 (0.05)	0.88 (0.02)	0.89 (0.01)	3.76 (0.03)	0.84 (0.01)	0.76 (0.01)
		2.83 (0.03)	0.93 (0.02)	1.00 (0.01)	4.38 (0.11)	0.88 (0.01)	0.82 (0.01)
	μ	0.10 (0.002)	0.06 (0.002)	0.08 (0.002)	0.05 (0.001)	0.05 (0.001)	0.09 (0.002)
		0.08 (0.002)	0.06 (0.002)	0.006 (0.002)	0.02 (0.001)	0.05 (0.001)	0.08 (0.003)
Mult.Richards							
Uni.Richards							
	α	270.88 (4.27)	28.57 (0.45)	45.09 (0.35)	201.17 (3.75)	74.66 (0.55)	91.49 (0.55)
		291.00 (5.90)	27.10 (0.34)	44.36 (0.37)	236.27 (2.11)	74.21 (0.68)	90.86 (1.36)
	μ	1.91 (0.21)	1.61 (0.39)	2.50 (0.26)	10.91 (1.15)	1.54 (0.20)	1.53 (0.25)
		1.00 (0.28)	2.66 (0.45)	2.33 (0.25)	4.40 (0.18)	1.74 (0.24)	1.17 (0.45)
	β	0.17 (0.01)	0.12 (0.01)	0.17 (0.01)	0.4 (0.04)	0.11 (0.06)	0.15 (0.01)
		0.14 (0.008)	0.16 (0.02)	0.17 (0.01)	0.17 (0.006)	0.11 (0.008)	0.14 (0.02)
	δ	0.83 (0.08)	2.13 (0.43)	3.05 (0.32)	4.3 (0.48)	2.31 (0.24)	2.31 (0.29)
		0.51 (0.08)	3.53 (0.06)	2.92 (0.29)	1.58 (0.07)	2.57 (0.31)	1.93 (0.49)

4.5 Summary: Growth of Grey-headed Gulls

This paragraph gives a summary of the growth process of a Grey-headed Gull chick by showing graphically the growth patterns for its different body features and by indicating the order in which the completion of the growth process occurs. Figure 4.20 indicates that about 40% or more of the growth process for foot, head, bill, and tarsus is completed before the chick hatches. It is also revealed that these body parts exhibited similar growth patterns (Figure 4.20). For wing and body mass, less than 20% of the growth process is completed during the incubation period. A sharp increase in body mass is observed in the first three weeks (about 20 days), followed by a slow change for about 10 days until the maximum mass is reached. The foot growth was estimated to attain its maximum at 30 days. After 40 days, the tarsus length was very close to asymptote length. Head and bill stopped growing approximately after 50 days. Wing growth was noted to take longer compared to other features. Figure 4.20 indicates that after 60 days the growth in wing length is still incomplete. Based on these observations, we may conclude that the growth for the five body features of Grey-headed Gulls attains the completion in the following order: (foot, body mass,tarsus)-(head,bill)-(wing).

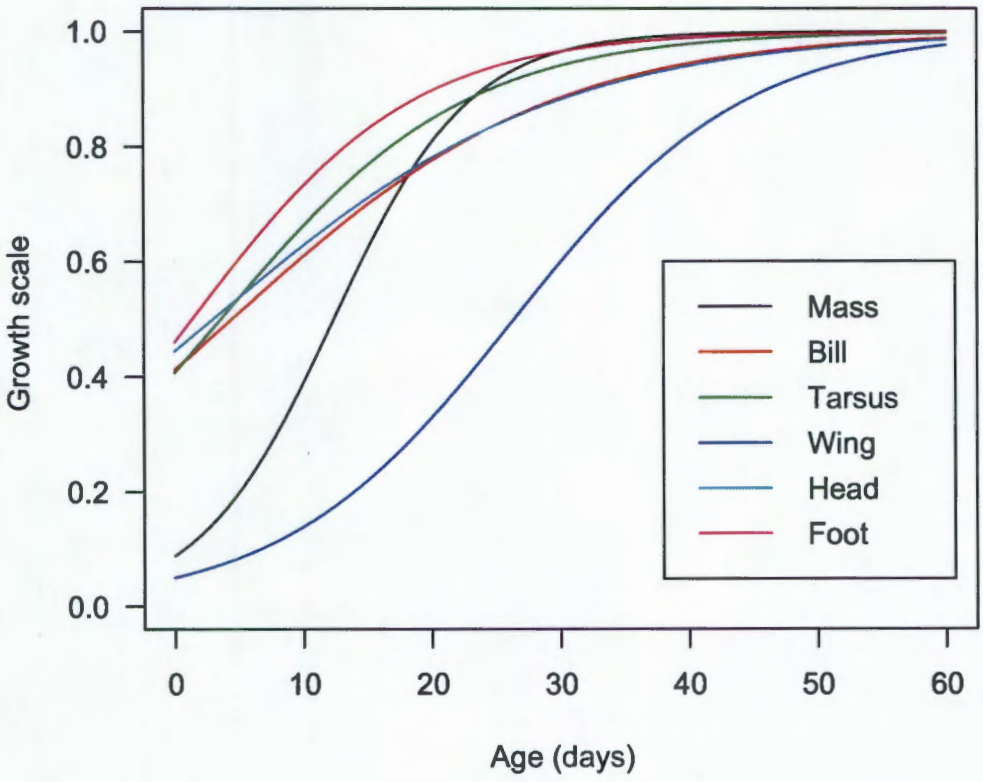

Figure 4.20: Scaled predicted curves obtained from the multivariate logistic model for the six body features of Grey-headed Gulls.

4.6 Analysis of Swift Tern data

The exact age at first capture was not known for each bird. Only the date and measurements taken from each body feature, at each occasion, were available for each bird. Figure 4.21 illustrates the different measurements taken on successive occasions for each feature. The separation between time points is clearly seen. Of note is the wide range of measurements at each time point. At day one of the follow up period, birds were classified into two age groups: nestling and runner. Therefore, it was imperative to determine the age at first capture in order to fit growth curves to this data. In section 4.6.1, we therefore describe the method used to determine age.

Richards, logistic, Gompertz and inverse exponential models were fitted to this data set and the best model was selected based on AIC. In fitting these growth curves to Swift Tern data, we followed all the steps described in section 4.1. For univariate modelling approach, a variance function with a constant plus a power of fitted values ($\text{var}(\varepsilon_{ij})=\sigma^2(\delta_1+|\mu_{ij}|^{\delta_2})^2$, was used for within-bird errors, whereas a first order autoregressive correlation for within-bird errors was assumed. With multivariate modelling approach, a *VarIdent* variance function model ($\text{var}(\varepsilon_{ij})=\sigma^2(\delta_k)$, which represents a variance model with different variances for each body feature, and a corAR1 correlation structure with features nested within bird (corAR1(form=$\sim$1|bird/feature)) were used for within-bird errors. k=1,...,6 and denotes body features. For both univariate and multivariate modelling approaches, the random effects were assumed to be independent of each other (a diagonal variance-covariance matrix for random effects was used).

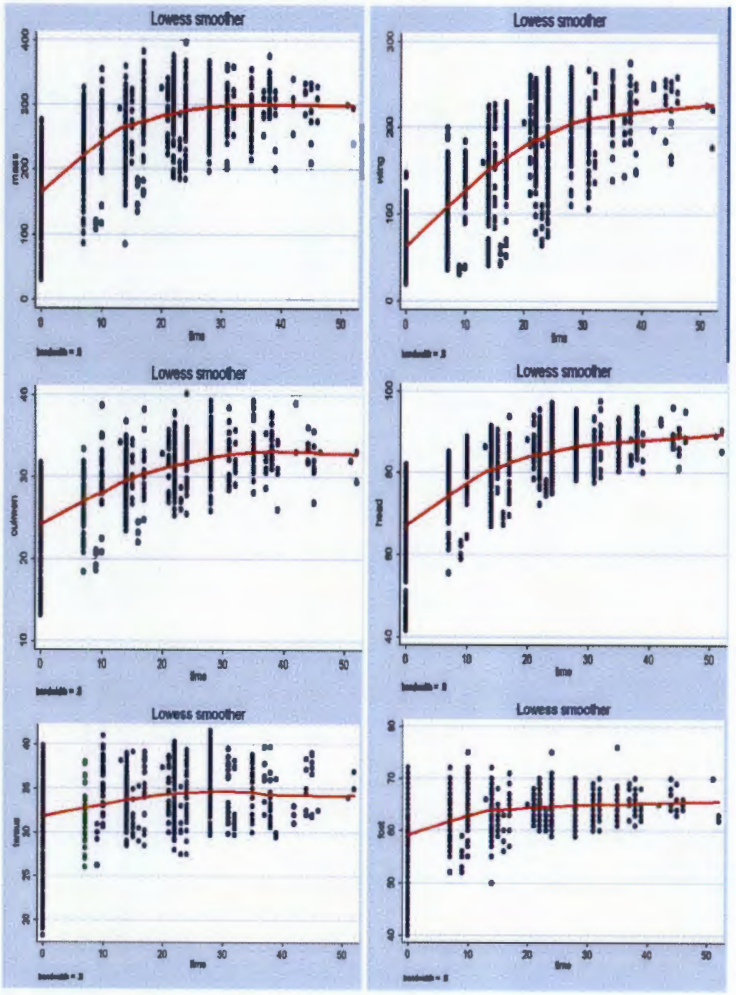

Figure 4.21: Loess curves superimposed on growth data for each of the six body features of Swift Terns before age of each chick at first capture was estimated.

4.6.1 Age determination

Qualitative and quantitative methods are often used to predict ages of young and adult birds. Emlen (1936) used the size, shape, and colour of body plumage and flight features to determine ages of American Crow. Quantitative methods use a sample of birds whose ages are known to construct models for age calculation for other birds (e.g. Scott and Ankney (1992), and Sanchez-Guzman and Viejo (1990)). For this study, a method based on optimization was used to determine the age at day one of the follow up period.

Method description

For the 34 nestling birds we assumed that age at first capture (t_0) was two days. We then fitted a logistic model to body mass for these nestling birds:

$$y_{it} = \frac{\alpha}{1 + \exp(-\frac{t-\mu}{\beta})} \tag{4.8}$$

We then fixed $\widehat{\alpha}$, $\widehat{\mu}$ and $\widehat{\beta}$ at the estimates generated from the above model given (equation 4.8). Then, for each of the runner birds, we found the logistic curve which fitted the observed measurements most closely by minimizing the sum of absolute residuals to the observed values (Figure 4.22) and by assuming that the growth rate parameters (μ and β) were equal for birds and that individuals should only differ in their asymptotic weights (i.e. allowed the asymptote (α) to differ from $\widehat{\alpha}$ by adding $\triangle\alpha_i$. Also, we allowed the age to differ from time 0 (day at first capture). The growth curve for runners can then be described as follows:

$$y_{it} = \frac{\widehat{\alpha} + \triangle\alpha_i}{1 + \exp(-\frac{t+\triangle t_i-\widehat{\mu}}{\widehat{\beta}})} \tag{4.9}$$

where y_{it} is the body mass for bird i measured at age t, $\triangle\alpha_i$ is the difference in asymptotes compared to $\widehat{\alpha}$ and $\triangle t_i$ is the actual age at first capture (days) . The aim was to determine $\triangle t_i$, which quantifies the age of the bird at day 0 (first capture for the particular bird). We used the "optim" function in R (R Development Core Team, 2006) to estimate $\triangle t_i$. $\triangle\alpha_i$ and $\triangle t_i$ were constrained to lie between $\widehat{\alpha}\pm$ 55 and 2 $\pm$30, respectively.

The impact of changing these bounds was assessed as follows. For $\triangle\alpha_i$ we used the bounds of $\pm$ 55, $\pm$65, $\pm$ 70 and for age we used the bounds of $\pm$ 10, $\pm$30, $\pm$ 40, $\pm$ 45, $\pm$ 50, and $\pm$ 100. Except for the bound $\pm$ 10 for age, more than 90 % of the estimates of $\triangle t_i$ were similar for other intervals. Table 4.16 gives some summary statistics of estimates of $\triangle t_i$ and $\triangle\alpha_i$. Age at each occasion was then calculated as $t + \triangle t_i$. Then y_{it} (growth measurements for each growth feature) was modeled against $t + \triangle t_i$. In the age determination method, body mass was used because this feature exhibits quite often a strong correlation with time. It was also assumed that asymptotes vary between birds since it is naturally unlikely that all birds have the same maximum mass even if their lower asymptotes were the same at hatching. The empirical growth plots of Swift Tern growth data against estimated age at each occasion $(t + \triangle t_i)$ (Figure 4.23), for each body feature, seem to give clear patterns of individual change over time.

Table 4.16: summary statistics for estimates of $\triangle t_i$ (the actual age at first capture) and $\triangle\alpha_i$ (the difference in asymptotes) for Swift Terns, using bounds of $\pm$55 for asymptote and $\pm$30 for age.

	Min	Lower quartile	Median	upper quartile	Max
$\triangle t_i$	0.89	11.71	16.87	19.50	40
$\triangle\alpha_i$	-55	-18.22	3.79	24.37	55

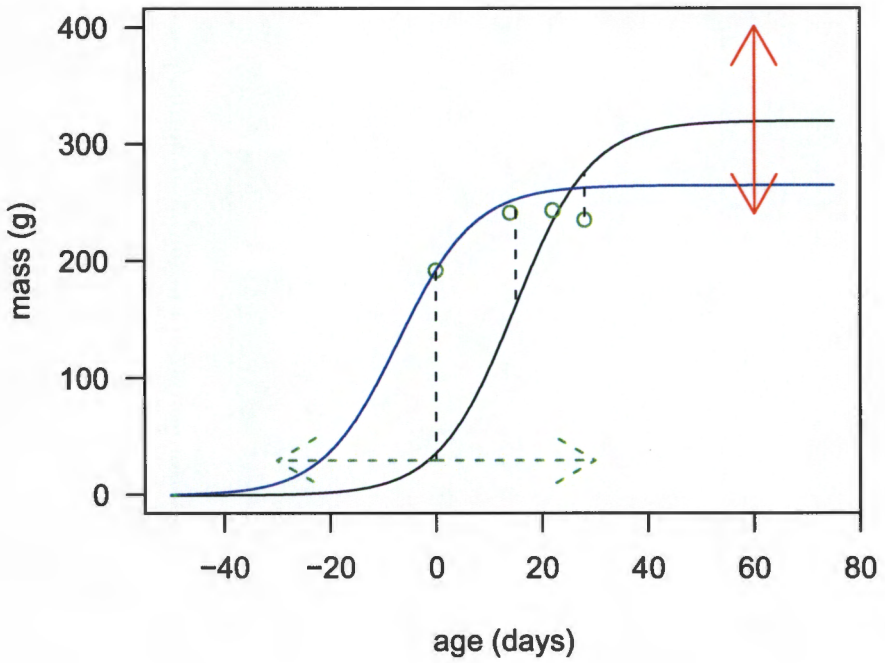

Figure 4.22: Predicted curve for nestling bird masses (black line) and the optimized curve for bird number 199 (blue line), arrows indicate the ranges over which $\Delta\alpha_i$ and Δt_i were allowed to vary $\Delta\alpha_i = -55$ and $\Delta t_i = 21.85$ for this bird.

4.6.2 Growth curve modelling

4.6.2.1 Univariate modelling

Logistic, Gompertz, Richards, and inverse exponential models were fitted to each of the growth variables. Based on the AIC statistic it was found that the inverse exponential model provided the best description of growth for culmen (bill), head, tarsus, and foot; but was a poor model for mass and could not be fitted to wing length (Table 4.17). Estimates of lower asymptotes, denoted by γ, obtained from Gompertz and inverse exponential models are very similar (Table 4.17) except for mass. The logistic model gave approximately the same asymptotes as the inverse exponential model (Table 4.17).

The Richards growth model could not be fitted to culmen (bill), head, tarsus, and foot length but it provided asymptotes for mass and wing that are close to those obtained from the logistic model (Table 4.17).

4.6.2.2 Multivariate modelling

Neither the Richards model nor the inverse exponential model could fit simultaneously all six variables. This was disappointing because the inverse exponential was the best univariate fit for 4 of the 6 features. However, we suspect the reason for this is the wing which, could not be modelled by the inverse exponential. The multivariate logistic model was considered as the best model since it had the smallest AIC (37385.75 against 37848.40 for multivariate Gompertz model, Table 4.18).

We assessed the goodness of fit of the best model (logistic model) through graphical method (i.e. inspection of diagnostic plots). The histogram of standardized residuals (4.24) indicates that there are some measurements over and under-estimated by the model from both tails, which causes deviation from normality. Figure 4.25 and 4.26 are plots of standardized residuals versus fitted values for all features together and for each feature, respectively. These figures show large within bird-errors were mostly for mass and wing measurements.

The results from multivariate Gompertz and logistic models (Table 4.18) are used for interpretation of results for swift tern data. The multivariate approach and univariate approach provided similar results (Table 4.19).

Gompertz model (Table 4.18) :

A nestling Swift Tern had a body mass that changed from approximately 30 g at hatching with an initial growth rate of 2.40 g/day with a decreasing rate of 0.09 g/day. The wing length of a Swift Tern chick grew from 5.96 mm at an initial instantaneous growth of 4.04 mm/day with a decreasing rate of 0.06 mm/day. At hatching, the culmen (bill) had a length of 14.71 mm, which increased at an initial growth of 0.87 mm/day with a decreasing rate of 0.06 mm/day. A hatched Swift Tern chick had a head length of 45.34 mm, which grew at rate of 0.74 mm/day with

a decreasing rate of 0.55 mm/day. The tarsus grew from an initial length of 18.88 mm with an initial instantaneous growth rate of 0.61 mm/day at a decreasing rate of 0.18 mm/day. At hatching day, a Swift Tern chick foot had grown almost up to 64 % (41.75 mm) of the asymptote (65.38 mm) and 50% of the growth had been reached approximately 6 days before hatching (-5.84).

Logistic model (Table 4.18) :

It was approximated that at week two (14 days after hatching) the body mass was half the asymptotic mass (317.58 g). Within about four weeks (28.18 days), the wing was estimated to be 142.69 mm long, which is the equivalent of half of the asymptote wing length (285.39 g). Approximately three days after hatching, the culmen (bill) had grown to 17.26 mm (half of the asymptote). It was approximated that even before hatching day (-0.07 days) the head length reached the half of the maximum head length. About two days (-2.64 days) before hatching, the tarsus had already reached half of the asymptotic length (34.91 mm), with foot attaining half of the maximum length (65.38 mm) within 6 days before hatching (μ=-5.84).

Table 4.17: Fixed effects estimates (with their standard errors in brackets) obtained from the univariate **logistic, Gompertz, inverse exponential and Richards** growth models for all six body features of Swift Terns.

		Body feature					
Model		Mass	Bill	Tarsus	Wing	Head	Foot
Logistic	AIC	**10465.84**	3656.967	4146.841	**8785.914**	4863.988	5169.982
	α	**316.34 (2.36)**	34.01 (0.21)	34.68 (0.15)	**286.15 (2.26)**	92.35 (0.31)	65.29 (0.17)
	μ	**14.00 (0.16)**	3.48 (0.32)	-0.94 (0.38)	**28.16 (0.22)**	0.46 (0.24)	−4.28 (0.33)
	β	**7.48 (0.11)**	11.11 (0.37)	5.14 (0.35)	**9.65 (0.09)**	13.54 (0.20)	7.33 (0.24)
Gompertz	AIC	10620.71	3633.416	4147.47	8872.747	4764.136	5168.414
	γ	34.80 (1.37)	14.45 (0.41)	18.26 (0.64)	7.51 (0.41)	46.32 (0.44)	40.43 (0.51)
	β	2.27 (0.04)	0.89 (0.02)	0.64 (0.03)	3.93 (0.05)	0.73 (0.01)	0.48 (0.01)
	μ	0.08 (0.002)	0.06 (0.003)	0.17 (0.012)	0.05 (0.001)	0.05 (0.001)	0.13 (0.004)
Inverse exponetial	AIC	10598.36	**3609.783**	**4146.343**	–	**4681.819**	**5121.345**
	γ	−6.72 (4.53)	**14.10 (0.45)**	**17.08 (0.15)**	–	**44.44 (0.55)**	**47.23 (0.89)**
	α	369.48 (4.91)	**36.18 (0.38)**	**34.72 (0.15)**	–	**98.07 (0.48)**	**66.17 (0.19)**
	β	0.04 (0.001)	**0.05 (0.002)**	**0.16 (0.011)**	–	**0.04 (0.001)**	**0.08 (0.004)**
Richards	AIC	10485.42	–	–	8976.06	–	–
	α	334.71 (3.32)	–	–	296.03 (4.86)	–	–
	μ	−2.18 (1.76)	–	–	2.54 (0.26)	–	–
	β	0.08 (0.004)	–	–	0.09 (0.005)	–	–
	δ	0.05 (0.08)	–	–	0.88 (0.10)	–	–

Table 4.18: Fixed effects estimates (with their standard errors in brackets) obtained from the multivariate **logistic and Gompertz** models for the six body features of Swift Terns.

		Body feature					
Model		Mass	Bill	Tarsus	Wing	Head	Foot
Logistic	AIC (37385.75)						
	α	317.58 (1.91)	34.52 (0.24)	34.91 (0.22)	285.39 (2.76)	93.25 (0.31)	65.38 (0.20)
	μ	14.06 (0.23)	2.81 (0.38)	−2.64 (0.51)	28.18 (0.29)	−0.07 (0.23)	−5.84 (0.44)
	β	7.85 (0.14)	12.27 (0.43)	5.78 (0.38)	9.87 (0.13)	14.56 (0.24)	7.98 (0.28)
Gompertz	AIC (37848.40)						
	γ	29.97 (1.95)	14.71 (0.34)	18.88 (0.84)	5.96 (0.54)	45.34 (0.36)	41.75 (0.65)
	β	2.40 (0.06)	0.87 (0.20)	0.61 (0.04)	4.04 (0.08)	0.74 (0.007)	0.44 (0.01)
	μ	0.09 (0.002)	0.06 (0.002)	0.18 (0.01)	0.06 (0.001)	0.055 (0.001)	0.13 (0.005)

Table 4.19: Comparison of parameter estimates obtained from univariate and multivariate **logistic and Gomprtz** models for the six body features of Swift Terns.

		Body feature					
Model		Mass	Bill	Tarsus	Wing	Head	Foot
Mult.logistic							
Uni.logistic							
	α	317.58 (1.91)	34.52 (0.24)	34.91 (0.22)	285.39 (2.76)	93.25 (0.31)	65.38 (0.20)
		316.34 (2.36)	34.01 (0.21)	34.68 (0.15)	286.15 (2.26)	92.35 (0.31)	65.29 (0.17)
	μ	14.06 (0.23)	2.81 (0.38)	-2.64(0.51)	28.18 (0.29)	-0.07 (0.23)	-5.84 (0.44)
		14.00 (0.16)	3.48 (0.32)	-0.94 (0.38)	28.16 (0.24)	0.46 (0.24)	-4.28 (0.33)
	β	7.85 (0.14)	12.27 (0.43)	5.78 (0.38)	9.87 (0.13)	14.56 (0.24)	7.98 (0.28)
		7.48 (0.11)	11.11 (0.37)	5.14 (0.35)	9.65 (0.09)	13.54 (0.20)	7.33 (0.24)
Mult.Gompertz							
Uni.Gompertz							
	γ	29.97 (1.95)	14.71 (0.34)	18.88 (0.84)	5.96 (0.54)	45.34 (0.36)	41.75 (0.65)
		34.80 (1.37)	14.45 (0.41)	18.26 (0.64)	7.51 (0.41)	46.32 (0.44)	40.43 (0.51)
	β	2.40 (0.06)	0.87 (0.20)	0.61 (0.04)	4.04 (0.08)	0.74 (0.007)	0.44 (0.01)
		2.27 (0.04)	0.89 (0.02)	0.64 0.03()	3.93 (0.05)	0.73 (0.01)	0.48 (0.01)
	μ	0.09 (0.002)	0.06 (0.002)	0.18 (0.01)	0.06 (0.001)	0.05 (0.001)	0.13 (0.005)
		0.08 (0.002)	0.06 (0.003)	0.17 (0.01)	0.05 (0.001)	0.05 (0.001)	0.13 (0.004)

4.6.3 Multiple comparisons of growth parameters

The multivariate logistic model provides an easy and meaningful multiple comparison of growth rates between features as all growth parameters have the same units (days) irrespective of units of the features. Tables(4.20, 4.21) provide differences between estimates of time to reach half of asymptotes among features and between estimates of time to increase from half to three quarters of the asymptotes for different features. A feature in a given row is compared to a feature in any column. For instance, 15.07 (second row and first column of Table 4.20) indicates that for a wing it took 15.07 days longer to reach half of the maximum wing length than it took mass to reach half of the asymptotic body mass. The value -10.67 (row 1 and column 1 of Table 4.20) implies that it took the culmen 10.67 days less to reach half of its asymptotic length than it took mass to reach half of the maximum body mass. The interpretation of the values in Table 4.21 is handled in a similar way as Table 4.20. From these two tables, it can be observed that wing took longer than other boy features to reach half of asymptotic values followed by mass. But not much differences between bill, tarsus, head and foot with respect to time taken to reach half of asymptotes. The head, culmen (bill) and wing took longer time to grow from half to three quarters of asymptotes compared to other body features which do not show much differences in growing from half to three quarters of asymptotes.

Table 4.20: Estimates of differences (in days) (with standard errors) between growth parameters μ for the body features of swift terns

Body feature	Mass	Wing	Culmen	Head	Tarsus	Foot
Mass	–					
Wing	14.11 (0.30)	–				
Culmen	-11.08 (0.36)	-25.20 (0.40)	–			
Head	-14.13 (0.24)	-28.24 (0.30)	-2.97 (0.39)	–		
Tarsus	-16.70 (0.51)	-30.82 (0.54)	-5.66 (0.60)	-2.57 (0.50)	–	
Foot	-19.90 (0.44)	-34.02 (0.48)	-8.89 (0.54)	-5.77 (0.42)	-3.20 (0.59)	–

Table 4.21: Estimates of differences (in days) (with standard errors) between growth parameters β for the body features of Swift Terns.

Body feature	Mass	Wing	Culmen	Head	Tarsus	Foot
Mass	–					
Wing	2.02 (0.19)	–				
Culmen	4.26 (0.42)	2.24 (0.42)	–			
Head	6.71 (0.27)	4.68 (0.27)	2.55 (0.50)	–		
Tarsus	-2.08 (0.41)	-4.10 (0.41)	-6.41 (0.58)	-8.78 (0.44)	–	
Foot	0.13 (0.31)	-1.89 (0.31)	-4.15 (0.52)	-6.57 (0.36)	2.21 (0.47)	–

4.7 Summary: Growth of Swift Tern chicks

For each body feature, the predictions obtained from the logistic multivariate model were scaled by dividing these predictions by the asymptotic value. The scaled values were plotted against time to produce Figure 4.28, which describes and compares growth of different body features. From this figure it is estimated that $\pm$ 20 days after hatching, the foot and tarsus of a tern chick have attained the maximum length. For the head, culmen and body mass, it appears that their growth is completed approximately within 50 days. The wing takes longer to reach the maximum length relative to other body parts because after 60 days the growth in wing length is still not completed. It was not determined at which age the wing is completely developed as no data were available for birds older than 60 days as at this time they are able to fly and cannot be easily captured. Figure 4.27 reveals that foot and tarsus exhibit similar growth patterns and also that head and bill have same growth patterns. It also shows that the univariate inverse exponential, univariate and multivariate Gompertz models fitted equally well the bill, head, tarsus and foot growth data of Swift Terns.

From these observations, it may be deduced that the growth of Swift Tern body features follows the following order: (Foot, Tarsus)- (body mass, bill, Head)-Wing. This growth pattern seems to be justified as it responds to the gradual adaptation of a chick to environmental conditions : adapt to the life in creche first (through developed feet and tarsus), followed by developing the capability of getting food on its own (with a developed culmen), and finally the development of wings so that a chick can fly with the parents in the hunt of best feeding areas.

The wing has the highest instantaneous growth rate (3.91 mm per day) but starting with low rate, followed by the body mass which has a growth rate of 2.09 g per day. The culmen and the head have a rate of 0.91 mm/day and 0.74 mm /day, respectively. The tarsus and the foot the last lowest instantaneous growth rates, 0.63 mm/day and 0.45 mm/day, respectively. In contrast, the tarsus and foot have their instantaneous growth rates decreasing at the highest rates (0.16 mm per day and 0.11 mm per day, respectively). This is the reason why these body features reach the completion of the growth while other features such as wing and culmen are still growing.

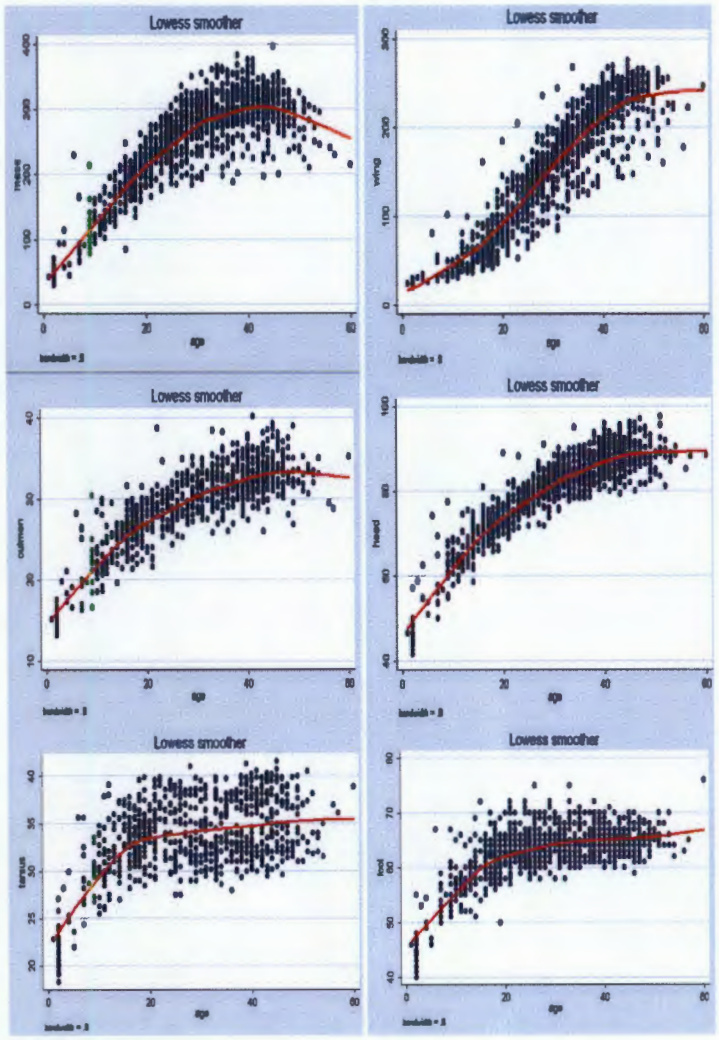

Figure 4.23: Loess curves superimposed on growth data for each of the six body features of Swift Terns after age of each chick at first capture was estimated.

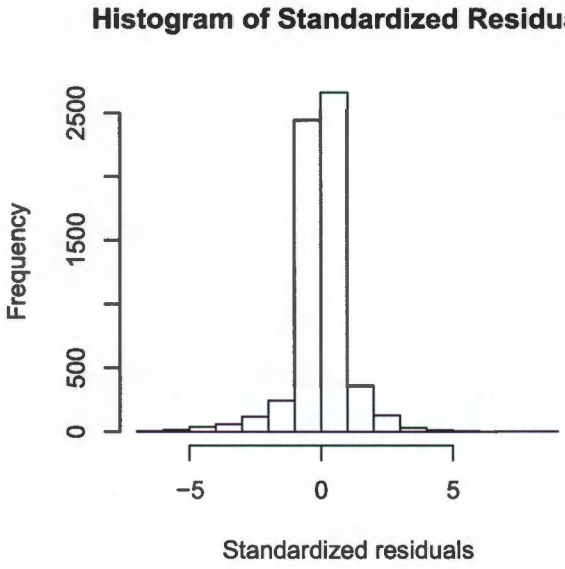

Figure 4.24: Histogram of standardized residuals obtained from the final multivariate logistic model for all six features of Swift Terns.

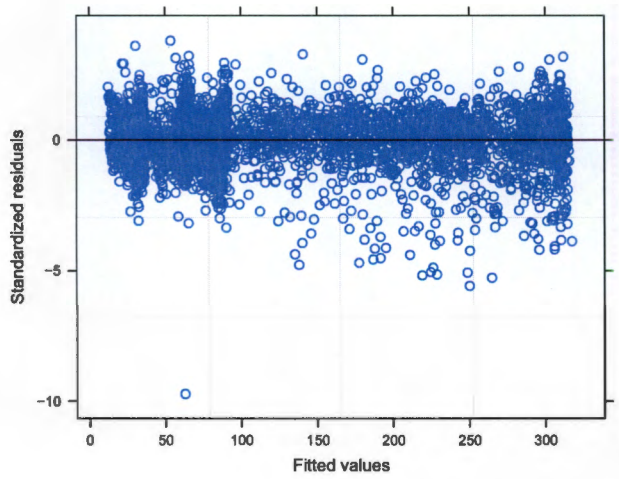

Figure 4.25: Standardized residuals obtained from the final multivariate logistic model versus fitted values for all six body features of Swift Terns.

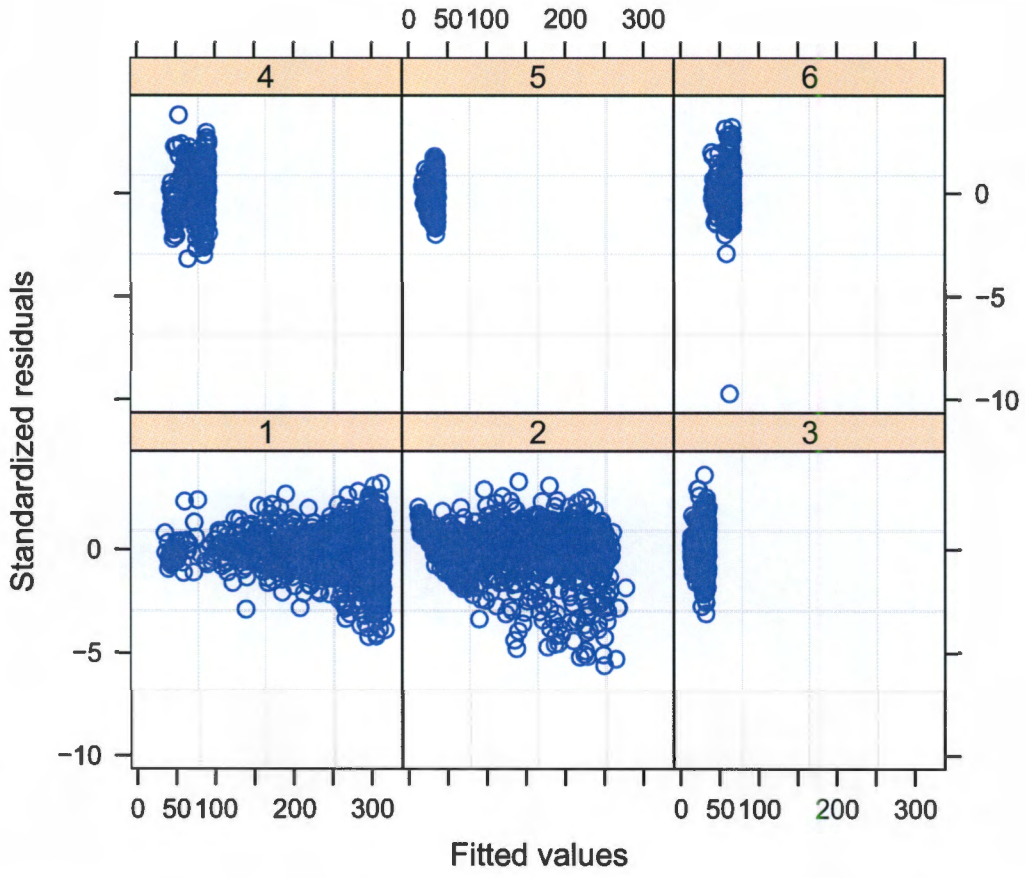

Figure 4.26: Standardized residuals obtained from the final multivariate logistic model versus fitted values for each feature of Swift Terns, 1=mass, 2=wing, 3=culmen (bill), 4=head, 5=tarsus, and 6=foot.

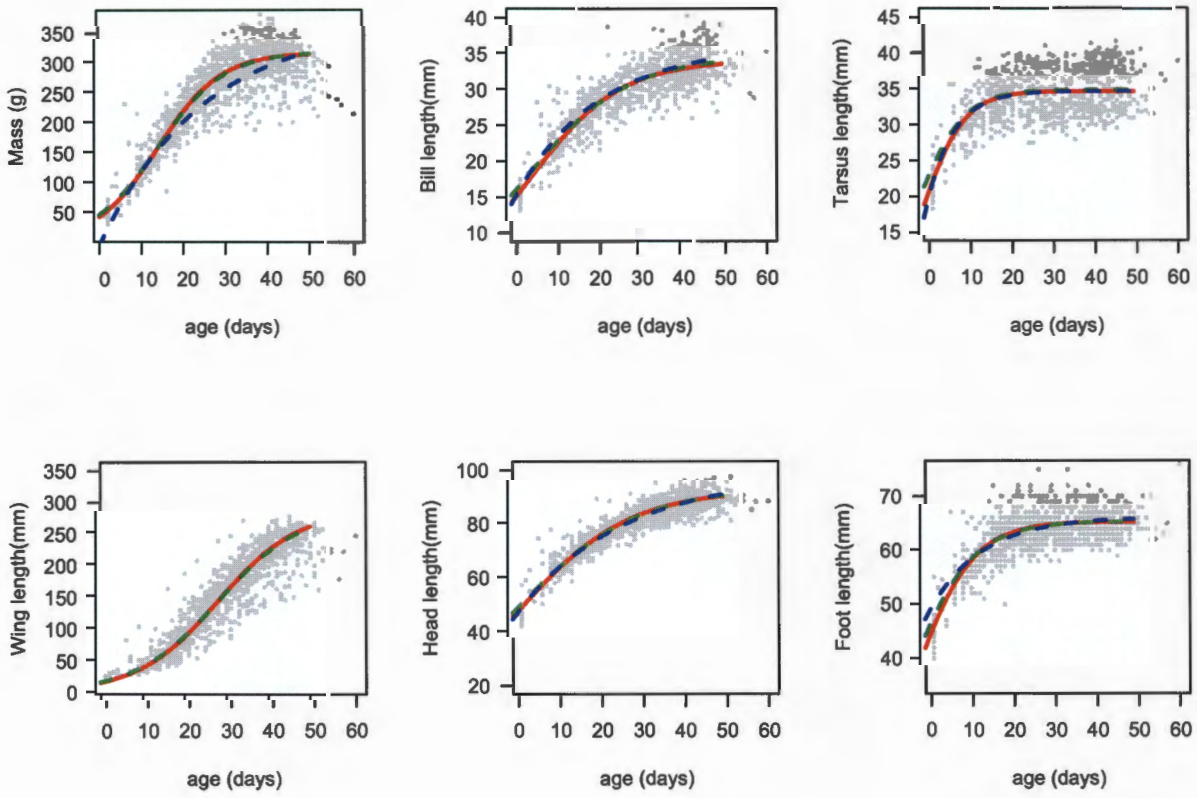

Figure 4.27: Predicted curves obtained from univariate inverse exponential (blue dotted line), univariate (red line) and multivariate (dotted green line)logistic growth models superimposed on growth data (grey dots) for the six body features of Swift Terns.

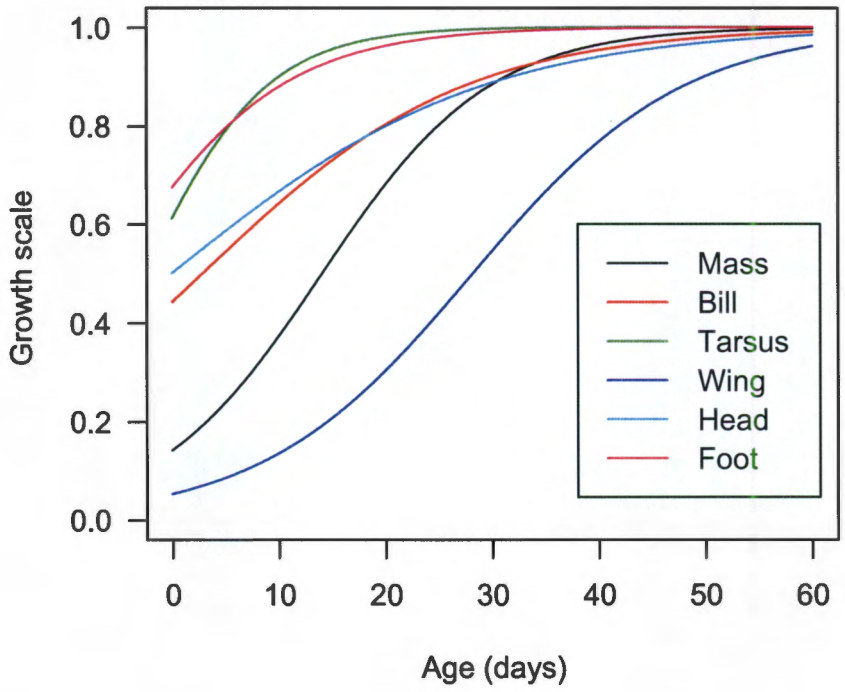

Figure 4.28: Scaled predicted growth curves obtained from the multivariate logistic growth models for the six body features of Swift Terns.

Chapter 5

Conclusions

In this chapter, we revisit our primary objectives in order to evaluate wether they have been achieved, we draw conclusions and make recommendations for improvements and further studies.

5.1 Review and evaluation of the objectives

- *Univariate and multivariate modelling.*
  With univariate modelling, we wanted to fit separate models to each body feature. We were able to fit logistic models with upper asymptotes but not with lower asymptotes. For Gompertz models, only growth models with lower asymptotes but not with upper asymptotes could be fitted. From our results we noted that the logistic models were most appropriate to describe the growth of body mass and wing length while the Gompertz models provided best fits for bill, tarsus, head and foot for Grey-headed Gulls. For Swift Terns, the inverse exponential model provided the best univariate fit for four of six features. But this model could not be fitted for wing. This may be the reason why we could not fit a multivariate inverse exponential and possibly highlights a problem with our approach of forcing the same structural form on all responses.

  The multivariate modelling approach:
  To fit growth curves to multiple responses simultaneously, we have used a different approach from that used in Davidian and Giltinan (1995).

Our approach can be used provided the same structural function is valid for all responses. We coped with heteroscedasticity by using feature-specific powers in the variance function. We specified the same within-subject correlation matrix for each feature but we were not able to include estimates of correlations from measurements from different features. The differences in scales for different features is to some extent taken into account by the fixed effect parameters in the model and to some extent by different powers for the variance function. But it did not entirely work since we noticed that large residuals related to measurements of the two features (wing and mass) with large values. The differently scaled responses is a problem in modelling all responses jointly when using non-linear mixed effects modes because of limitations in being able to specify different variances for different responses (Davidian and Giltinan, 1995), and the use of different powers for variance function did not solve this problem. The logistic model gave the best model to describe the growth of all body features taken simultaneously for both Grey-headed Gull and Swift Tern data.

Although the AIC and LR tests indicated the need for random effects, it turned out that the random effects were very small so that we could not distinguish between fixed effect and bird-specific curves. This questions the need for random effects and the usefulness of AIC and LR statistics in testing for their contribution to the model.

- *Intra-specific comparisons of growth for different body features.*
  The multivariate modelling allowed to compare growth rates of features to one another. The results showed that the multivariate logistic provided meaningful comparisons of growth rates as all growth parameter estimates were expressed in the same units (time taken to grow to a certain level). Standardized growth curves, which are curves obtained by plotting scaled predictions (predictions divided by the asymptotic value) against age, allowed us to determine the sequence in which the completion of the growth took place in all features.

- *Age determination for Swift Tern.*
  The necessity to achieve this objective arises from the fact that for terns captured when they were already runners their ages at first capture were unknown. A method based on optimization was used to estimate ages at first occasion of the follow-up period for these birds. This method seemed to work well in that curves (Figure 4.23) are much improved (as shown by narrower ranges and better defined curves). But this method was based on the following assumptions: the growth rate parameters are assumed to be the same for all birds, the asymptotes vary between birds but lie between $\widehat{\alpha} \pm 55$, and the age at first capture lies between 2 ± 30. We recommend to further investigate to see whether these assumptions hold in a data set for which ages are known so that the predictions can be compared to true ages.

5.2 Conclusions and recommendations

This study focused on fitting growth curves to Grey-headed Gull and Swift Tern growth data using univariate and multivariate non-linear mixed effects modelling approaches. Prior to fitting growth curves to Swift Tern data, an optimization method was used to estimate the ages of Swift Terns at first catch of the follow up period.

Logistic and Gompertz models gave a good description of growth of body features of Grey-headed Gulls and Swift Terns compared to other growth models investigated in this study.

From the investigated growth models (logistic, Gompertz, inverse exponential, and Richards models), the logistic and Gompertz models provide good fits for growth variables (body features). In this study, a combination of the logistic model, which provides an upper asymptote, an estimate of time to reach the point of inflection, and an estimate of time to increase from half to three quarters of the asymptote, with the Gompertz, that provides a lower asymptote and instantaneous growth rates, was used to describe the growth of body features. The inverse exponential and Richards models could not fit for all body features of Grey-headed Gulls and Swift Terns.

In addition, parameter estimates of Richards models are not easy to interpret.

Univariate and multivariate modelling approaches yielded approximately the same parameter estimates.

Estimates obtained from univariate models did not differ substantially from those obtained from the multivariate models. With the multivariate modelling approach, it was possible to explore correlation between body features to some extent. We could also carry out multiple comparisons between growth rates of different features. However, in the multivariate modelling approach, estimation problems (convergence problems) were often encountered.

The completion of growth for the body features occurs in a specific sequence.

The body features do not all grow at the same rate and the growth is not completed at the same time. For foot, tarsus, head, and culmen (bill), more than 40% of the growth occurred during the incubation period whereas body mass and wing length have less than 20% of their growth completed during incubation. The asymptotes are reached at different times. For both the Grey-headed Gulls and Swift Terns, the completion of the growth for different body features occurs closely in a similar pattern: (foot, body mass, tarsus)-(bill, head)-(wing) for Grey-headed Gulls and (tarsus, foot)-(body mass, bill, head)-(wing) for Swift Terns.

Comparison of our results to previous studies of the Grey-headed Gull and Swift Tern data.

The Grey-headed Gull data was analyzed in a previous study (McIntyre, 2006) using a non-parametric approach to fitting growth curves pioneered by Le Roux (2006). It was claimed that logistic and Gompertz models provide poor fits. However, in the current study, we fitted non-linear mixed effects logistic and Gompertz models and these models yielded similar results (lower and upper asymptotes) to those obtained by non-parametric methods in McIntyre (2006). It was also noted that both methods provided similar shapes of growth curves for the gull body features.

In this study we found the site effect on parameter estimates to be not significant while site effect was found to be significant in McIntyre (2006)'s analysis.

Swift Tern data was analyzed by Le Roux (2006) using the above non-parametric method. Our non-linear mixed effects method and the non-parametric method (Le Roux, 2006) gave similar shapes of growth curves for the body features of Swift Terns. According to Ricklefs (1973), the Gompertz model is a reasonable approximation to growth patterns of seabirds. Le Roux (2006) showed that Gompertz model did not provide good fit to Swift Tern data. Our findings however suggest that the (multivariate) Gompertz model gives a good description of growth of body features of Swift Terns. Our estimates of asymptotic growth lengths for the tarsus and foot are similar to the mean adult lengths given in Le Roux (2006). Asymptotic mass, maximum wing length and asymptotic head length obtained from our results are reasonably close to mean adult measurements, given in Le Roux (2006), for these features. However, a large discrepancy between our maximum bill length estimate (34.52 mm) and mean adult bill length (Le Roux, 2006) (63.6 mm) was observed. One reason for this discrepancy is that measurements have stopped well before the bill has completed its growth, and our asymptote estimate is an extrapolation beyond the range of available data. From our results it seems that development of the body features of Swift Terns is as follows (foot, tarsus, body mass)-(bill-head)-(wing) whereas legs-wing-bill was the order given in Le Roux (2006). This implies that the bill growth was estimated to reach the maximum length before the wing but in reality the bill of a Swift Tern is believed to continue to grow at very low rate for longer period after fledging. We recommend to further study the growth of body features of Swift Terns followed for a period including after fledging stage. The main difference between the non-parametric approach by McIntyre (2006) and Le Roux (2006) and our approach is that with the former the data dictate the shape of the growth curve whereas with the later a specific functional form is imposed to the data.

Variance-covariance structure in multivariate non-linear mixed effects modelling:

In this study we fitted different variance functions successfully for the univariate modelling approach. However, for the multivariate modelling approach, we could only impose the same variance functions (albeit with differential power parameters for each feature) and correlation functions (compound symmetry or first order autoregressive correlation structure) for all features with errors from different body features within the same bird were assumed to be independent, for convergence purpose. Thus, we recommend future investigation in variance functions and correlation structures such as autoregressive structure of higher order for each feature within the same bird for the multivariate approach.
Due to estimation problems, we were restricted to a block diagonal structure for the variance-covariance structure for random effects. Other forms of variance-covariance matrix for random effects, such as an unstructured form, may improve the model.

Multivariate with different structural forms for groups of responses:

In our study, we assumed the same structural model for all response variables (body features). Although this approach allowed us to solve a multivariate problem, it presents a major drawback if different features requires different structural functions. Attempts to fit different structural models to responses from different features using the approach described by Davidian and Giltinan (1995); Hall and Clutter (2004) ran into estimation problems when using nlme (non-linear mixed effects) procedure in R. More success was achieved using a generalized non-linear least square procedure (gnls). Initial results (not presented) showed models with higher AICs than the ones reported in this thesis. However, further work is needed to refine these models, especially in terms of fitting of variance and correlation functions. With our approach, based on fixed effects parameters, we can carry out comparisons between different responses and easily generate estimates of confidence intervals (CI) for differences in parameter estimates for different responses whereas with the approach described by Davidian and Giltinan (1995); Hall and Clutter (2004) these comparisons would be based on comparing predicted outcome.

Since we can bring in the feature covariate into our variance function (in our case, especially by allowing different power functions for different features) we are able to some extent to overcome the problem of differential scales for responses. However, this method is only of use when the same structural form is applicable for all responses.

Bibliography

Benoit, L. and Henri, W. (1990). Influence of Parental experience on the Growth of Wandering Albatross, *The Condor* **92**: 726–731.

Berrow, S. D., Huin, N., Humpidge, R., Murray, A. W. A. and Prince, P. A. (2002). Wing and Primary Growth Wandering Albatross, *The Condor* **101**: 360–368.

Brooke, R. (1997). Grey-headed Gull *Larus cirrocephalus*. In: Non-passerines. Harrison, J. A., Allan, D.G., Underhill, L.G., Herremans, M., Tree, A.J., Parker, V. and Brown, C.J., *Atlas* 1: 464–465.

Brooke, R. K., Allan, D. G., Cooper, J., Cyrus, D. P., Dean, W. R. J., Dyer, B. M., Martin, A. P. and Taylor, R. H. (1999) Breeding distribution, population size and conservation of Grey-headed Gull *Larus cirrocephalus* in southern Africa, *Ostrich* **70**: 157–163.

Burchinal, M. and Appelbaum, M. (1991). Estimating Individual Developmental Functions: Methods and their assumptions, *Journal of the Operational Research Society* **62**: 23–43.

Calegario, N., F.Daniels, R., Maestri, R. and Neiva, R. (2005). Modeling dominant height growth based on non-linear mixed effects model: a clonal case Eucalyptus plantation case study, *Forest Ecology and Management* **204**: 11–21.

Cooper, J., Crawford, R. J. M. and Williams, A. J. (1990). Distribution, population size and conservation of the Swift Tern *Sterna bergii* in southern Africa, *Ostrich* **61**: 56–65.

Davidian, M. and Giltinan, D. M. (1995). *Nonlinear Models for Repeated Measurement Data*, Chapman & Hall, New York.

Emlen, J. T. J. (1936). Age Determination in the American Crow, *The Condor* **38**: 99–102.

Gamito, S. (1998). Growth models and their use in ecological modeling. An application to a fish population , *Ecological Modelling* **113**: 83–94.

Hall, D. B. and Clutter, M. (2004). Multivariate Multilevel Nonlinear Mixed Effects Models for Timber Yield Predictions, *Biometrics* **60**: 16–24.

Hockey, P. A. R., Dean, W. R. J. and Ryan, P. G. (2005). *Roberts - Birds of southern Africa.*

Holmes, D. I. (1983). A graphical identification procedure for growth curves, *The Statistician* **32**: 405–415.

Jacoby, W. G. (2000). Loess: a non-parametric graphical tool for depicting relationships between variables, *Electoral Studies* **19**: 577–613.

Kumar, K. (1998). Fitting of Sigmoidal Growth Curves, *The Mathematical Gazette* **82**: 306–309.

Le Roux, J. (2006). *The Swift Tern* Sterna bergii *in Southern Africa: Growth and Movement, Masters thesis*, University of Cape Town.

McIntyre, M. A. (2006). *Biology of the Grey-headed Gull Larus cirrocephalus in South Africa: Masters thesis*, University of Cape Town.

Mendenhall, W., Beaver, R. J. and Beaver, B. M. (1996). *A course in Business Statistics*, Duxbury press, New York.

Nagarajan, R., Thiyagesan, K., Natarajan, R. and Kanakasabai, R. (2002). Patterns of growth in nestling Indian Barn-Owls, *The Condor* **104**: 885–890.

Narushin, V. G. and Takma, C. (2003). Sigmoid Model for the Evaluation of Growth and Production Curves in Laying Hens, *Biosystems Engineering* **84**: 343–348.

Olshansky, S. J. and Bruce, A. C. (1997). Ever since Gompertz, *The Demograhy of Aging* **34**: 1–15.

Philip, H. F. (1994). Fitting a Gompertz Curve, *The Journal of the Operational Research Society* **45**: 109–113.

Pinheiro, J. C. and Bates, D. M. (2000). *Mixed Effects Models in S-Plus*, Springer-Verlag, New York.

R Development Core Team (2006). *R: A Language and Environment for Statistical Computing*, R Foundation for Statistical Computing, Vienna, Austria.

Ratkowsky, D. A. (1983). *Nonlinear Regression Modelling. A Unified Practical Approach*, Marcel Dekker, New York.

Ratkowsky, D. A. (1990). *Handbook of Nonlinear Regression Models*, Marcel Dekker, New York.

Raudenbush, S. W. and Bryk, A. S. (2002). *Hierarchical Linear Models: Applications and Data Analysis Methods*, International Educational and Professional Thousand Oaks. London.

Ricklefs, R. E. (1967). A graphical Method of Fitting Equations to Growth Curves, *Journal of Ecology* **48**: 978–983.

Ricklefs, R. E. (1973). Patterns of growth in birds. II. Growth and rate of mode of development, *Ibis* **115**: 177–201.

Sanchez-Guzman, J. M. and Viejo, A. M. D. (1990). A Method of Age Determination for Nestling Gull-Billed Terns, *Colonial Waterbirds* **21**: 427–430.

Scott, G. G. and Ankney, C. D. (1992). Estimating age of young birds with a multivariate measure of body size, *The Auk* **109(3)**: 444–450.

Seber, G. and Wild, C. J. (1989). *Nonlinear regression*, John Wiley & Sons, New York.

Singer, J. D. and Willett, J. B. (2003). *Applied Longitudinal Data Analysis. Modeling change and event occurrence*, Oxford University Press, New York.

Sterman, J. D. (2000). *Business Dynamics. Systems thinking and modeling a complex world*, Irwin & Mc Graw-Hill, New York.

Tom, A. D. S. and Roel, J. B. (2002). *Multivariate Analysis. An Introduction to Basic and Advanced Multilevel Modeling*, SAGE Publications, London.

Vieira, S. and Hoffmann, R. (1977). Comparison of the Logistic and the Gompertz Functions Considering Additive and Multiplicative Error Terms, *Applied.Statistics* **26**: 143–148.

Weisstein, E. W. (1999). Logistic Growth curves.
URL: *http://mathworld.wolfram.com/LogisticEquation.ht*

Wiener, J., Kinsman, S. and Williams, S. (1998). Modeling the Growth of Individuals in Plant Populations: Local Density Variation in a Strand Population of Xanthium strumarium (Asteraceae), *American Journal of Botany* **85**: 1638–1645.

Winsor, C. P. (1932). Gompertz Curve as a Growth Curve, *Proceedings of the National Academy of Sciences* **18**: 1–8.

Appendix A

Appendix: R Code

This appendix is subdivided into three main parts, namely, univariate modelling codes, multivariate modelling codes, and age determination method codes. R programmes require that all comments and other documentations are preceded by the symbol # and the commands are just statements. To avoid any confusion our codes are written within R program requirements so that these codes can be used by anyone without changing anything.

A.1 Univariate modelling

```
# \textbf{Read data from an excel file saved as text document.}

data1<-read.table(''BonaeroModderfontein-mass.txt'', header=TRUE,sep=''\ t'').
data<-na.omit(data1) data2<-groupedData(mass~ age|bird,data=data).

#Defining site as categorical variable

bird<-data2[,1] # this  represents a bird id.
age<-data2[,2] mass<-data2[,4]
site<-as.factor(data2$site)
data3<-data.frame(bird,age,mass,site)
data4<-groupedData(mass~ age|bird,data=data3). is.factor(data4\site)
```

Fitting Logistic, Gompertz, Inverse exponential and Richards' models:

1. Logistic models

single non-linear model

```
Lmodel1<-nls(mass~ SSlogis(age,Asym,Xmid,Scal), data=data4,
start=c(Asym=317,Xmid=13.06,Scal=7.04))
```

Separate model for each bird

```
Lmodel2<-nlsList(mass~SSlogis(age,Asym,Xmid,Scal), data=data4,
start=c(Asym=317,Xmid=15,Scal=8))
```

Mixed effects models

```
Lmodel3<-nlme(mass ~ SSlogis(age,Asym,Xmid,Scal), data=data4,
random=pdDiag(Asym+Xmid+Scal~ 1),fixed=(Asym+Xmid+Scal~ 1),
start=c(Asym=317,Xmid=13.06,Scal=7.04)) Lmodel4<-nlme(mass ~
SSlogis(age,Asym,Xmid,Scal), data=data4, random=pdDiag(Asym+Xmid~
1),fixed=(Asym+Xmid+Scal~ 1), start=c(Asym=317,Xmid=13.06,Scal=7.04))
Lmodel6<-nlme(mass~ SSlogis(age,Asym,Xmid,Scal), data=data4, random=(Asym+Xmid ~
1),fixed=(Asym+Xmid+Scal ~ 1), start=c(Asym=317,Xmid=13.06,Scal=7.04))
Lmodel7<-nlme(mass ~ SSlogis(age,Asym,Xmid,Scal), data=data4,
random=pdDiag(Asym+Scal~ 1),fixed=(Asym+Xmid+Scal~1),
start=c(Asym=317,Xmid=13.06,Scal=7.04)) Lmodel8<-nlme(mass ~
SSlogis(age,Asym,Xmid,Scal), data=data4, random=(Asym+Scal~
1),fixed=(Asym+Xmid+Scal~ 1), start=c(Asym=317,Xmid=13.06,Scal=7.04))
Lmodel9<-nlme(mass~ SSlogis(age,Asym,Xmid,Scal), data=data4,
random=pdDiag(Asym+Scal~ 1),fixed=(Asym+Xmid+Scal~ 1),
start=c(Asym=317,Xmid=13.06,Scal=7.04)) Lmodel10<-nlme(mass~
SSlogis(age,Asym,Xmid,Scal), data=data4, random=(Xmid+Scal~
1),fixed=(Asym+Xmid+Scal~ 1), start=c(Asym=317,Xmid=13.06,Scal=7.04))
Lmodel11<-nlme(mass~SSlogis(age,Asym,Xmid,Scal), data=data4,
random=pdDiag(Xmid+Scal~ 1),fixed=(Asym+Xmid+Scal~ 1),
start=c(Asym=317,Xmid=13.06,Scal=7.04))
Lmodel12<-nlme(mass~SSlogis(age,Asym,Xmid,Scal), data=data4, random=pdDiag(Asym ~
```

```
1),fixed=(Asym+Xmid+Scal~ 1), start=c(Asym=317,Xmid=13.06,Scal=7.04))
Lmodel13<-nlme(mass~ SSlogis(age,Asym,Xmid,Scal), data=data4, random=pdDiag(Scal~
1),fixed=(Asym+Xmid+Scal~ 1), start=c(Asym=317,Xmid=13.06,Scal=7.04))
Lmodel14<-nlme(mass~ SSlogis(age,Asym,Xmid,Scal), data=data4, random=pdDiag(Xmid ~
1),fixed=(Asym+Xmid+Scal~ 1), start=c(Asym=317,Xmid=13.06,Scal=7.04))
```

Comparing the models using AIC

```
anova(Lmodel3,Lmodel4,Lmodel5,Lmodel6,Lmodel7,Lmodel8,Lmodel9,Lmodel10,
Lmodel11,Lmodel12,Lmodel13,Lmodel14,test=F)
```

Fitting Variance functions in nlme:

```
Lmodel6<-update(Lmodel3,weights=varPower(fixed=0.5))
Lmodel7<-update(Lmodel3,weights=varIdent(form=~ 1| site))
Lmodel8<-update(Lmodel3,weights=varConstPower(power=0.5))
Lmodel9<-update(Lmodel3,weights=varComb(varConstPower(power=0.5), varIdent(form=~
1|site))) Lmodel10<-update(Lmodel,weights=varPower(form=~  fitted(.)| site))
```

Fitting Correlation structure functions in nlme:

```
Lmodel11<-update(Lmodel8,correlation=corAR1(),method="ML")
Lmodel12<-update(Lmodel8,correlation=corCompSymm(),method="ML")
Lmodel13<-update(Lmodel8,correlation=corARMA(q=2),method="ML")
```

Fitting covariates in nlme models:

```
 #Graphical exploration of variability between sites
 #Generating random.effects associated to parameters according to  site

Lmodel11.nlmeCE<-ranef(Lmodel11,augFrame=T) \#Plot of boxplots

par(mfrow=c(1,3)) boxplot(Lmodel11.nlmeCE\Asym ~
Lmodel11.nlmeCE\site,ylab="Asym",xlab="Site") boxplot(Lmodel11.nlmeCE\Xmid ~
Lmodel11.nlmeCE\site,ylab="Xmid",xlab="Site") boxplot(Lmodel11.nlmeCE\Scal~
Lmodel11.nlmeCE\site,ylab="Scal",xlab="Site")
```

```
#Expressing parameters as  functions of site

Lmodel16<-update(Lmodel11,fixed=c(Asym ~ 1,Xmid ~ site,Scal ~ site),
start=c(Asym=317,Xmid=13.06,0,Scal=7.04,0) , random=pdDiag(Asym+Xmid+Scal~ 1))
Lmodel17<-update(Lmodel11, fixed=c(Asym ~ site,Xmid~ 1,Scal~ site),
start=c(Asym=317,0,Xmid=13.06,Scal=7.04,0) , random=pdDiag(Asym+Xmid+Scal~1))
Lmodel18<-update(Lmodel11, fixed=c(Asym ~ site,Xmid ~ site,Scal~
1),start=c(Asym=317,0,Xmid=13.06,0,Scal=7.04) , random=pdDiag(Asym+Xmid+Scal~ 1))
Lmodel19<-update(Lmodel11, fixed=c(Asym ~ site,Xmid ~ site,Scal~ site),
start=c(Asym=317,0,Xmid=13.06,0,Scal=7.04,0) , random=pdDiag(Asym+Xmid ~ 1)) \#best
```

Assessing assumptions

```
#1. Constant
variation plot(Lmodel18,id=0.05,adj=-0.3) plot(Lmodel18)

#2. Normality qqnorm(Lmodel18,abline=c(0,1))
qqnorm(Lmodel11,abline=c(0,1),id=0.05,adj=-0.3)
qqnorm(Lmodel18,~ranef(.),layout=c(3,1))

#3. Generating augmented plots to visualize the model
plot(augPred(Gmodel3,level=0:1),layout=c(7,5,4))

#4.Otherdiagnostic plots

plot(Lmodel00$fitted[,2],data4\mass,ylab="Observed mass",xlab="Fitted mass")
abline(0,1) plot(Lmodel15$fitted[,2],abs(Lmodel15$residuals[,2]),ylab="|
Residuals|",xlab="Fitted Values")

plot(data4$age, Lmodel$residuals[,2],ylab="Residuals",xlab="age") abline(h=0)
```

2. Gompertz models

```
gomp<-function(age, w, mu,k){w*exp(mu*(1-exp(-k*age)))}
```

Single non-linear model

```
Gmodel1<-nls(mass~gomp(age,w,mu,k),data=data4,start=c(w=8.6,mu=5,k=0.08))
```

Separate model for each bird

```
Gmodel2<-nlsList(mass~gomp(age,w,mu,k),data=data4,start=c(w=8.6,mu=5,k=0.08))
```

Mixed models

```
Gmodel3<-nlme(mass~gomp(age,w,mu,k), data=data4,
random=pdDiag(w+mu+k~1),fixed=(w+mu+k~1), start=c(w=8.6,mu=5,k=0.08))
```

Variance functions:

```
Gmodel4<-update(Gmodel3,weights=varPower(fixed=0.5))
Gmodel5<-update(Gmodel3,weights=varIdent(form=~ 1 | site))
Gmodel6<-update(Gmodel3,weights=varConstPower(power=0.5))
Gmodel7<-update(Gmodel3,weights=varComb(varConstPower(power=0.5),
varIdent(form=~1|site)))

Gmodel8<-update(Gmodel3,weights=varPower(form=~ fitted(.)| site))#best
```

Correlation structure:

```
Gmodel9<-update(Gmodel6,correlation=corCompSymm())
Gmodel10<-update(Gmodel6,correlation=corAR1())\#best
Gmodel11<-update(Gmodel6,correlation=corARMA(q=2),method="ML")
```

Modeling covariates

```
Gmodel12<- update(Gmodel10, fixed=c(w~site,mu~site,k~site),
start=c(w=8.6,0,mu=5,0,k=0.08,0),random=pdDiag(mu+k~1))
```

3. Inverse Exponential model

```
expo<-function(age,B1,B2,B3){B1-(B1-B2)*exp(-B3*age)}
```

Mixed models

```
Invmodel3<-nlme(mass ~ expo(age,B1,B2,B3), data=data4, random=pdDiag(B1+B2+B3 ~
1),fixed=(B1+B2+B3 ~ 1), start=c(B1=350,B2=20,B3=0.05)) Invmodel4<-nlme(mass ~
expo(age,B1,B2,B3), data=data4, random=pdDiag(B1+B2 ~ 1),fixed=(B1+B2+B3 ~ 1),
start=c(B1=350,B2=20,B3=0.05))
```

Variance functions

```
Invmodel4<-update(Invmodel3,weights=varPower(fixed=0.5))
Invmodel5<-update(Invmodel3,weights=varIdent(form= ~ 1 | site))
Invmodel6<-update(Invmodel3,weights=varConstPower(power=0.5))
Invmodel7<-update(Invmodel3,weights=varComb(varConstPower(power=0.5),varIdent(form=
~ 1| site)))

Invmodel8<-update(Invmodel3,weights=varPower(form=~fitted(.)| site))\#best
```

Correlation structure

```
Invomodel8<-update(Invmodel8,correlation=corCompSymm())
Invmodel9<-update(Invmodel8,correlation=corAR1())
Invmodel10<-update(Invmodel8,correlation=corARMA(q=2),method="ML")
```

Covariate modelling

```
Invmodel11<-update(Invomodel8,fixed=c(B1 ~ site,B2~ site,B3~ site),start=
c(B1=350,0,B2=20,0,B3=0.05,0), random=pdDiag(B1~ 1))
```

4. Richards models

```
rich<-function(age, a,b ,g ,d){a/(1+exp(b-g*age))^(1/d)}
```

Single non-linear model

```
Rmodel1<-nls(mass~rich(age,a,b,g,d), data=data4,start=c(a=175,b=1.85,g=0.15,d=0.75))
```

Separate model for each bird

```
Rmodel2<-nlsList(mass ~ rich(age,a,b,g,d),
data=data4,start=c(a=175,b=1.85,g=0.15,d=0.75))
```

Mixed effects models

```
Rmodel3<-nlme(Rmodel2,random=pdDiag(a+b+g+d ~ 1))
Rmodel4<-nlme(Rmodel2,random=pdDiag(a ~ 1),method="ML")
Rmodel5<-nlme(Rmodel2,random=pdDiag(a+b ~ 1),method="ML")
Rmodel6<-nlme(Rmodel2,random=pdDiag(a+b+g ~ 1),method="ML")\#best
```

Variance functions

```
Rmodel8<-update(Rmodel6,weights=varPower(fixed=0.5))
Rmodel9<-update(Rmodel6,weights=varIdent(form= ~ 1 | site))
Rmodel10<-update(Rmodel6,weights=varConstPower(power=0.5))
Rmodel11<-update(Rmodel6,weights=varComb(varConstPower(power=0.5),varIdent(form= ~
1|site))) Rmodel12<-update(Rmodel6,weights=varPower(form=~fitted(.)|site))\#best
```

Correlation function

```
Rmodel13<-update(Rmodel8,correlation=corAR1(),method="ML")
Rmodel14<-update(Rmodel8,correlation=corCompSymm(),method="ML")
Rmodel15<-update(Rmodel8,correlation=corARMA(q=2),method="ML")
Rmodel16<-update(Rmodel8,correlation=corARMA(p=1,q=1),method="ML")
```

Comparing Gompertz,Logistic ,Inverse exponential Richards's models using AIC

```
anova(Gmodel12 ,Lmodel18,Invomodel8, Rmodel17,test=F)
```

Standardized predicted curves for all variables

```
x <- seq(0,60,by = 0.2) # Declaring the parameters' values

#1.Mass
 A.m <- 268.42
 xmid.m <- 12.45
 scal.m <- 5.21
# 2.Bill
 A.b <- 29.2
 xmid.b <- 3.59
 scal.b <- 11.68
# Tarsus
 A.t <- 46.24
 xmid.t <- 3.39
 scal.t <- 9.24
# Wing A.w <- 266.99
xmid.w <- 23.76
scal.w <- 8.29
#Head
 A.h <- 78.04
 xmid.h <- 2.59
 scal.h <- 12.96
# Foot
 A.f <- 93.51
 xmid.f <- 1.42
 scal.f <- 8.81
mult.logf <- 1 / (1 + exp(- (x - xmid.f)/scal.f))

mult.logh <- 1 / (1 + exp(- (x - xmid.h)/scal.h))

mult.logw <- 1 / (1 + exp(- (x - xmid.w)/scal.w))

mult.logt <- 1 / (1 + exp(- (x - xmid.t)/scal.t))
```

```
mult.logm <- 1 / (1 + exp(- (x - xmid.m)/scal.m))

mult.logb <- 1 / (1 + exp(- (x -xmid.b)/scal.b))

plot(x, mult.logm, type = "l", col = 1, ylim = c(0,1),ylab="Growth scale ",xlab="Age
(days)",lty=1,las=1)

lines(x, mult.logb, col = 2,lty=1,las=1) lines(x, mult.logt, col = 3,lty=1,las=1)
lines(x, mult.logw, col = 4,lty=1,las=1) lines(x, mult.logh, col = 5,lty=1,las=1)
lines(x, mult.logf, col = 6,lty=1,las=1)

text(locator(6), c("Mass", "Bill", "Tarsus", "Wing", "Head", "Foot"))
```

Predicted curves for body mass of Grey-headed Gull chicks in Bonaero Park and Modderfontein Pan

```
dis1<-read.table("dimas.txt",header=TRUE,sep="\t")
dis2<-read.table("bonamass.txt",header=TRUE,sep="\t")
dis3<-read.table("moddermass.txt",header=TRUE,sep="\t") age <- seq(0,50,by = 0.2)

#1.Mass A.b <- 268.42
xmid.b <- 12.45 scal.b<- 5.21
A.m <- 252.96 xmid.m <- 12.40
scal.m <- 4.87
Bonaero <- A.b / (1 + exp(- (age - xmid.b)/scal.b))

Modderfontein <- A.m / (1 +exp(- (age - xmid.m)/scal.m))

plot(dis2\ageb, dis2\massb, pch =2,col=2, cex = 0.3,ylab="Mass (g)",xlab="Age
(days)",ylim = c(20,320),las=1) points(dis3$agem, dis3$massm, pch =7,col=3, cex =
0.3,ylab="mass (g)",xlab="Age(day)", las=1)

lines(age, Bonaero, type = "l", col = 2, ylim = c(20,320),ylab="mass
(g)",xlab="Age(day)",lty=1,lwd=2,las=1)
```

```
lines(age, Modderfontein, col =3,lty=1,cex=0.8,lwd=2,las=1)

legend(20, 100,c("Bonaero","Modderfontein"),col=c(2,3),lty=1,lwd=2,pch=c(2,7))
```

A.2 Multivariate modelling

Multivariate logistic models

Separate models

```
Lmodel1 <- nls(response ~SSlogis(age,Asym,Xmid,Scal), data=dis4,
start=c(Asym=317,Xmid=13.06,Scal=7.04)) Lmodel2 <- nlsList(response ~
SSlogis(age,Asym,Xmid,Scal), data=dis4, start=c(Asym=317,Xmid=15,Scal=8))

Lmodel3 <- nlme(response~ SSlogis(age,Asym,Xmid,Scal), data=dis4,
random=pdDiag(Asym+Xmid+Scal ~ 1),fixed=(Asym+Xmid+Scal ~ 1),
start=c(Asym=317,Xmid=13.06,Scal=7.04))\# best

Lmodel4 <- nlme(response~SSlogis(age,Asym,Xmid,Scal), data=dis4,
random=(Asym+Xmid+Scal ~ 1),fixed=(Asym+Xmid+Scal ~ 1),
start=c(Asym=317,Xmid=13.06,Scal=7.04))

Lmodel5 <- nlme(response~SSlogis(age,Asym,Xmid,Scal), data=dis4,
random=pdDiag(Asym+Xmid ~ 1),fixed=(Asym+Xmid+Scal ~ 1),
start=c(Asym=317,Xmid=13.06,Scal=7.04))

Lmodel6 <- nlme(response ~ SSlogis(age,Asym,Xmid,Scal), data=dis4, random=(Asym+Xmid
~ 1),fixed=(Asym+Xmid+Scal ~ 1), start=c(Asym=317,Xmid=13.06,Scal=7.04))

Lmodel7 <- nlme(response ~ SSlogis(age,Asym,Xmid,Scal), data=dis4,
random=pdDiag(Asym+Scal ~ 1),fixed=(Asym+Xmid+Scal ~ 1),
start=c(Asym=317,Xmid=13.06,Scal=7.04))

Lmodel8 <- nlme(response ~ SSlogis(age,Asym,Xmid,Scal), data=dis4, random=(Asym+Scal
~ 1),fixed=(Asym+Xmid+Scal ~ 1), start=c(Asym=317,Xmid=13.06,Scal=7.04))

Lmodel9 <- nlme(response~SSlogis(age,Asym,Xmid,Scal), data=dis4, random=pdDiag(Asym
~ 1),fixed=(Asym+Xmid+Scal ~ 1), start=c(Asym=317,Xmid=13.06,Scal=7.04))
```

```
Lmodel10 <- nlme(response~SSlogis(age,Asym,Xmid,Scal), data=dis4, random=(Asym ~
1),fixed=(Asym+Xmid+Scal ~ 1), start=c(Asym=317,Xmid=13.06,Scal=7.04))
```

Variance function:

```
Lmodel13<-update(Lmodel3,weights=varPower(fixed=0.5))

Lmodel14 <-update(Lmodel3,weights=varIdent(form= ~ 1 | site))

Lmodel15<- update(Lmodel3,weights=varIdent(form= ~ 1| feature))

Lmodel16<- update(Lmodel3,weights=varIdent(form=~ 1 | feature*site))

Lmodel17<- update(Lmodel3,weights=varConstPower(power=0.5))
Lmodel12<-update(Lmodel11,weights=varComb(varConstPower(power=0.5), varIdent(form=~1
| site*feature)))

Lmodel18<-update(Lmodel2,weights=varPower(form= ~ fitted(.)| site*feature))
Lmodel17<-update(Lmodel2,weights=varPower(form=~ fitted(.)| feature))# best
```

Correlation structure

```
Lmodel19<-update(Lmodel17,correlation=corAR1(),method="ML") Lmodel20<-
update(Lmodel17,correlation=corCompSymm(),method="ML") Lmodel21<-
update(Lmodel17,correlation=corARMA(q=2),method="ML")
Lmodel22<-update(Lmodel7,correlation=corAR1(form=~1|bird/feature),method="ML") #best
```

Covariates in the model

```
Lmodel23<- update(Lmodel22, fixed=c(Asym~feature,Xmid ~ feature,Scal ~ feature),
start=c(Asym=317,0,0,0,0,0,Xmid=13.06,0,0,0,0,0,Scal=7.04,0,0,0,0,0) ,
random=pdDiag(Asym+Xmid+Scal ~ 1))

Lmodel24<- update(Lmodel22, fixed=c(Asym ~ site+feature,Xmid ~ site+feature,Scal ~
site+feature),start=c(Asym=317,0,0,0,0,0,0,Xmid=13.06,0,0,0,0,0,0,Scal=7.04,0,0,0,0,0
, random=pdDiag(Asym+Xmid+Scal ~ 1))
```

Multivariate Gompertz models

```
gomp<-function(age, w, mu,k){w*exp(mu*(1-exp(-k*age)))}

#Single model: Gmodel1<-nls(response~gomp(age,w,mu,k),
data=dis4,start=c(w=8.6,mu=5,k=0.08))
```

Separate models

```
Gmodel2<-nlsList(response~gomp(age,w,mu,k), data=dis4,start=c(w=8.6,mu=5,k=0.08))
```

Mixed models

```
Gmodel3<-nlme(response~gomp(age,w,mu,k), data=dis4,
random=pdDiag(w+mu+k~1),fixed=(w+mu+k~1), start=c(w=8.6,mu=5,k=0.08))
Gmodel4<-nlme(response~gomp(age,w,mu,k), data=dis4,
random=pdDiag(w+mu~1),fixed=(w+mu+k~1), start=c(w=8.6,mu=5,k=0.08))
Gmodel5<-nlme(response~gomp(age,w,mu,k), data=dis4,
random=(w+mu+k~1),fixed=(w+mu+k~1), start=c(w=8.6,mu=5,k=0.08))
Gmodel6<-nlme(response~gomp(age,w,mu,k), data=dis4,
random=(w+mu~1),fixed=(w+mu+k~1), start=c(w=8.6,mu=5,k=0.08))
```

Variance functions:

```
Gmodel6<-update(Gmodel4,weights=varPower(fixed=0.5))
Gmodel7<-update(Gmodel4,weights=varIdent(form=~1|site))
Gmodel8<-update(Gmodel4,weights=varIdent(form=~1|feature))
Gmodel9<-update(Gmodel4,weights=varIdent(form=~1|feature*site))
Gmodel10<-update(Gmodel4,weights=varConstPower(power=0.5))
Gmodel11<-update(Gmodel4,weights=varComb(varConstPower(power=0.5),varIdent(form=~1|fe
Gmodel12<-update(Gmodel4,weights=varPower(form=~fitted(.)|site*feature))\#best
Gmodel13<-update(Gmodel4,weights=varPower(form=~fitted(.)|feature))
```

Correlation structure:

```
Gmodel14<-update(Gmodel13,correlation=corCompSymm())
Gmodel15<-update(Gmodel12,correlation=corAR1())#best
Gmodel16<-update(Gmodel13,correlation=corARMA(q=2),method="ML")
```

```
Gmodel17<-update(Gmodel13,correlation=corARMA(p=1,q=1),method="ML")
Gmodel18<-update(Gmodel13,correlation=corAR1(form=~1| bird/feature),method="ML")

#best
```

Modelling covariate

```
Gmodel19<- update(Gmodel18, fixed=c(w~feature,mu~feature,k~feature),
start=c(w=8.6,0,0,0,0,0,mu=5,0,0,0,0,0,k=0.08,0,0,0,0,0) ,random=pdDiag(w+mu~1))
```

Multivariate Richards models

```
rich<-function(age, a,b ,g ,d){a/(1+exp(b-g*age))^(1/d)}
Rmodel1<-nls(response~rich(age,a,b,g,d),
data=dis4,start=c(a=175,b=1.85,g=0.15,d=0.75))
Rmodel2<-nlsList(response~rich(age,a,b,g,d),
data=dis4,start=c(a=175,b=1.85,g=0.15,d=0.75))
Rmodel3<-nlme(Rmodel2,random=pdDiag(a+b+g+d~1))
Rmodel4<-nlme(Rmodel2,random=pdDiag(a~1),method="ML")
Rmodel5<-nlme(Rmodel2,random=pdDiag(a+b~1),method="ML")
Rmodel6<-nlme(Rmodel2,random=pdDiag(a+b+g~1),method="ML")\#best
```

Variance function

```
Rmodel8<-update(Rmodel6,weights=varPower(fixed=0.5))
Rmodel9<-update(Rmodel6,weights=varIdent(form=~1|site))
Rmodel10<-update(Rmodel6,weights=varConstPower(power=0.5))
Rmodel11<-update(Rmodel6,weights=varComb(varConstPower(power=0.5),varIdent(form=~1|
site))) Rmodel12<-update(Rmodel6,weights=varPower(form=~fitted(.)| site))\#best
```

Correlation function

```
Rmodel13<-update(Rmodel12,correlation=corAR1(),method="ML")
Rmodel14<-update(Rmodel12,correlation=corCompSymm(),method="ML")
Rmodel15<-update(Rmodel12,correlation=corARMA(q=2),method="ML")
Rmodel16<-update(Rmodel12,correlation=corARMA(p=1,q=1),method="ML")
```

Covariate modelling

```
Rmodel17<-update(Rmodel13, fixed=c(a~site,b~site,g~site,d~site),
start=c(a=175,0,b=1.85,0,g=0.15,0,d=0.75,0) , random=pdDiag(a+g~1))
```

Multivariate inverse exponential models

```
expo<-function(age,B1,B2,B3){B1-(B1-B2)*exp(-B3*age)}
Invmodel3<-nlme(response~expo(age,B1,B2,B3), data=dis4,
random=pdDiag(B1+B2+B3~1),fixed=(B1+B2+B3~1), start=c(B1=350,B2=20,B3=0.05))
Invmodel4<-nlme(response~expo(age,B1,B2,B3), data=dis4,
random=(B1+B2+B3~1),fixed=(B1+B2+B3~1), start=c(B1=350,B2=20,B3=0.05))
Invmodel5<-nlme(response~expo(age,B1,B2,B3), data=dis4,
random=pdDiag(B1+B2~1),fixed=(B1+B2+B3~1), start=c(B1=350,B2=20,B3=0.05))
Invmodel6<-nlme(response~expo(age,B1,B2,B3), data=dis4,
random=(B1+B2~1),fixed=(B1+B2+B3~1), start=c(B1=350,B2=20,B3=0.05))
```

Variance function

```
Invmodel7<-update(Invmodel3,weights=varPower(fixed=0.5))
Invmodel8<-update(Invmodel3,weights=varIdent(form=~1| site))
Invmodel9<-update(Invmodel3,weights=varIdent(form=~1| feature))
Invmodel10<-update(Invmodel3,weights=varIdent(form=~1| feature*site))
Invmodel11<-update(Invmodel3,weights=varConstPower(power=0.5))
Invmodel12<-update(Invmodel3,weights=varComb(varConstPower(power=0.5),
varIdent(form=~1| site*feature)))
Invmodel13<-update(Invmodel3,weights=varPower(form=~fitted(.)| site*feature))
```

Correlation structure

```
Invomodel14<-update(Invmodel7,correlation=corCompSymm())
Invmodel15<-update(Invmodel7,correlation=corAR1())
Invmodel16<-update(Invmodel7,correlation=corARMA(q=2),method="ML")
```

Covariate modeling

```
Invmodel11<-update(Invmodel7,fixed=c(B1~feature+site,B2~feature+site,
B3~feature+site),
start=c(B1=350,0,0,0,0,0,0,B2=20,0,0,0,0,0,0,B3=0.05,0,0,0,0,0,0,),
random=pdDiag(B1~1))
```

A.3 Age determination: Optimization method

Details of this optimization include the following

- Reading the data from comma delimited file into R
- Declaration of parameters
- Defining functions
- Optimization
- Printing parameters
- Plotting predicted and optimized curves of one Swift Tern chick

```
dis1<-read.table("Swiftern-nozeroage-atleast4obs.txt",header=TRUE,sep="\t")
  Xmid <- 14.795
  Scal <- 7.189
  Asym <- 318.9684
  pinit<-c(326, 1)
  logss<-function(p)
  { rss <- sum(abs(dy - (Asym + p[1]) /(1 + exp(-((dx + p[2]) - Xmid) / Scal))))
  }
            # p[1] is change in asymptote value
            # p[2] is a shift parameter for difference in age

logist <- function(x, asym, xmid, scal) asym /(1 + exp(-(x - xmid)/scal))

diffs <- matrix(nrow = 224, ncol = 2) for(i in 1:224)
 { dx <- dis1$time[dis1$bird==i & ! is.na(dis1$mass)]
   dy <- dis1$mass[dis1$bird==i & ! is.na(dis1$mass)]
   out <- optim(par = pinit, fn = logss, lower = c(-55, -30), upper = c(55,30),
   method = "L-BFGS-B")
   diffs[i,] <- out$par
 }
print(diffs)
```

```
# Plots

x <- seq(-50, 75, length = 1000) y <- logist(x, Asym, Xmid, Scal)

# plot estimated growth curve plot(x, y, type = "l",ylim = c(0,400), las = 1, xlab =
"age (days)", ylab = "mass (g)")

# select one bird and plot on top of nestling curve

j <- 199

dx <- dis1$time[dis1$bird==j & ! is.na(bdis1$mass)]

dy <- dis1$mass[dis1$bird==j & ! is.na(dis1$mass)] points(dx,dy, col = "green")

dy.new <-$ logist(x + diffs[j,2],Asym + diffs[j,1], Xmid, Scal)

lines(x,dy.new, col = "blue") segments(0,30,0,200,lty=2)
segments(15,168,15,250,lty=2) segments(28,238,28,275,lty=2)
arrows(60,320,60,400,col=2) arrows(60,320,60,240,col=2)
arrows(0,30,30,30,col=3,lty=2) arrows(0,30,-30,30,col=3,lty=2)
text(locator(2),c("estimated curve", "optimal curve for bird199 "))
```